Universidade do Estado do Rio de Janeiro
Centro de Tecnologia e Ciências
Instituto de Química

Aline Rayboltt da Cruz Souza

Optimal design of sieve trays in distillation columns

Rio de Janeiro
2022

Aline Rayboltt da Cruz Souza

Optimal design of sieve trays in distillation columns

Tese apresentada, como requisito parcial para a obtenção do grau de Doutor, ao Programa de Pós-Graduação em Engenharia Química, da Universidade do Estado do Rio de Janeiro.
Área de concentração: Processos Químicos, Petróleo e Meio Ambiente.

Orientador: Prof. Dr. André Luiz Hemerly Costa
Coorientador: Prof. Dr. Miguel Jorge Bagajewicz

Rio de Janeiro
2022

CATALOGAÇÃO NA FONTE
UERJ / REDE SIRIUS / BIBLIOTECA CTC/Q

S729 Souza, Aline Rayboltt da Cruz.

Optimal design of sieve trays in distillation columns. – 2022.
164 f.

Orientador (a): André Luiz Hemerly Costa.

Tese (Doutorado) – Universidade do Estado do Rio de Janeiro. Instituto de Química.

1. Engenharia química – Teses. 2. Engenharia de processos – Teses. 3. Destilação – Teses. I. Costa, André Luiz Hemerly. II. Universidade do Estado do Rio de Janeiro. Instituto de Química. III. Título.

CDU 66.048

Aline Rayboltt da Cruz Souza
Assinatura

25/03/2024
Data

Aline Rayboltt da Cruz Souza

Optimal design of sieve trays in distillation columns

Tese apresentada, como requisito parcial para a obtenção do grau de Doutor, ao Programa de Pós-Graduação em Engenharia Química, da Universidade do Estado do Rio de Janeiro. Área de concentração: Processos Químicos, Petróleo e Meio Ambiente.

Aprovada em 04 de novembro de 2022.

Banca Examinadora:

Prof. Dr. André Luiz Hemerly Costa (Orientador)
Instituto de Química – UERJ

Prof. Dr. Miguel Jorge Bagajewicz (Coorientador)
School of Chemical – University of Oklahoma

Heloísa Lajas Sanches Fernandes

Prof.ª Dra. Heloísa Lajas Sanches
Escola de Química – UFRJ

Prof. Dr. Víctor Rolando Ruiz Ahón
Escola de Engenharia – UFF

Prof. Dr. André Luís Alberton
Instituto de Química – UERJ

Rio de Janeiro

2022

DEDICATÓRIA

Dedico este trabalho aos meus pais, Aldery (*in memorian*) e Angela, por me apoiarem sempre e me incentivarem a seguir os meus sonhos.

AGRADECIMENTOS

A Deus, pela vida e por ter me dado forças para conseguir chegar ao fim desta tese.

Aos meus pais Aldery (*in memorian*) e Angela, pelo amor, carinho e compreensão, que sempre me dedicaram, sempre me apoiando para eu melhorar nos estudos, o que me fez chegar até o doutorado.

Ao meu noivo Ricardo Faustino, pelo amor, carinho e cuidado, o companheiro de vida que Deus me deu, sempre pronto para me apoiar em todos os momentos!

Ao orientador André Luiz Hemerly Costa, pela orientação, pelos ensinamentos, pela dedicação, pelo seu exemplo como professor e pesquisador e pelo grande incentivo. Obrigada por sempre estar aberto as minhas dúvidas e questionamentos!

Ao coorientador Miguel Jorge Bagajewicz, pela orientação, pelos conhecimentos transmitidos e pela participação em reuniões mesmo que à distância.

À minha amiga Maria Zenaide, pelo incentivo e apoio. Sempre me dando forças em todos os momentos!

Às minhas amigas Michaela, Luana e Rachel, pelo carinho e pela compreensão de nem sempre estar por perto como gostaria.

À minha amiga Ana Levy, que me acompanhou no doutorado. Obrigada por ter compartilhado esta caminhada comigo, foi muito melhor com você por perto!

Aos amigos do PPGEQ, Marco Thiago, Alice, Júlia e Carol, obrigada pelo apoio e incentivo, com a pandemia nos afastamos um pouco, mas quando precisava de ajuda sempre estavam prontos a me ajudar. Muito Obrigada!

À UERJ, que foi minha segunda casa nestes últimos 15 anos.

À CAPES, pelo apoio financeiro.

E tantos outros, que de alguma forma contribuíram para o presente trabalho.

Muitas vezes, a dor vem para nos ensinar. Não vem para nos embrutecer, mas para nos fortalecer e elevar, para aperfeiçoar nossa alma com o difícil aprendizado da aceitação e da superação.

Padre Marcelo Rossi, Philia

RESUMO

SOUZA, Aline Rayboltt da Cruz. *Projeto ótimo de pratos perfurados em colunas de destilação.* 2022. 164 f. Tese (Doutorado em Engenharia Química) – Instituto de Química, Universidade do Estado do Rio de Janeiro, Rio de Janeiro, 2022.

A abordagem tradicional do projeto de colunas de destilação é o procedimento heurístico, baseado no método de tentativa e erro. Nas últimas décadas, a literatura apresenta diversos trabalhos de otimização de colunas de destilação integrados, em sua maioria, a um simulador comercial. Entretanto, nestes trabalhos somente há a preocupação do dimensionamento do diâmetro e altura da coluna, que fazem parte do custo total da coluna, as outras variáveis importantes para a funcionalidade da coluna não são dimensionadas. Neste contexto, o presente trabalho apresenta a otimização do projeto ótimo de pratos de colunas de destilação usando duas técnicas diferentes: programação não linear inteira mista e *Set Trimming*. Além disso, se propõe a aperfeiçoar os parâmetros das correlações de inundação e arraste da literatura, a fim de melhorar a acurácia da formulação do projeto. O objetivo desta otimização é dimensionar todas as variáveis geométricas do prato, respeitando as restrições hidráulicas do mesmo (inundação, arraste, gotejamento e *downcomer backup*). Duas possíveis funções objetivas são testadas, a minimização do custo da coluna e a minimização da massa da coluna. A abordagem proposta é aplicada em um exemplo da literatura, o resultado ótimo obtido através da programação matemática e *Set Trimming* são comparados com o resultado obtido pelo procedimento heurístico (retirado da literatura e descrito no texto) e as diferentes técnicas são comparadas entre si. A comparação indica que ambas as técnicas apresentam resultados melhores que o procedimento heurístico, porém o *Set Trimming* é mais robusto que a programação matemática. Na estimação dos parâmetros das correlações utilizou-se programação matemática. Os novos parâmetros são aplicados em três exemplos de projetos de colunas da literatura e comparados com as correlações já existentes. Os resultados obtidos apresentaram uma redução significativa no erro médio e máximo das correlações em relação aos dados originais.

Palavras-chave: destilação; otimização; projeto; estimação de parâmetros; *Set Trimming*.

ABSTRACT

SOUZA, Aline Rayboltt da Cruz. *Optimal design of sieve trays in distillation columns.* 2022. 164 f. Tese (Doutorado em Engenharia Química) – Instituto de Química, Universidade do Estado do Rio de Janeiro, Rio de Janeiro, 2022.

The traditional approach to distillation column design is the heuristic procedure, based on the trial-and-error method. In recent decades, the literature presents several works on the optimization of distillation columns, mostly integrated with a commercial simulator. However, these works are only concerned with the sizing of the diameter and height of the column, which are part of the total cost of the column; the other important variables for the functionality of the column are not measured. In this context, this work presents the optimization of the optimal design of distillation column trays using two different techniques: mixed integer nonlinear programming and Set Trimming. In addition, it is proposed to refine the parameters of the flooding and entrainment correlations in the literature in order to improve the accuracy of the design formulation. The objective of this optimization is to size all the geometric variables of the tray while respecting its hydraulic constraints (flooding, entrainment, weeping, and downcomer backup). Two possible objective functions are tested, the column cost minimization and the column mass minimization. The proposed approach is applied to an example from the literature, the optimal result obtained by mathematical programming and Set Trimming are compared with the result obtained by the heuristic procedure (taken from the literature and described in the text), and the different techniques are compared with each other. Mathematical programming was used to estimate the parameters of the correlations. The new parameters are applied to three example column designs from the literature and compared with preexisting correlations. The results obtained showed a significant reduction in the mean and maximum error of the correlations compared to the original data.

Keywords: distillation; optimization; design; parameter estimation; Set Trimming.

LISTA DE FIGURAS

LISTA DE TABELAS

LISTA DE SÍMBOLOS

Ac	Total column area (m²)
Adc	Downcomer area (m²)
An	Vapor flow area (m²)
Aa	Active area (m²)
Ah	Total area of all the active holes (m²)
$\widehat{wcz}_{in}$	Width of inlet calming zone (m)
$\widehat{wcz}_{out}$	Width of outlet calming zone (m)
wus	Width of the unperforated strip (m)
lt	Tray spacing (m)
hw	Weir height (m)
how	Height of the liquid crest over the weir (m)
hap	Height of the clearance under the downcomer (m)
$hdwap$	Difference between weir and clearance height under the downcomer (m)
hb	Height of the downcomer backup (m)
sNt	Set of column trays
$\widehat{Lw}$	Liquid mass flow rate (kg/s)
$\widehat{Vw}$	Vapor mass flow rate (kg/s)
$\widehat{\rho l}$	Specific mass of liquid (kg/m³)
$\widehat{\rho v}$	Specific mass of vapor (kg/m³)
$\hat{\sigma}$	Sufarce tension (N/m)
$\widehat{Flv}$	Liquid-vapor flow factor (dimensionless)
$\widehat{hr}$	Residual head loss (m)
Dc	Column diameter (m)
dh	Hole diameter (m)
lw	Weir length (m)
lp	Hole pitch (m)
tt	Tray thickness (m)
lay	Hole layout
sDc	Set of column diameter
$\widehat{pDc}$	Available values of the column diameter (m)

yDc	Binary variable of the column diameter
sdh	Set of hole diameter
$\widehat{pdh}$	Available values of the hole diameter (m)
ydh	Binary variable of the hole diameter
shdwap	Set of difference between weir and clearance height under the downcomer
$\widehat{phdwap}$	Available values of the difference between weir and clearance height
yhdwap	Binary variable of the difference between weir and clearance height under the downcomer
shw	Set of weir height
$\widehat{phw}$	Available values of the weir height (m)
yhw	Binary variable of the weir height (m)
slt	Set of tray spacing
$\widehat{plt}$	Available values of the tray spacing (m)
ylt	Binary variable of the tray spacing
slw	Set of weir length
$\widehat{plw}$	Available values of the weir length (m) under the downcomer (m)
ylw	Binary variable of the weir length
slp	Set of hole pitch
$\widehat{plp}$	Available values of the hole pitch (m)
ylp	Binary variable of the hole pitch
stt	Set of tray thickness
$\widehat{ptt}$	Available values of the tray thickness (m)
ytt	Binary variable of the tray thickness
slay	Set of the hole layout
$\widehat{play}$	Available values of the hole layout
ylay	Binary variable of the hole layout
Asector	Circular sector area (m^2)
Atriangle	Triangle area (m^2)
θ	Weir angle (rad)
δ	Ratio between the weir length and the column diameter (dimensionless)
Acz	Calming zone area (m^2)
lcz_{in}	Length of the inlet calming zone (m)
lcz_{out}	Length of the outlet calming zone (m)

β	calming zone angle (rad)
Aus	Unperforated strip area (m²)
α	active area angle (rad)
ywus	Binary variable of the width of the unperforated strip
swus	Set of the width of unperforated strip
$\hat{\varepsilon}$	Small positive valor equal to 10^{-6}
k	parameters (dimensionless)
φ	Ratio between the hole diameter and the hole pitch (dimensionless)
un	Vapor flow velocity (m/s)
uflood	Flooding velocity (m/s)
Csb	Sounders-Brown coefficient (m/s)
K1	Parameter of the Fair's flooding correlation (dimensionless)
yK1	Binary variable of the K1 parameter
sK1	Set of the K1 constant
ψ	Fractional entrainment (kg/kg gross liquid flow)
Fflood	Factor of flooding (dimensionless)
uh	Flow velocity throughout the tray holes (m/s)
uhmin	Minimum vapor flow velocity (m/s)
K2	Parameter of the weeping correlation (dimensionless)
ht	Total tray head loss (m)
hdc	Head loss in the downcomer (m)
hd	Dry tray head loss (m)
Co	Orifice coefficient
ω	Ratio between the tray thickness and the hole diameter (dimensionless)
Aap	Clearance area under the downcomer (m²)
time	Residence time (s)
min	lower bound
max	upper bound
Wshell	Mass of the column shell (kg)
twall	Column wall thickness (m)
Ctotal	Total column cost ($)
$\widehat{Nt}$	Number of trays
$\widehat{\rho shell}$	Specific mass of shell material (kg/m³)

Hc	Height of column between tangent lines (m)
$\widehat{Ptwall}$	Available values of the wall thickness (m)
$Wtotal$	Mass of the distillation column (kg)
Wt	Mass of the trays (kg)
$Wcolumn$	Mass of the column shell and internals (kg)
$\widehat{Cw}$	Factor of cost equation (dimensionless)
Dm	Mean diameter of column (m)
Vt	Volume of the tray deck (m³)
$Vwdc$	Volume of the combination weir/downcomer (m³)
$\widehat{\rho t}$	Specific mass of tray material (kg/m³)
Hdc	Height of downcomer (m)
$FAdc$	Factor of downcomer area (%)
$\widehat{\rho w}$	Specific mass of carbon steel (kg/m³)
Be	Bernoulli number
ΔP	Pressure drop (N/m²)
$\hat{g}$	Gravity acceleration (m^2/s)
$\hat{A}_{i,j}$	Parameters (dimensionless)
$\hat{B}_j$	Parameters (dimensionless)
ρl	Specific mass of liquid (kg/m³)
ρv	Specific mass of vapor (kg/m³)
σ	Surface tension (N/m)
K	Constant of Fair flooding correlation (dimensionless)
Flv	Liquid-vapor flow factor (dimensionless)
L	Liquid mass flow rate (kg/s)
V	Vapor mass flow rate (kg/s)
$\theta_{Csb,k}$	Flooding correlation parameters (dimensionless)
$\theta_{\psi,k}$	Entrainment correlation parameters (dimensionless)
$Fobj$	Objective function (dimensionless)
$\boldsymbol{x}_i$	Vector of the independent variable values at the data point i (dimensionless)
y_i^{graph}	Data obtained from the Fair's graph (dimensionless)
y_i^{model}	Data obtained from the model (dimensionless)
$\sigma_{y,i}^2$	Variance of the data points (dimensionless)

TABLE OF CONTENTS

INTRODUCTION

Distillation columns are of great important in the chemical industry, being the main equipment for purification and separation. The traditional method of design distillation column trays consists of a trial and error procedure, where the designer selects certain characteristics of the tray and checks whether the tray is feasible for its hydraulic constraints, this is done sequentially until he finds the tray that respects these constraints. However, the speed of such a process depends on the experience of the professional.

Due to the wide use of distillation columns, the capital invested in this equipment is of great importance, becoming a crucial point in the search for cost reduction in industrial plants. The traditional method is not flawed, it is possible to obtain a feasible column, but there is no way to guarantee that the solution found will be the one with the lowest cost.

Nowadays, with the development of more powerful computational tools and algorithms, optimization works for the design of distillation columns have emerged. The main focus of these works has been to optimize the column diameter, the number of trays, and the reflux ratio, seeking to minimize the total annualized cost. However, few works seek to optimize a set of tray dimensions.

In this context, this thesis aims to present the optimization of the design of distillation column trays, focusing on sizing all geometric variables in order to respect the hydraulic constraints (flooding, entrainment, dripping, and downcomer backup) and minimize the cost/mass of the column. The solution to this problem is explored using different optimization techniques in order to find the one associated with the lowest computational effort with a guarantee of the global optimum.

This thesis is organized in the form of articles. Then, Chapter 1 represents the first article and presents the mathematical formulation of the problem of Mixed Integer Nonlinear Programing (MINLP) to the design of distillation column trays using commercial global solvers; Chapter 2 represents the second article and presents the design of distillation column trays by applying the Set Trimming technique.

In the search for better correlations of flooding and entrainment that best fit Fair's curves to use in formulations, it was observed that the correlations in the literature have some large errors in certain regions, which can generate a suboptimal design. Therefore, a third article was done seeking to refine the parameters of the literature correlations and improve the fit to the original data. This article is presented in Chapter 3. Finally, the conclusions and suggestions are presented.

1 GLOBALLY OPTIMAL DISTILLATION TRAY DESIGN USING A MATHEMATICAL PROGRAMMING APPROACH

This article presents the optimization of the design of distillation column trays. We develop a mixed-integer nonlinear optimization model, which we solve using mathematical programming. The objective of this formulation is to size all geometric variables of the tray. Two possible alternative objective functions are tested: column cost and column mass. The utilization of the proposed approach is illustrated through a design example from the literature. In this example, the optimal result obtained through the proposed approach is compared with the one obtained following the spirit of a traditional heuristic design procedure employed in process equipment design textbooks. The comparison indicates a reduction of both objective functions tested as compared to the result of the heuristic procedure.

1.1 Introduction

In the United States, it is estimated that there are more than 40,000 distillation columns in operation, accounting for 90 % of the separation and purification processes. It is estimated that the capital invested in these systems is around US$ 8 billion (Humphrey, 1995). Because the costs associated with this equipment are high, a considerable number of papers have addressed the optimal design of distillation columns. The main focus of these procedures is to optimize the column diameter, the number of trays, and the reflux ratio to minimize the total annualized cost.

Several different mathematical programming approaches were used to address this design problem: nonlinear programming (NLP) (Dowling; Biegler, 2015; Yeoh; Hui, 2021), mixed-integer nonlinear programming (MINLP) (Viswanathan; Grossmann, 1993; Kong; Maravelias, 2019), and generalized disjunctive programming (GDP) (Yeomans; Grossmann, 2000). Additionally, a combination of mathematical programming and commercial simulators was proposed by Caballero *et al.* (2005) and Caballero (2015).

Aiming at avoiding convergence drawbacks and local optimality problems associated with mathematical programming, some authors proposed the utilization of stochastic optimization methods for the solution of the aforementioned optimal design problem.

Different techniques were tested, such as, particle swarm optimization (PSO) (Javaloyes-Antón; Ruiz-Femenia; Caballero, 2013), genetic algorithms (GA) (Ibrahim; Jobson; Guillén-Gosálbez, 2017) and differential evolution (DE) associated with parallel computing (Lyu *et al.*, 2021).

In all the aforementioned approaches, the dimensions of the column internals, namely, tray spacing, weir length, weir height, etc., have been not included. The traditional approach for the design of distillation column trays is based on trial and verification schemes, as depicted in several textbooks: Fair (1963), Wankat (1988), Kister (1992), Chuang and Nandakumar (2000), and Towler and Sinnott (2013). These schemes are considered reliable, but they depend on the designer's experience to attain a feasible choice of the tray geometric dimensions, with no guarantee that the solution found will feature the lowest cost. We know of only two works that employ optimization techniques for identifying the optimal set of tray dimensions: Ogboja and Kuye (1990) and Lahiri (2014, 2020). Ogboja and Kuye (1990) developed a sieve tray optimization formulation, solved using the Complex method (Box, 1965). The objective function was represented for the tray efficiency and the constraints are related to geometrical and phenomenological features. The decision variables was column diameter, spacing trays, tray thickness, weir length and height, hole diameter, and clearance height under the downcomer. As a way of validating the method, they used an exhaustive method that analyzes all sets of variables and determines their efficiency. Lahiri (2014, 2020) employed the PSO method together with the Aspen Plus simulator for the optimization of the distillation column including the specifications of the column tray. Lahiri (2014, 2020) considered complex tray configurations, such as multiple passes, sieve and valved trays, and segmental downcomer. The objective function to be minimized is the total annualized cost, considering the column capital costs and the costs associated with utility consumption.

In this article, we address the design of distillation column trays including the column diameter and all the geometric variables. We formulate the problem as a mixed-integer nonlinear model and we solve it using commercial global solvers (BARON and ANTIGONE). Previous approaches that addressed the tray design optimization employed local optimization methods (Ogboja; Kuye, 1990) or stochastic methods, which can escape to a local optima, i.e. global optimality cannot be guaranteed (Lahiri, 2014, 2020). Additionally, the aforementioned works consider continuous variables, whereas the optimization method proposed in this work is based on discrete design variables. Indeed, the utilization of continuous variables to later use of commercial/standard geometric discrete values demands rounding procedures that can imply suboptimal or even infeasible solutions.

The article is organized as follows. Section 1.2 presents the tray operating limits that define the design constraints. Section 1.3 presents the dimensions of the sieve trays that are employed as optimization variables in the design problem. Sections 1.4 and 1.5 present the constraints and the objective functions of the Mixed Integer Nonlinear Model (MINLM), respectively. Section 1.6 presents the heuristic design procedure employed in the comparison of the results. Section 1.7 illustrates the performance of the proposed formulation and compares it with the heuristic procedure. The conclusions are finally presented in Section 1.8.

1.2 Tray operating range limits

In a given distillation column, the liquid and vapor flows must be between within certain limits. Different authors characterize the phenomena associated with the operating limits of a tray in a different manner, often using different nomenclatures. In this work, we will use the terminology adopted by Kister (1992). The operational limits that must be obeyed by the designer are flooding, entrainment, downcomer flooding, and weeping, as illustrated in Figure 1. These operational limits origin the mathematical relations that compose the constraints of the optimization problem.

Figure 1 – Tray performance diagram

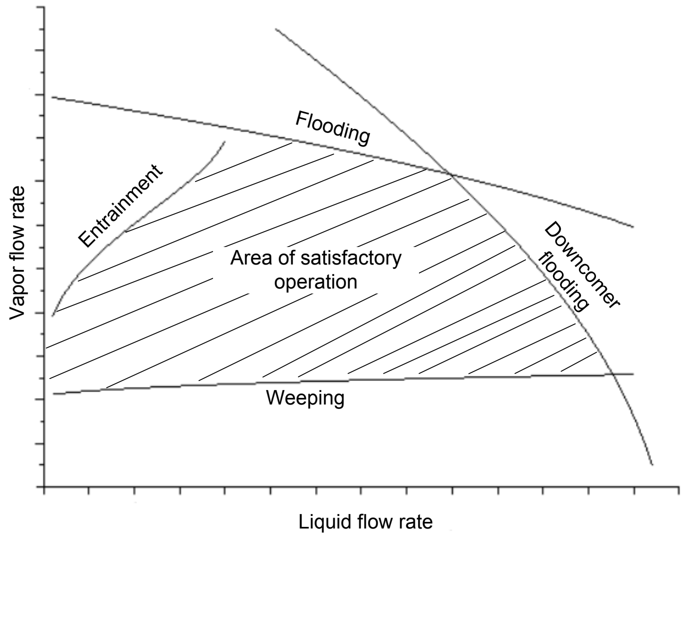

Source: The author, 2022.

1.3 Sieve tray layout

Sieve trays feature different types of configurations for downcomer (segmental, circular, etc.), weir (straight, picket fence, etc.), and the number of passes (one or multiple passes, the latter option mostly employed for large diameters). Figure 2 depicts the simplest configuration, which is the one we use in this work. The total column area (Ac) is Figure 2a. The downcomer area (Adc) is equivalent to the area of the inlet downcomer of the liquid flow from the tray above or the area of the outlet downcomer of the liquid flow to the tray below (Figure 2b). The vapor flow area (An) corresponds to the difference between the cross-sectional area of the column and the downcomer area (Figure 2c). The active area (Aa) is the tray area where liquid and vapor get in contact (Figure 2d). The hole area (Ah) is the total area of the perforations on the tray (Figure 2e).

Figure 2 – Area definition

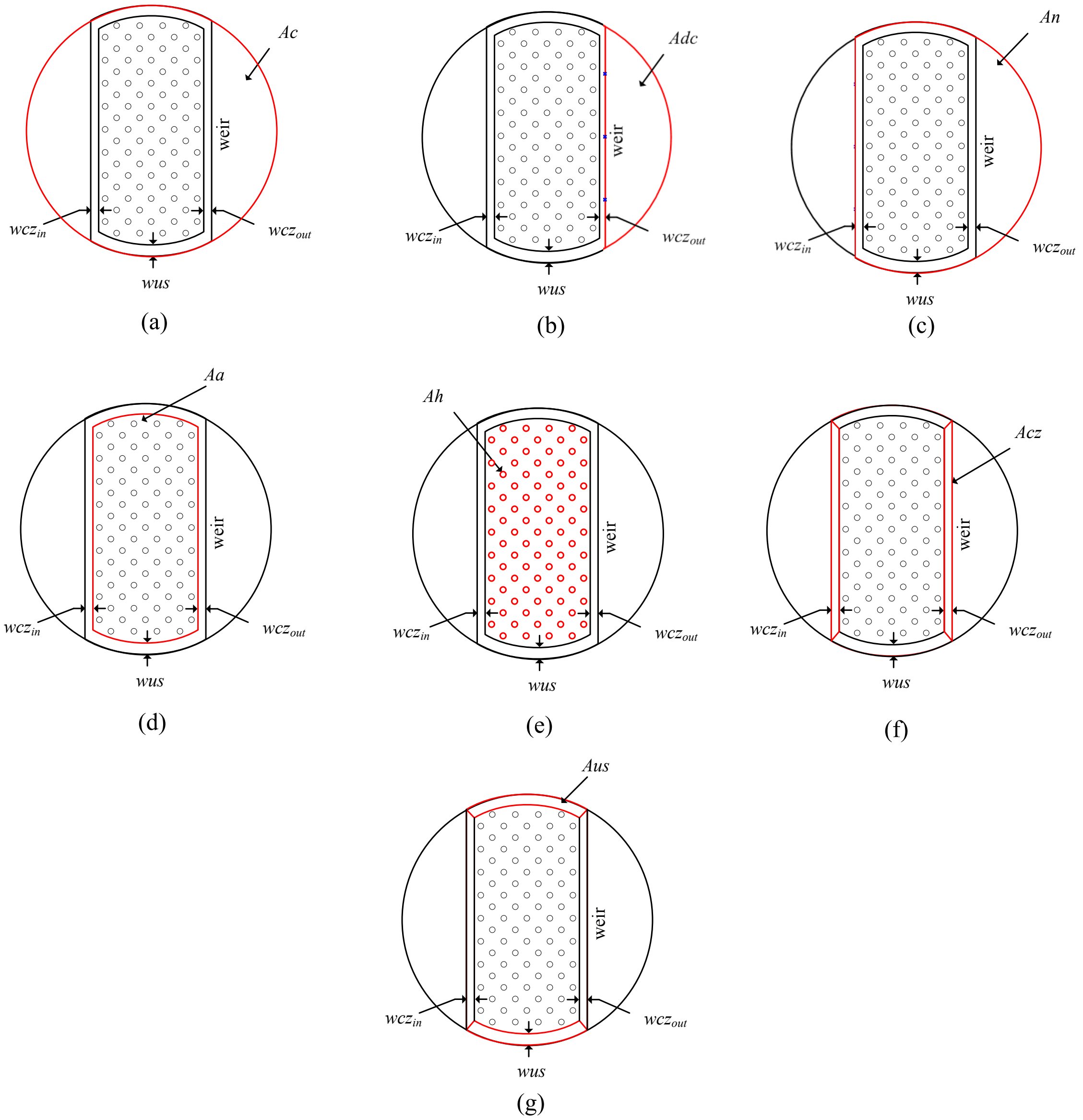

Subtitle: (a) Total column area, (b) downcomer area, (c) vapor flow area, (d) active area, (e) hole area, (f) calming zone area, (g) unperforated strip area.

Source: The author, 2022.

Surrounding the active area, there are strips without holes. The almost rectangular strips, close to the downcomer slit and close to the weir, are referred to as “calming zones”. The calming zone region (Figure 2f). close to the downcomer, with width wcz_{in}, aims to reduce the vorticity of the flow from the downcomer connected to the tray above. In turn, the calming zone region close to the weir, characterized by the width wcz_{out}, aims to reduce instabilities of the flow close to the weir, thus reducing the turbulence associated to vapor bubbling through the liquid and allowing complete vapor-liquid separation so that bubbles are not carried towards the downcomer (Wankat, 1988). The circular gap with width *wus* between the column shell and the active area is called "unperforated strip" (Figure 2g). This gap is used for the support ring and does not have an explicitly hydraulic role (Towler; Sinnott, 2013).

Figure 3 depicts a side view of the tray, showing the tray spacing (*lt*), the weir height (*hw*), the height of the liquid crest over the weir (*how*), the clearance height under the downcomer (*hap*), the difference between weir and clearance height under the downcomer (*hdwap*), and the downcomer backup height (*hb*).

Figure 3 – Tray side view

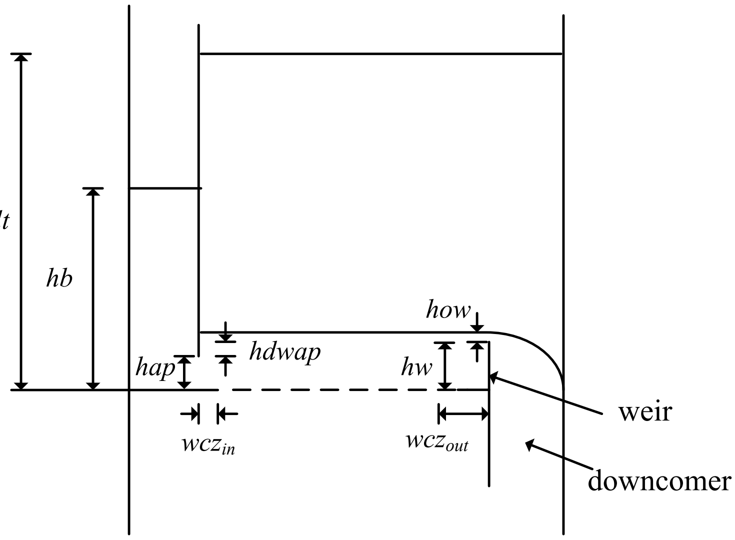

Source: The author, 2022.

1.4 Tray design constraints

The optimization is focused on the design of the trays of a distillation column. It is assumed that the flow rates of the liquid and vapor and the corresponding physical properties were already previously calculated for each tray. These data are obtained from the distillation design, through a traditional approach based on heuristics or any of the optimization procedures available in the literature (see Section 1.1). Therefore, the model parameters associated with each tray *sNt*, represented here with a symbol "^" on top, are: the liquid mass flow rate ($\widehat{Lw}_{sNt}$), the vapor mass flow rate ($\widehat{Vw}_{sNt}$), the density of the liquid ($\widehat{\rho l}_{sNt}$), the density of the vapor ($\widehat{\rho v}_{sNt}$), and the surface tension of the liquid ($\hat{\sigma}_{sNt}$).

Some additional parameters are calculated based on the values of the parameters listed above, as the liquid-vapor flow factor ($\widehat{Flv}_{sNt}$) used in the Fair correlation (Fair, 1961):

$$\widehat{Flv}_{sNt} = \frac{\widehat{Lw}_{sNt}}{\widehat{Vw}_{sNt}}\sqrt{\frac{\widehat{\rho v}_{sNt}}{\widehat{\rho l}_{sNt}}} \qquad \forall\ sNt \tag{1}$$

and the residual pressure drop in the column tray ($\widehat{hr}_{sNt}$), as proposed by Hunt et al. (1955):

$$\widehat{hr}_{sNt} = \frac{12.5}{\widehat{\rho l}_{sNt}} \qquad \forall\ sNt \tag{2}$$

Other specific parameters associated with the objective function are presented later.

1.4.1 Discrete representation of geometric variables

All the dimensions of the tray are represented by a set of discrete values. This representation is associated with the physical nature of some variables (e.g. hole layout: triangular or square); availability of commercial standards (e.g. tray thickness); or constructional patterns (e.g. manufacturing of mechanical pieces in inches or fractions of an inch).

The discrete representation of the design variables uses binary variables. Let *x* be a design variable that is associated with a set of possible values $\widehat{px}_i$. The selection of the discrete values $\widehat{px}_i$ is represented by the binary variables yx_i. Therefore, the variable *x* is related to the corresponding set of binary variables by:

$$x = \sum_i \widehat{px}_i yx_i \tag{3}$$

$$\sum_i yx_i = 1 \tag{4}$$

This representation is applied to the following set of variables associated with the tray design: column diameter (*Dc*), hole diameter (*dh*), the difference between weir and clearance height under the downcomer (*hdwap*), weir height (*hw*), tray spacing (*lt*), weir length (*lw*), hole pitch (*lp*), tray thickness (*tt*), and hole layout (*lay*):

$$Dc = \sum_{sDc=1}^{sDcmax} \widehat{pDc}_{sDc}\, yDc_{sDc} \tag{5}$$

$$dh = \sum_{sdh=1}^{sdhmax} \widehat{pdh}_{sdh}\, ydh_{sdh} \tag{6}$$

$$hdwap = \sum_{shdwap=1}^{shdwapmax} \widehat{phdwap}_{shdwap}\, yhdwap_{shdwap} \tag{7}$$

$$hw = \sum_{shw=1}^{shwmax} \widehat{phw}_{shw}\, yhw_{shw} \tag{8}$$

$$lt = \sum_{slt=1}^{sltmax} \widehat{plt}_{slt}\, ylt_{slt} \tag{9}$$

$$lw = \sum_{slw=1}^{slwmax} \widehat{plw}_{slw}\, ylw_{slw} \tag{10}$$

$$lp = \sum_{slp=1}^{slpmax} \widehat{plp}_{slp}\ ylp_{slp} \tag{11}$$

$$tt = \sum_{stt=1}^{sttmax} \widehat{ptt}_{stt}\ ytt_{stt} \tag{12}$$

$$lay = \sum_{slay=1}^{slaymax} \widehat{play}_{slay}\ ylay_{slay} \tag{13}$$

$$\sum_{sDc=1}^{sDcmax} yDc_{sDc} = 1 \tag{14}$$

$$\sum_{sdh=1}^{sdhmax} ydh_{sdh} = 1 \tag{15}$$

$$\sum_{shdwap=1}^{shdwapmax} yhdwap_{shdwap} = 1 \tag{16}$$

$$\sum_{shw=1}^{shwmax} yhw_{shw} = 1 \tag{17}$$

$$\sum_{slt=1}^{sltmax} ylt_{slt} = 1 \tag{18}$$

$$\sum_{slw=1}^{slwmax} ylw_{slw} = 1 \tag{19}$$

$$\sum_{slp=1}^{slpmax} ylp_{slt} = 1 \tag{20}$$

$$\sum_{stt=1}^{sttmax} ytt_{stt} = 1 \tag{21}$$

$$\sum_{slay=1}^{slaymax} ylay_{slay} = 1 \tag{22}$$

1.4.2 Tray dimensions

The geometric equations are based on the sieve tray description presented in Towler and Sinnott (2013). The downcomer area is obtained by the difference between the circular sector area (*Asector*) and the triangle area (*Atriangle*), as illustrated in Figure 4.

Figure 4 – Graphical representation of the downcomer area evaluation

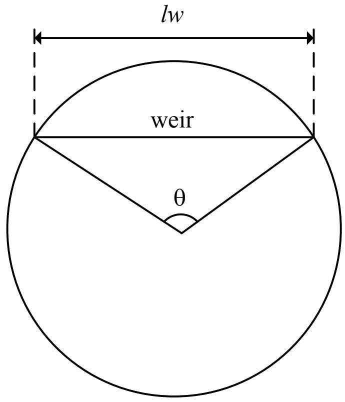

Source: The author, 2022.

Let θ be the weir angle, i.e. the central angle associated with the column circumference and the chord referring to weir length. Thus:

$$\theta - 2\arcsin(\delta) = 0 \qquad (23)$$

where δ is the ratio between the weir length and the column diameter:

$$\delta\, Dc - lw = 0 \qquad (24)$$

The area of the sector defined by the weir angle is:

$$Asector - \frac{Dc^2\theta}{8} = 0 \qquad (25)$$

The area of the isosceles triangle is defined by the weir angle and the weir length as follows:

$$Atriangle - \frac{lw}{2}\sqrt{\left(\frac{Dc}{2}\right)^2 - \left(\frac{lw}{2}\right)^2} = 0 \qquad (26)$$

Therefore, the total column area, the downcomer area, and the vapor flow area are given by:

$$Ac - \frac{\pi Dc^2}{4} = 0 \qquad (27)$$

$$Adc - Asector + Atriangle = 0 \qquad (28)$$

$$An - Ac + Adc = 0 \qquad (29)$$

The calming zone area (*Acz*) is approximated by the area of two trapezoids, as illustrated in Figure 5, and is given by:

$$Acz - \frac{(lcz_{in} + lw)}{2}\widehat{wcz}_{in} - \frac{(lcz_{out} + lw)}{2}\widehat{wcz}_{out} = 0 \qquad (30)$$

where lcz_{in} and lcz_{out} are the lengths of the inlet and outlet calming zones. These lengths are related to other variables by:

$$lcz_{in} - lw + 2(wcz\beta_{in}) = 0 \qquad (31)$$

$$lcz_{out} - lw + 2(wcz\beta_{out}) = 0 \qquad (32)$$

where:

$$wcz\beta_{in}\tan(\beta) - \widehat{wcz}_{in} = 0 \qquad (33)$$

$$wcz\beta_{out}\tan(\beta) - \widehat{wcz}_{out} = 0 \qquad (34)$$

The angle β is the calming zone angle:

$$2\beta - \pi + \theta = 0 \qquad (35)$$

Figure 5– Calming zones and unperforated strip areas

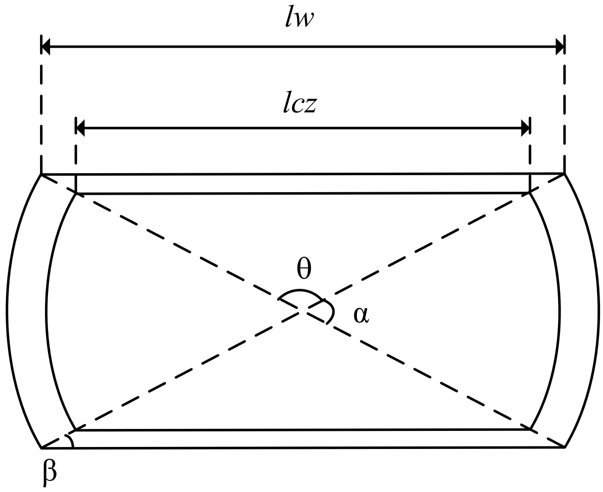

Source: The author, 2022.

Several references suggest a value for the width of the calming zone between 2 and 5 in, without differing inlet and outlet values (Wankat, 1988; Dutta, 2007; Towler; Sinnott, 2013; AMACS Process Tower Internals, 2020). Then, we consider the width of the inlet and outlet calming zones ($\widehat{wcz}_{in}$ and $\widehat{wcz}_{out}$) equal to 0.050 m (2 in) in the proposed formulation.

The unperforated strip area (*Aus*) is determined using the angle of active area (α) and the width of the unperforated strip (Towler; Sinnott, 2013):

$$Aus - wus\ \alpha(Dc - wus) = 0 \tag{36}$$

$$\alpha - \pi + \theta = 0 \tag{37}$$

The width of the unperforated strip varies according to the column diameter (AMACS Process Tower Internals, 2020), as follows:

$$wus = \begin{cases} 0.0381, & Dc \leq 0.7620 \\ 0.0508, & 0.7620 < Dc \leq 1.6764 \\ 0.0635, & 1.6764 < Dc \leq 3.8100 \\ 0.0762, & 3.8100 < Dc \leq 5.9436 \\ 0.0889, & 5.9436 < Dc \leq 7.4676 \\ 0.1143, & Dc > 7.4676 \end{cases} \tag{38}$$

The reorganization of Eq. (38) into a set of inequalities using a set of auxiliary binary variables yields:

$$wus - 0.0381\ ywus_1 - 0.0508\ ywus_2 - 0.0635\ ywus_3 - 0.0762\ ywus_4 - 0.0889\ ywus_5 - 0.1143\ ywus_6 = 0 \tag{39}$$

$$Dc - 0.7620\ ywus_1 - 1.6764\ ywus_2 - 3.8100\ ywus_3 - 5.9436\ ywus_4 - 7.4676\ ywus_5 \leq 0 \tag{40}$$

$$Dc - 0.7620\, ywus_2 - 1.6764\, ywus_3 - 3.8100\, ywus_4 - 5.9436\, ywus_5 - 7.4676\, ywus_6 - \hat{\varepsilon} \geq 0 \quad (41)$$

$$\sum_{swus=1}^{6} ywus_{swus} = 1 \quad (42)$$

where $\hat{\varepsilon} = 10^{-6}$.

The active area corresponds to the cross-sectional area of the column minus the areas of the downcomers, unperforated strip, and calming zone.

$$Aa - Ac + 2\, Adc + Aus + Acz = 0 \quad (43)$$

The total area of all the active holes is a fraction of the active area, which depends on the hole layout:

$$Ah - k\varphi^2 Aa = 0 \quad (44)$$

where:

$$\varphi\, lp - dh = 0 \quad (45)$$

$$k - 0.785 ylay_1 - 0.905 ylay_2 = 0 \quad (46)$$

where $ylay_1$ and $ylay_2$ are associated with the square and triangular layouts, respectively.

1.4.3 Geometric Constraints

The weir length must be smaller than the column diameter:

$$lw \leq Dc \quad (47)$$

The hole pitch must be higher than twice the hole diameter (Towler; Sinnott, 2013):

$$lp \geq 2dh \quad (48)$$

Assuming that the tray holes are punched, the tray thickness cannot be higher than the hole diameter (Chuang; Nandakumar, 2000):

$$dh \geq tt \quad (49)$$

The range of the ratio between the hole area and the active area must be:

$$0.06Aa \leq Ah \leq 0.16Aa \quad (50)$$

The lower bound on Eq. (50) is necessary to use the Fair flooding correlation (Fair, 1961) and the upper bound avoids conditions where significant weeping and entrainment may coexist and the design equations may not apply (Chuang; Nandakumar, 2000).

Finally, to use the Fair flooding correlation, the following bound must be applied (Fair, 1961):

$$hw \leq 0.15\ lt \tag{51}$$

1.4.4 Operational constraints

These constraints consist of equations representing the limits of flooding, entrainment, weeping, downcomer backup, and residence time in the downcomer.

1.4.4.1 Flooding

To avoid flooding, an upper bound on the vapor flow velocity is used:

$$un_{sNt} - 0.85\ uflood_{sNt} \leq 0 \qquad \forall\ sNt \tag{52}$$

where *un* is the vapor flow velocity and *uflood* is the flooding velocity, both based on the vapor flow area.

The vapor flow velocity can be evaluated as follows:

$$un_{sNt} An - \frac{\widehat{Vw}_{sNt}}{\widehat{\rho v}_{sNt}} = 0 \qquad \forall\ sNt \tag{53}$$

The determination of the flooding condition is given by Fair (1961):

$$uflood_{sNt} - K1\ Csb_{sNt} \sqrt{\frac{\widehat{\rho l}_{sNt} - \widehat{\rho v}_{sNt}}{\widehat{\rho v}_{sNt}}} \left(\frac{\hat{\sigma}_{sNt}}{0.02}\right)^{0.2} = 0 \qquad \forall\ sNt \tag{54}$$

where *Csb* is the Sounders-Brown coefficient.

In turn, the parameter *K1* varies with the fraction of the hole area:

$$K1 = \begin{cases} 0.8, & 0.06 \leq k\varphi^2 \leq 0.08 \\ 0.9, & 0.08 \leq k\varphi^2 \leq 0.10 \\ 1.0, & 0.10 \leq k\varphi^2 \leq 0.16 \end{cases} \tag{55}$$

The parameter *K1* had to be rearranged into inequalities using binary variables to represent the different options in purely algebraic form:

$$K1 - 0.8\ yK1_1 - 0.9\ yK1_2 - 1.0\ yK1_3 = 0 \tag{56}$$

$$k\varphi^2 - 0.08yK1_1 - 0.10yK1_2 - 0.16yK1_3 \leq 0 \tag{57}$$

$$k\varphi^2 - 0.06yK1_1 - 0.08yK1_2 - 0.10yK1_3 \geq 0 \tag{58}$$

$$\textstyle\sum_{sK1=1}^{3} yK1_{sK1} = 1 \tag{59}$$

Several authors have presented curve fitting of the Fair's correlation (Economopoulos, 1978; Lygeros; Magoulas, 1986; Ogboja; Kuye, 1990). The expression we use is the proposed by Ogboja and Kuye (1990):

$$Csb_{sNt} - 0.0129 - 0.1674\, lt - 0.0063\widehat{Flv}_{sNt} + 0.2686\, lt\, \widehat{Flv}_{sNt} + 0.008\widehat{Flv}_{sNt}{}^{2} - 0.01448 lt\, \widehat{Flv}_{sNt}{}^{2} = 0 \qquad \forall\, sNt \tag{60}$$

1.4.4.2 Entrainment

The constraint to avoid entrainment is represented by an upper bound on the fractional entrainment variable (ψ_{sNt}):

$$\psi_{sNt} - 0.1 \leq 0 \qquad \forall\, sNt \tag{61}$$

The fractional entrainment can be estimated by the correlations proposed by Economopoulos (1978) or Ogboja and Kuye (1990). We choose to use the correlation of Ogboja and Kuye (1990):

$$\psi_{sNt} - \left\{ exp \left[\begin{array}{c} -7.9196 + 1.0891 Fflood_{sNt} \\ -(0.0705 + 2.1916 Fflood_{sNt}) \ln \widehat{Flv}_{sNt} \\ +(0.046 - 0.605 Fflood_{sNt} + 1.2669 Fflood_{sNt}{}^{2} \\ -0.9563 Fflood_{sNt}{}^{3})\left(\ln \widehat{Flv}_{sNt}\right)^{2} \end{array} \right] \right\} = 0 \qquad \forall\, sNt \tag{62}$$

where *Fflood* is the factor of flooding:

$$Fflood_{sNt}\; uflood_{sNt} - un_{sNt} = 0 \qquad \forall\, sNt \tag{63}$$

1.4.4.3 Weeping

The constraint to assure that the tray design will not be subjected to weeping is represented by a lower bound on the flow velocity throughout the tray holes:

$$uh_{sNt} - uhmin_{sNt} \geq 0 \qquad \forall\, sNt \tag{64}$$

where *uh* is the vapor flow velocity throughout the tray holes and it can be calculated by:

$$uh_{sNt} Ah - \frac{\widehat{Vw}_{sNt}}{\widehat{\rho v}_{sNt}} = 0 \qquad \forall\, sNt \tag{65}$$

and the weeping point associated with the minimum vapor flow velocity (*uhmin*) can be determined by the following correlation (Eduljee, 1959):

$$uhmin_{sNt} - \frac{K2_{sNt} - 0.9(25.4 - 10^3 dh)}{(\widehat{\rho v}_{sNt})^{\frac{1}{2}}} = 0 \qquad \forall\, sNt \tag{66}$$

where $K2$ is evaluated by the correlation proposed by Ogboja and Kuye (1990):

$$K2_{sNt} - 23.48 - 1.66 \ln[10^3(hw + how_{sNt})] = 0 \qquad \forall\, sNt \tag{67}$$

The height of the liquid crest over the weir (*how*) can be estimated using the Francis weir formula:

$$how_{sNt} - 750 \cdot 10^{-3} \left(\frac{\widehat{Lw}_{sNt}}{\widehat{\rho l}_{sNt}\, lw}\right)^{\frac{2}{3}} = 0 \quad \forall\, sNt \tag{68}$$

1.4.4.4 Downcomer backup

The constraint to avoid flooding in the downcomer must impose an upper bound on the downcomer backup height:

$$hb_{sNt} - \frac{1}{2}(lt + hw) \leq 0 \qquad \forall\, sNt \tag{69}$$

$$hb_{sNt} - hw - how_{sNt} - ht_{sNt} - hdc_{sNt} = 0 \qquad \forall\, sNt \tag{70}$$

where *ht* is total tray head loss and *hdc* is head loss in the downcomer.

The total tray head loss is the sum of the head of clear liquid on the tray (*hw*+*how*) and the dry tray drop (*hd*):

$$ht_{sNt} - hw - how_{sNt} - hd_{sNt} - \widehat{hr}_{sNt} = 0 \qquad \forall\, sNt \tag{71}$$

The dry tray head loss is given by:

$$hd_{sNt} Co^2 - 51 \cdot 10^{-3} uh_{sNt}{}^2 \frac{\widehat{\rho v}_{sNt}}{\widehat{\rho l}_{sNt}} = 0 \qquad \forall\, sNt \tag{72}$$

where *Co* is the orifice coefficient that can be estimated by the correlations proposed by Economopoulos (1978) or Ogboja and Kuye (1990). We choose to use the correlation of Ogboja and Kuye (1990):

$$Co - 0.6323 + 0.0255\omega - 0.1495\omega^2 - 0.777k\varphi^2 = 0 \tag{73}$$

where:

$$\omega\, dh = tt \tag{74}$$

Cicalese *et al*. (1947) estimated the head loss in the downcomer by:

$$hdc_{sNt}Aap - 166 \cdot 10^{-3}\left(\frac{\widehat{Lw}_{sNt}}{\widehat{\rho l}_{sNt}}\right) = 0 \qquad \forall\, sNt \tag{75}$$

where Aap is the clearance area under the downcomer that can be determined by:

$$Aap - hap\; lw = 0 \tag{76}$$

The height of the clearance under the downcomer (*hap*) is given by:

$$hap - hw + hdwap = 0 \tag{77}$$

1.4.4.5 Residence time

The downcomer residence time (*time*) must be enough for promoting vapor and liquid separation and preventing that the heavily aerated liquid be transported under the downcomer (Towler; Sinnott, 2013):

$$time_{sNt} - 3 \geq 0 \qquad \forall\, sNt \tag{78}$$

where:

$$time_{sNt} - Adc\; hb_{sNt}\frac{\widehat{\rho l}_{sNt}}{\widehat{Lw}_{sNt}} = 0 \qquad \forall\, sNt \tag{79}$$

1.4.5 Variable bounds

Bounds on the design variables (*Dc, dh, hdwap, hw, lt, lw, lp, tt,* and *lay*) are aggregated considering the available options associated with the tray manufacturing process, usual alternatives employed in practice and literature recommendations:

$$\widehat{Dc}_{min} \leq Dc \leq \widehat{Dc}_{max} \tag{80}$$

$$\widehat{dh}_{min} \leq dh \leq \widehat{dh}_{max} \tag{81}$$

$$\widehat{hdwap}_{min} \leq hdwap \leq \widehat{hdwap}_{max} \tag{82}$$

$$\widehat{hw}_{min} \leq hw \leq \widehat{hw}_{max} \tag{83}$$

$$\widehat{lt}_{min} \leq lt \leq \widehat{lt}_{max} \tag{84}$$

$$\widehat{lw}_{min} \leq lw \leq \widehat{lw}_{max} \tag{85}$$

$$\widehat{lp}_{min} \leq lp \leq \widehat{lp}_{max} \tag{86}$$

$\widehat{tt}_{min} \leq tt \leq \widehat{tt}_{max}$ (87)

$\widehat{lay}_{min} \leq lay \leq \widehat{lay}_{max}$ (88)

Bounds are also imposed to the variables *Wshell* and *twall* that appears in the objective function to represent the mass of the column shell and the column thickness (Towler; Sinnott, 2013):

$\widehat{Wshell}_{min} \leq Wshell \leq \widehat{Wshell}_{max}$ (89)

$\widehat{twall}_{min} \leq twall \leq \widehat{twall}_{max}$ (90)

Finally, bounds on the following variables are related to their physical nature:

$0.0381 \text{ m} \leq wus \leq 0.143 \text{ m}$ (91)

$0.8 \leq K1 \leq 1.0$ (92)

$0 \leq \beta \leq \frac{\pi}{2}$ (93)

1.5 Objective function

The optimization seeks to minimize the capital cost associated with the distillation column. An equation for evaluation of the capital cost of a distillation column, provided by Towler and Sinnott (2013), is employed as the objective function:

$\text{Min } Ctotal = (130 + 440Dc^{1.8})\widehat{Nt} + 11600 + 34\ Wshell^{0.85}$ (94)

where $\widehat{Nt}$ is the number of trays and *Wshell* is the mass of the column shell. This equation is valid for carbon steel columns with 0.5 m ≤ *Dc* ≤ 5.0 m and 160 kg ≤ *Wshell* ≤ 250,000 kg.

The mass of the column shell is given by:

$Wshell - \pi\ \widehat{\rho shell}\ Dc\ Hc\ twall = 0$ (95)

where $\widehat{\rho shell}$ is the density of the shell material and *Hc* is the height of the column between tangent lines i.e. without heads, given by:

$Hc - \widehat{Nt}\ lt = 0$ (96)

The column wall thickness depends on the column diameter:

$twall\ - \sum_{sDc=1}^{SDcmax} \widehat{Ptwall}_{sDc}\ yDc_{sDc} = 1$ (97)

where $\widehat{Ptwall}_{sDc}$ is the thickness value corresponding to the mechanical design associated with the column diameter related to the binary variable yDc_{sDc}.

Another alternative of the objective function consists in minimizing the mass of the distillation column (*Wtotal*), considering the mass of the column (*Wcolumn*) and trays (*Wt*).

$$\text{Min } Wtotal = Wcolumn + Wt\,\widehat{Nt} \tag{98}$$

The mass of the column is given by (Towler; Sinnott, 2013):

$$Wcolumn - \widehat{Cw}\,\pi\,\widehat{\rho shell}\,Dm\,(Hc + 0.8Dm)\,twall = 0 \tag{99}$$

where $\widehat{Cw}$ is a factor responsible for the mass of nozzles, manways, internal supports, etc, (assumed equal to 1.15), and *Dm* is the mean diameter of the column. The mean diameter is given by:

$$Dm - Dc - twall = 0 \tag{100}$$

The mass of the tray is determined by the volume of the tray deck (*Vt*) and the volume of the weir together with the downcomer (*Vwdc*).

$$Wt - (Vt + Vwdc)\widehat{\rho t} = 0 \tag{101}$$

where $\widehat{\rho t}$ is the specific mass of tray material.

The *Vwdc* is given by a rectangular plate:

$$Vwdc - \ (hw + tt + Hdc)tt\,lw = 0 \tag{102}$$

where *Hdc* is the height of the downcomer:

$$Hdc - lt + hap = 0 \tag{103}$$

The volume for each tray is given by the area of the column minus the areas of the downcomer and holes.

$$Vt - \ (Ac - Adc - Ah)tt = 0 \tag{104}$$

1.6 Heuristic design procedure

Aiming at comparing the performance of the proposed approach for the sizing of distillation columns with traditional schemes, a heuristic procedure based on Towler and Sinnott (2013) is presented in this section.

The original design discussion in Towler and Sinnott (2013) does not describe in detail all the steps of the procedure, deferring implicitly to the designer certain decisions. We seek to provide a design scheme that could be as systematic as possible, avoiding as much as possible from calls to vague changes. However, some decisions from a practitioner are still needed.

In the next paragraphs, we present an analysis based on the literature about the selection of certain dimensions of the sieve tray. The values presented here serve as initial guesses in the design procedure.

a) Tray spacing: Towler and Sinnott (2013) do not provide guidelines. Kister (1992) shows a range for tray spacing from 8 in until 36 in, but adopting 24 in, other authors (Fair, 1963; Wankat, 1988) agree with him. Therefore, we settle in adopting 24 in as a first choice.
b) Downcomer area: we use the direct recommendation given by Towler and Sinnott (2013), that is, 12 % of the total column area as the starting point.
c) Vapor velocity: The recommendation provided by Towler and Sinnott (2013) and Fair (1963) is to pick a vapor velocity equal to 85 % of the flooding velocity. Other values used are 80 % by Kister (1992) and Couper et al. (2012) and 75 % by Wankat (1988). We adopt the largest value of the literature.
d) Hole area: The hole area is initially estimated at 10 % of the active area by different authors (Wankat, 1988; Kister, 1992; Towler; Sinnott, 2013; Couper *et al.*, 2012). We use this choice as the initial guess.
e) Tray thickness: Towler and Sinnott (2013) do not recommend the use of any specific value, but they use 5 mm in their example. We choose 3.4 mm, which is the smallest thickness used in the literature (Kister, 1992; Chuang; Nandakumar, 2000).
f) Hole diameter: Towler and Sinnott (2013) offer the following limits: $0.0025\ \text{m} \leq dh \leq 0.012\ \text{m}$. They also state that the diameter is subject to a limit related to the tray thickness $(dh/tt \geq 1)$. Towler and Sinnott (2013) do not offer a criterion and in their example, they use 5 mm, pretty much in the middle of the range. For Kister (1992) the choice depends on the service, for clean services is 3/16 in, for fouling services is 1/2 in. Other authors also choose 3/16 in (Fair, 1963; Wankat, 1988; Kooijman; Taylor, 2006). Engel (2020) indicates that small holes are preferable due to hydraulic reasons, but penalize the fabrication costs. We adopt the valor shared by most of the literature 3/16 in (≈ 4.8 mm) and later change it if there is a need to do it.
g) Weir height: For Towler and Sinnott (2013) the choice depends on the operation, for columns operating above atmospheric pressure is $0.040\ \text{m} \leq hw \leq 0.090\ \text{m}$, for vacuum operation is $0.006\ \text{m} \leq hw \leq 0.012\ \text{m}$. It must be $hw < 0.15\ lt$. Other authors also choose 2 in (0.051 m) (Fair, 1963; Wankat,

1988; Kister, 1992; Kooijman; Taylor, 2006; Couper *et al.*, 2012; Towler; Sinnott, 2013). Larger heights have a significant effect on pressure drop, so from this point of view, smaller values should be preferred. We adopt the valor shared by most of the literature (2 in).

h) Difference between weir and clearance height under the downcomer: Towler and Sinnott (2013) consider the following values $0.005 \text{ m} \leq hdwap \leq 0.010 \text{ m}$. Kister (1990) explains that the largest value is to avoid an excessive increase in the pressure drop, which would cause a downcomer backup flooding. The smallest value is adopted to avoid that the vapor flows up the downcomer. Other authors specify certain valor (Fair, 1963; Kister, 1990; Kooijman; Taylor, 2006) for this variable as 10 mm. We decided to adopt this value.

Our procedure mimics the one suggested by Towler and Sinnott (2013) and complemented with our considerations and is the following:

Step 1: Data collection: Obtain flow rates and physical properties of the vapor and liquid streams of two representative trays, one from the rectifying section and another from the stripping section (one can extend this exercise to all trays in each section and then somehow find compromise solutions for each section, but we do not pursue this here, thus sticking to the classical recommendation).

Step 2: Perform preliminary specifications: Select values of tray spacing, downcomer area fraction of total area ($FAdc$), and flooding fraction to determine the column diameter (0.85).

Step 3: Determine the column diameter corresponding to both trays (rectifying and stripping section representatives) based on flooding considerations:

$$Dc = \left[\frac{4\widehat{Vw}}{\pi\, 0.85\, uflood\, \widehat{\rho v}(1-FAdc)}\right]^{0.5} \tag{105}$$

Because only one diameter is sought after (unless there are serious mismatches and the column needs more than one diameter), the largest of both diameters is picked.

The column diameter must be higher than 0.60 m to avoid difficulties of installation (Towler; Sinnott, 2013). If the value obtained is smaller than 0.60 m, then return to Step 2 and reduce the tray spacing or increase the downcomer area fraction. We offer the following rationale. If the diameter obtained violates the above inequality by a small amount, it is advisable to change the downcomer area criteria (increase 12 % by a small amount), to make the calculated diameter fit the inequality. If the diameter obtained is far away from the limit established by the inequality, that is, it is very small in comparison, then it is advisable to reduce the tray spacing.

Step 4: Finalize tray geometry specifications

a) Evaluate an initial estimative of the active area:

$$Aa = Ac - 2Adc \tag{106}$$

b) Hole area: use 10 % of the active area or other value if needed for respecting the constraint for the use of the Fair correlation $0.06 < Ah/Aa < 0.16$ (Fair, 1963).

c) Tray thickness: We use the smallest value (3.4 mm) as discussed above.

d) Hole diameter: We use the recommendations discussed above (4.8 mm). Because the thickness has already been set in the previous step, we choose a hole diameter that respects the limit established by the thickness ($dh/tt \geq 1$).

e) Weir height: We use 51 mm (2 in) as discussed above.

f) Difference between weir and clearance height under the downcomer: We use the largest value (10 mm) as discussed above.

g) Weir length: It is determined based on a graphical relation present in Towler and Sinnott (2013) ($lw < Dc$).

Step 5: Check the weeping safety factor (Eq. (64)); if unsatisfactory, return to Step 4, reducing the hole area.

Step 6: Check the downcomer backup safety factor (Eq. (69)). If unsatisfactory return to Step 4, increasing the hole area, reducing the downcomer area, and/or increasing the tray spacing.

Step 7: Check the downcomer residence time safety factor (Eq. (78)); if unsatisfactory, return to Step 4, reducing the hole area or increasing the downcomer area.

Step 8: Specify tray layout details:

a) Width of the calming zone: We choose 0.050 m for the input and output calming zones (the same values adopted in our optimization model).

b) Width of unperforated areas: We choose what we use in our model (Eq. (38)).

c) Hole layout: We adopt the option shared by most of the literature as triangular layout (Fair, 1963; Wankat, 1988; Kister, 1992; Kooijman; Taylor, 2006; Towler; Sinnott, 2013).

d) Recalculate the active area considering calming zone area and unperforated strip area:

$$Aa = Ac - 2Adc - Acz - Aus \tag{107}$$

Step 9: Determine the hole pitch by Eq. (108) and check the safety factor ($lp \geq 2dh$), if unsatisfactory, then return to Step 4, increasing the hole diameter.

$$lp = dh\left(\frac{0.905Aa}{Ah}\right)^{0.5} \tag{108}$$

Step 10: Check the flooding safety factor (Eq. (52)), if unsatisfactory, then return to Step 4, increasing the tray spacing.

Step 11: Check the entrainment safety factor (Eq. (61)), if unsatisfactory then return to Step 4, increasing the tray spacing. Otherwise, stop.

Other procedures and equations used in the literature exist and they are all based on trial and verification steps. The intervention of an experienced designer becomes important in Steps 2, 4, and 8 to adequately select the values of the design variables to be verified. In the verification steps, a check is made to see if the design is feasible or not (Steps 5, 6, 7, 9, 10, and 11).

1.7 Results

The performance of the proposed MINLP procedure for the optimal design of distillation columns trays is illustrated by the solution of an example from the literature (Towler; Sinnott, 2013) together with a comparison with the corresponding results of the heuristic procedure.

The example considers a distillation column with an aqueous waste stream as feed, where it is desired to recover acetone. The feed is a stream with 454.5 kmol/h of a mixture containing 10 % of acetone (all compositions are expressed here using a molar basis). The top stream must contain 95 % of acetone and the bottom stream must not contain more than 1 % of acetone. The example considers ten equilibrium stages with a total condenser. The operation pressure some equal to 1 atm for all trays.

The column was simulated in the Aspen Plus software using the property method UNIQ-RK, which employs the Redlich-Kwong equation of state (Redlich; Kwong, 1979) and the UNIQUAC activity coefficient model (Abrams; Prausnitz, 1975). The reflux ratio is 1.24 and the feed tray corresponds to stage 8. The results of the simulation for the nine ideal stages are presented in Table 1 (the equilibrium stage 10 corresponds to the kettle reboiler).

Table 1 – Operational parameters of the example

Parameters/ Tray	1	2	3	4	5	6	7	8	9
$\widehat{Lw}$ (kg/s)	0.82	0.80	0.78	0.76	0.72	0.66	0.51	3.12	2.78
$\widehat{Vw}$ (kg/s)	1.50	1.48	1.46	1.43	1.40	1.34	1.18	1.02	0.68
$\widehat{\rho l}$ (kg/m³)	753.76	754.64	755.64	756.92	758.84	762.57	776.27	873.01	900.73
$\widehat{\rho v}$ (kg/m³)	2.10	2.09	2.07	2.04	2.01	1.95	1.78	1.61	1.02
$\hat{\sigma}$ (N/m)$\times 10^3$	22.28	23.20	24.21	25.45	27.21	30.28	38.60	59.14	60.79

Source: The author, 2022.

The overall efficiency was assumed to be equal to 60 %. Excluding the reboiler, the nine ideal stages correspond to 15 real stages. This value was employed for the evaluation of the column height in the objective function. The column material was carbon steel ($\widehat{\rho w}$ = 7900 kg/m^3).

Table 2 displays the standard alternatives of the discrete geometric variables employed in the design problem. This set of options corresponds to a search space composed of 7,931,520 candidates (total number of possible combinations of the values of the design variables). The lower and upper bounds are outlined by Eqs. (80-88) correspond to the minimum and maximum values displayed in Table 2. The lower and upper bounds on the variable $Wshell$ are $\widehat{Wshell}_{min} = 160\ kg$ and $\widehat{Wshell}_{max} = 250000\ kg$, according to the validity range of the correlation in Eq. (94).

Table 2 – Discrete values of the design variables

Variables	Discrete values																
Dc (m)	0.61	0.76	0.91	1.07	1.27	1.47	1.68	1.93	2.18	2.44	2.74	3.05	3.35	3.71	4.06	4.42	4.83
dh (mm)	3.60	4.00	4.40	4.80	5.20	5.60	6.00	6.40									
hdwap (mm)	5.00	6.00	7.00	8.00	9.00	10.0											
hw (cm)	3.81	4.44	5.08	5.71	6.35	6.98	7.62	8.25	8.89								
lt (m)	0.15	0.23	0.31	0.47	0.62	0.91											
lw (m)	0.41	0.66	0.91	1.17	1.42	1.68	1.93	2.18	2.44	2.69	2.95	3.20	3.45	3.71	3.96		
lp (mm)	9.00	12.0	15.0	18.0	21.0	24.0											
tt (mm)	3.40																
lay	square		triangular														

Source: The author, 2022.

The column diameters vary between 0.6096 m (2 in) and 4.826 m (19 in), the diameter lower bound being necessary to avoid difficulties of installation (Towler; Sinnott, 2013), and the upper bound is related to the maximum that the column cost equation allows (Eq. (94)) (Towler; Sinnott, 2013). The discrete values of the diameters employed in the optimization were selected in such a way that the differences between them increase as the diameter increases.

The diameters of the holes correspond to the commercial standardization of drills (Oberg *et al.*, 2004). Their limits are chosen to respect the Fair entrainment correlation limits (Fair, 1961), that is, between 1.6 mm (1/16 in) and 6.4 mm (1/4 in). Moreover, hole diameters must respect the geometric constraints (Eqs. (48-49)). The limits of the variables *hdwap*, *hw* and *lt* were established based on their corresponding typical values (Towler; Sinnott, 2013). Finally, the limits of the variables *lw* and *lp* were generated from the limits of the variables *Dc* and *dh* according to the relations suggested by Towler and Sinnott (2013):

$$0.6 \leq \frac{lw}{Dc} \leq 0.85 \tag{109}$$

$$2.5 \leq \frac{lp}{dh} \leq 4.0 \tag{110}$$

The values of the column shell thickness related to each column diameter alternative are shown in Table 3, according to Towler and Sinnott (2013). The lowest and highest values of thicknesses are employed as lower and upper bounds on the variable *twall*.

Table 3 – Shell thickness for each column diameter

Dc (m)	0.61	0.76	0.91	1.07	1.27	1.47	1.68	1.93	2.18	2.44	2.74	3.05	3.35	3.71	4.06	4.42	4.83
twall (mm)	5	5	5	7	7	7	7	7	9	9	10	12	12	12	12	12	12

Source: The author, 2022.

The MINLM formulation of the design optimization problem is composed of 79 binary variables, 169 discrete variables and 309 constraints for the cost minimizing. For the mass minimizing has an addition of 1 discrete variable and 1 constraint. The formulation was solved by MINLP procedures using the GAMS software interface (version 24.7.1) and the global optimization solvers ANTIGONE (version 1.1) (Misener; Floudas, 2014), and BARON (version 16.3.4) (Sahinidis, 1996).

Because ANTIGONE and BARON do not accept trigonometric functions, Taylor series expansions to represent those functions were used (Gradshteyn; Ryzhik, 2015):

$$\tan x = \sum_{k=1}^{\infty} \frac{2^{2k}(2^{2k}-1)}{(2k)!} |Be_{2k}| x^{2k-1}, \qquad |x| < \frac{\pi}{2} \tag{111}$$

$$arcsin\, x = \sum_{k=0}^{\infty} \frac{(2k)!}{2^{2k}(k)!^2(2k+1)} x^{2k-1} \tag{112}$$

where *Be* is the Bernoulli number obtained from Plouffe (2001). The series representing the tangent function was evaluated using 81 terms and the series of the arcsine function involved 14 terms, which have an error below 0.001.

The computational times associated with the optimization using the solver ANTIGONE were 73 s and 20 s for cost and mass as objective functions, respectively. The corresponding computational times using the solver BARON were 136 s and 36 s. These times were collected in a computer with an Intel Core i7 processor with 8 Gb of RAM.

The comparison of the solutions obtained using ANTIGONE and BARON indicates that BARON did not attain the global optimum in the minimization of the cost (the value of the objective function obtained using BARON was 13 % higher than the solution using ANTIGONE). The results obtained using ANTIGONE are displayed in Table 4, for different objective functions. These solutions are similar, exhibiting different masses: 1,339.42 kg for the cost objective function and 1,335.52 kg for the mass objective function. The total cost is the same ($ 28,915.69) because the cost function is not detailed enough to be sensitive to the minor differences between these similar solutions.

The heuristic design procedure was also applied to the solution of the same design example. The details of the application of the heuristic procedure are present in the Appendix A, including all the candidates tested during the search. The final feasible solution found is also presented in Table 4. This solution is associated with a cost and a mass equal to $ 31,822.12 and 1,831.70 kg, respectively.

The comparison of the optimal values of the objective function with the results obtained using the heuristic procedure indicates that the optimization attained a reduction of 9 % of the cost and 27 % of the mass of steel.

Table 4 – Results

	MINLP – Minimization of the column cost	MINLP – Minimization of the column mass	Heuristics
$Ctotal$ (\$)	28,915.69	28,915.69	31,822.12
$Wtotal$ (kg)	1,339.42	1,335.52	1,831.70
Dc (m)	0.9144	0.9144	0.7307
dh (m)	0.0036	0.0036	0.0048
$hdwap$ (m)	0.008	0.005	0.010
hw (m)	0.0381	0.0381	0.0508
lt (m)	0.4572	0.4572	0.9144
lw (m)	0.6604	0.6604	0.5550
lp (m)	0.009	0.009	0.011
lay	square	triangular	triangular

Source: The author, 2022.

1.8 Conclusions

This paper presented a Mixed Integer Nonlinear Model solved using a MINLP procedure for the tray design of distillation columns. For a given set of flow rates and physical properties, the optimization determines the optimal value of the column diameter and all the dimensions of the trays. Two alternative objective functions were used: cost and mass. The method can be also extended for other internals (e.g. valve trays, bubble cap trays, etc.) or objective functions (e.g. more detailed cost functions based on mechanical design). Additionally, a step-by-step heuristic procedure, based on the literature, was presented and used for comparison. Significant reductions were obtained in both objective functions.

Besides the advantages of the mathematical programming approach, the heuristic procedures have another disadvantage: they rely on experienced practitioners. Therefore, a novice engineer may obtain a more expensive solution than an experienced one. Comparatively, the application of the optimization approach is automatic and the least cost design is attained, no matter the experience of the user.

2 SET TRIMMING APPROACH FOR THE GLOBALLY OPTIMAL DESIGN OF SIEVE TRAYS IN SEPARATION COLUMNS

In this article, we use Set Trimming to obtain the globally optimal design of distillation column trays, that is, the column diameter and the geometrical design of the trays (weir, downcomer, etc.) that minimize mass or cost. We assume that the operating conditions (vapor and liquid flow rates, compositions, temperatures) are given. The design task is, to this day, presented in textbooks as a trial and verification procedure. We show that Set Trimming guarantees global optimality and is amenable to exploring alternative global optima. Compared with the employment of a mixed-integer nonlinear programming (MINLP) approach using commercial global optimizers, we show that Set Trimming is a more robust option with competitive computational times for individual design problems. It also exhibits a significant reduction in computational effort when alternative optimal solutions are sought.

2.1 Introduction

The design of column trays in separation columns has been traditionally handled using trial-and-verification procedures through step-by-step procedures (Fair, 1963; Wankat, 1988; Douglas, 1988; Kister, 1992; McCabe; Smith; Harriott, 1993; Seader; Henley; Roper, 2011; Chuang; Nandakumar, 2000; Towler; Sinnott, 2013). Some of these procedures are based on bold assumptions and heuristics that facilitate obtaining viable answers, with the intended effect of keep changing the trial geometries until one is viable. For example, the area of the downcomer is assumed to be 10% of the total area right after the diameter is selected based on a flooding velocity (Towler; Sinnott, 2013).

The utilization of optimization techniques for the design of column trays was addressed by a few works. Ogboja and Kuye (1990) used the Complex Method (Box, 1965) to solve a sieve tray optimization. They obtained the optimal tray design by maximizing tray efficiency according to geometrical and phenomenological constraints. The problem formulation was restricted to optimizing only one plate and not the total set of column trays. Lahiri (2014, 2020) presented a method to obtain the optimal tray design based on the minimization of the total annualized cost, showing better results when compared with a commercial simulator. More recently, Souza *et al*. (2022) presented a mixed-integer nonlinear mathematical model (MINLM) solved using a global optimizer for the design of column trays, based on the equations presented in Towler and Sinnott (2013).

As shown by Souza *et al*. (2022), the solution to the tray design-optimization problem using mathematical programming can attain better results than the traditional trial and verification approach. However, further numerical tests indicate that the global solution of the tray design problem using mathematical programming may be difficult sometimes. Aiming at providing a fast and reliable optimization tool for the solution of the optimal tray design problem, we present in this work the application of Set Trimming (Costa; Bagajewicz, 2019). According to the results presented in this article, the proposed technique for solving the tray design problem is more robust than mathematical programming using global solvers, presenting competitive computational times.

Another important aspect of the proposed technique is the solution based on optimal sets, instead of optimal points. Conventional optimization techniques identify a single optimal solution. However, Set Trimming can identify all of the optimal solutions with the lowest value of the objective function (if there is more than one). Therefore, the user can choose one of these solutions considering other additional criteria that were not originally contemplated in the problem formulation. The identification of this set using conventional optimization techniques demands a recursive solution to the optimization problem, but Set Trimming can do it in a single run. We discuss more details about Set Trimming later in the article.

This article is organized as follows: Section 2.2 presents the geometric variables that are employed in the design problem, Section 2.3 presents the problem constraints, Section 2.4 presents different objective functions employed for the formulation of the design optimization problem, Section 2.5 presents the Set Trimming technique, and Section 2.6 illustrates the performance of the proposed formulation and compares it with mathematical programming. The conclusions are finally presented in Section 2.7.

2.2 Sieve tray geometry

The proposed optimization procedure is applied here for the design of sieve trays (the same optimization technique can be also employed for bubble cap or valve trays). A sieve tray is composed of the active and downcomer areas, with some calming zones. There are several types of configurations that use multiple passes (mostly for large diameters) and others, as well as different downcomer geometries (segmental, circular, etc.).

Figure 6 shows the simplest configuration (one pass and segmental downcomer), which is the one we use in this article and our previous one (Souza; Bagajewicz; Costa, 2022). Summarizing the detailed description given in the aforementioned article, we cite the components: active area (*Aa*), downcomers areas (*Adc*), hole area (*Ah*), calming zones (wcz_{in} and wcz_{out}), and unperforated strips (*wus*).

Figure 6 – Sieve tray top view

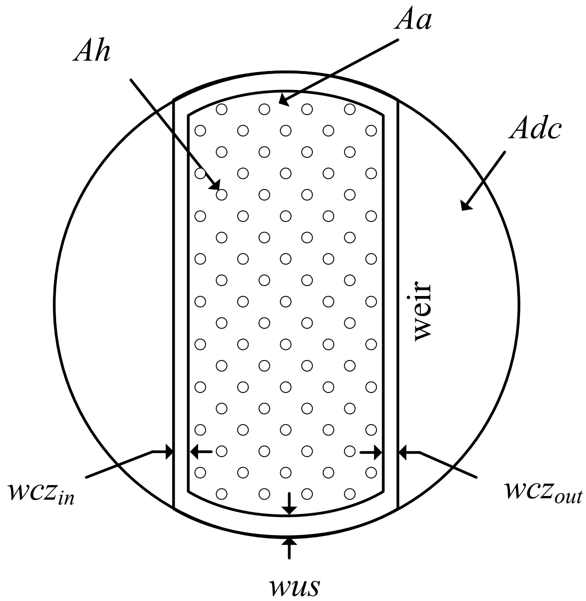

Source: The author, 2022.

Figure 3 shows a side view of the tray highlighting another set of model variables: tray spacing (*lt*), weir height (*hw*), height of the liquid crest over the weir (*how*), clearance height under the downcomer (*hap*), the difference between weir and clearance height under the downcomer (*hdwap*), and the height of the downcomer backup (*hb*). The independent geometric variables we use are introduced in Table 5. The optimization problem consists of the determination of the values of these variables associated with the optimal value of one of the objective functions described in Section 2.4. These variables are discrete in practice, namely *dh*, *tt* and *lt*, because are standardized, while many other variables, namely *Dc*, *hdwap*, *hw*, *lw* and *lp* are usually considered continuous, but fabrication forces the use of discrete values. The tray mathematical model allows the determination of the values of the other model variables based on a given set of values of this set of independent variables

Figure 3 – Tray side view

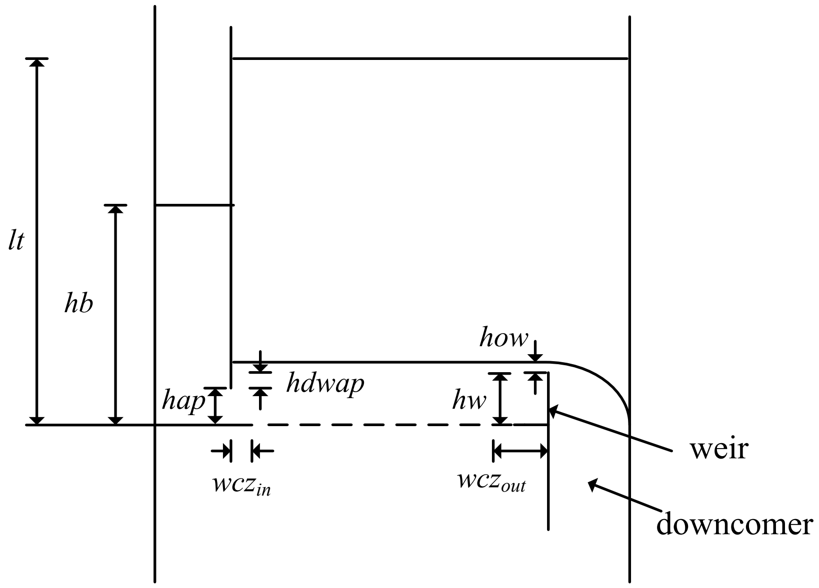

Source: The author, 2022.

Table 5 – Independent geometric variables

Variable	Definition	Unit
Dc	Column diameter	m
dh	Hole diameter	m
hdwap	Difference between weir and gap height	m
hw	Weir height	m
lt	Tray spacing	m
lw	Weir length	m
lp	Hole pitch	m
tt	Tray thickness	m
lay	Hole layout (triangle and squared)	-

Source: The author, 2022.

Figure 4 depicts the downcomer area, which is obtained as the difference between the circular sector area (*Asector*) and the triangle area (*Atriangle*). The following equations show the geometrical relations among the several tray dimensions. Details of their development and source are given by Souza *et al.* (2022).

Figure 4– Tray downcomer area

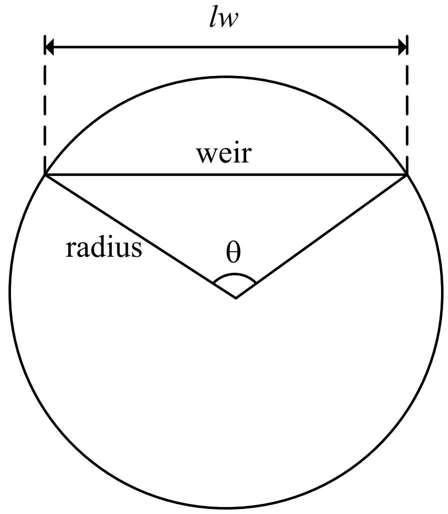

Source: The author, 2022.

The central angle of the circle that spans the weir is given by:

$$\theta = 2\arcsin\left(\frac{lw}{Dc}\right) \tag{113}$$

The area of the sector defined by the weir angle is:

$$Asector = \frac{Dc^2\theta}{8} \tag{114}$$

and the area of the triangle defined by the column radius and the weir length is:

$$Atriangle = \frac{lw}{2}\sqrt{\left(\frac{Dc}{2}\right)^2 - \left(\frac{lw}{2}\right)^2} \tag{115}$$

The total column cross-sectional area (*Ac*), the cross-sectional area of the downcomer (*Adc*), and the net area available for vapor-liquid interaction (*An*) are given by:

$$Ac = \frac{\pi Dc^2}{4} \tag{116}$$

$$Adc = Asector - Atriangle \tag{117}$$

$$An = Ac - Adc \tag{118}$$

Additional geometric relations involving the calming zones and unperforated strip areas are shown below, associated with the representation in Figure 5.

Figure 5 – Calming zones and unperforated strip areas

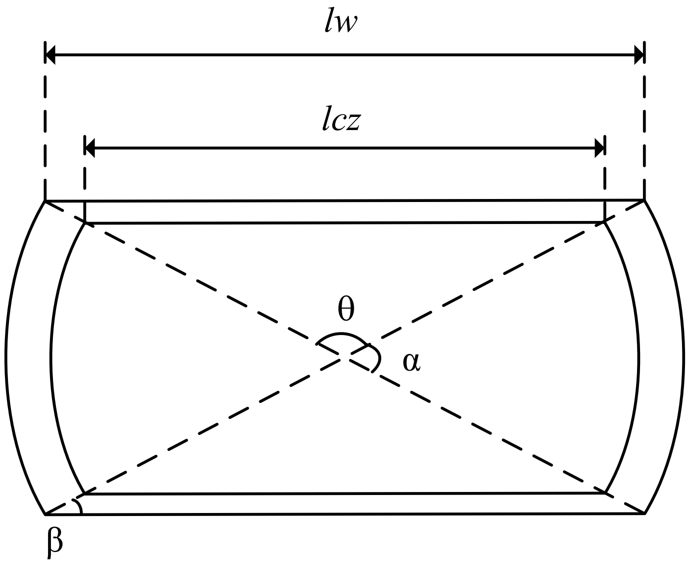

Source: The author, 2022.

The calming zone area (Acz) is the area of two trapezoids, as illustrated in Figure 5, and it is given by:

$$Acz = \frac{(lcz_{in}+lw)}{2}\widehat{wcz}_{in} + \frac{(lcz_{out}+lw)}{2}\widehat{wcz}_{out} \tag{119}$$

The length of the calming zone (lcz) is given by:

$$lcz_{in} = lw - 2\left(\frac{\widehat{wcz}_{in}}{\tan\beta}\right) \tag{120}$$

$$lcz_{out} = lw - 2\left(\frac{\widehat{wcz}_{out}}{\tan\beta}\right) \tag{121}$$

where β is the calming zone angle:

$$\beta = \frac{\pi-\theta}{2} \tag{122}$$

The width of the inlet and outlet calming zone has been suggested to be between 2 and 5 in (AMACS Process Tower Internals, 2020; Dutta, 2007; Towler; Sinnott, 2013; Wankat, 1988). Then, we consider $\widehat{wcz}_{in}$ and $\widehat{wcz}_{out}$ equal to 0.050 m (2 in).

As a consequence, the unperforated strip area (Aus) is determined using the angle of the active area (α) and the width of the unperforated strip (wus) (Towler; Sinnott, 2013).

$$Aus = wus\,\alpha(Dc - wus) \tag{123}$$

$$\alpha = \pi - \theta \tag{124}$$

The width of the unperforated strip varies according to diameter (AMACS Process Tower Internals, 2020):

$$wus = \begin{cases} 0.0381, & Dc \leq 0.7620 \\ 0.0508, & 0.7620 < Dc \leq 1.6764 \\ 0.0635 & 1.6764 < Dc \leq 3.8100 \\ 0.0762 & 3.8100 < Dc \leq 5.9436 \\ 0.0889 & 5.9436 < Dc \leq 7.4676 \\ 0.1143 & Dc > 7.4676 \end{cases} \tag{38}$$

The active area is the column cross-sectional area less the downcomer area, the unperforated strip area, and the calming zone areas:

$$Aa = Ac - 2\,Adc - Aus - Acz \tag{125}$$

The hole area (Ah) can be determined as follows (Kister, 1990):

$$Ah = k\left(\frac{dh}{lp}\right)^2 Aa \tag{126}$$

where k is 0.785 or 0.905 from square or triangular hole layout, respectively.

2.3 Optimization constraints

The set of constraints involves geometric and operational constraints.

2.3.1 Geometric constraints

The weir length must be limited to the column diameter:

$$lw \leq Dc \tag{127}$$

The hole pitch must be equal to or greater than twice the hole diameter (Towler; Sinnott, 2013).

$$lp \geq 2\,dh \tag{128}$$

The thickness must be limited by the hole diameter (Chuang; Nandakumar, 2000):

$$\frac{dh}{tt} \geq 1 \tag{129}$$

The ratio of the hole area to the active area is bounded:

$$0.06 \leq \frac{Ah}{Aa} \leq 0.16 \tag{130}$$

Finally, to use the Fair flooding correlation, the following constraint holds: (Fair, 1961)

$$hw \leq 0.15\,lt \tag{131}$$

Except for Eqs. (127) and (128), which are logical constraints, all the rest are heuristics.

2.3.2 Operational constraints

The operational constraints are the limits of flooding, entrainment, weeping, downcomer backup, and residence time in the downcomer of the sieve tray design. Because the flow rates and physical properties of the vapor and liquid stream vary along the column, these constraints must be applied for each tray, identified by the index *sNt*. These constraints are also reproduced below from Souza *et al.* (2022) without further discussion.

- Flooding:

$$un_{sNt} \leq 0.85\, uflood_{sNt} \qquad \forall\, sNt \tag{132}$$

$$un_{sNt} = \frac{\widehat{Vw}_{sNt}}{\widehat{\rho v}_{sNt}\ An} \qquad \forall\, sNt \tag{133}$$

$$uflood_{sNt} = K1\ Csb_{sNt}\sqrt{\frac{\widehat{\rho l}_{sNt}-\widehat{\rho v}_{sNt}}{\widehat{\rho v}_{sNt}}}\left(\frac{\widehat{\sigma}_{sNt}}{0.02}\right)^{0.2} \qquad \forall\, sNt \tag{134}$$

$$\widehat{Flv}_{sNt} = \frac{\widehat{Lw}_{sNt}}{\widehat{Vw}_{sNt}}\sqrt{\frac{\widehat{\rho v}_{sNt}}{\widehat{\rho l}_{sNt}}} \qquad \forall\, sNt \tag{135}$$

$$K1 = \begin{cases} 0.8, & 0.06 \leq \frac{Ah}{Aa} \leq 0.08 \\ 0.9, & 0.08 \leq \frac{Ah}{Aa} \leq 0.10 \\ 1.0, & 0.10 \leq \frac{Ah}{Aa} \leq 0.16 \end{cases} \tag{136}$$

$$Csb_{sNt} = 0.0129 + 0.1674\, lt + 0.0063\widehat{Flv}_{sNt} - 0.2686\, lt\, \widehat{Flv}_{sNt} - 0.008\widehat{Flv}_{sNt}^{\ 2} + 0.01448\, lt\, \widehat{Flv}_{sNt}^{\ 2} \qquad \forall\, sNt \tag{137}$$

- Entrainment

$$\psi_{sNt} \leq 0.1 \qquad \forall\, sNt \tag{138}$$

$$\psi_{sNt} = \left\{ exp\begin{bmatrix} -7.9196 + 1.0891 Fflood_{sNt} \\ -(0.0705 + 2.1916 Fflood_{sNt}) \ln \widehat{Flv}_{sNt} \\ +(0.046 - 0.605 Fflood_{sNt} + 1.2669 Fflood_{sNt}^{\ 2} \\ -0.9563 Fflood_{sNt}^{\ 3})\left(\ln \widehat{Flv}_{sNt}\right)^2 \end{bmatrix} \right\} \qquad \forall\, sNt \tag{139}$$

$$Fflood_{sNt} = \frac{un_{sNt}}{uflood_{sNt}} \qquad \forall\, sNt \tag{140}$$

- Weeping:

$$uh_{sNt} \geq uhmin_{sNt} \qquad \forall\, sNt \tag{141}$$

$$uh = \frac{\widehat{Vw}_{sNt}}{\widehat{\rho v}_{sNt}\,Ah} \qquad \forall\, sNt \tag{142}$$

$$uhmin_{sNt} = \frac{K2_{sNt} - 0.9\left(25.4 - 10^3\,dh\right)}{(\widehat{\rho v}_{sNt})^{\frac{1}{2}}} \qquad \forall\, sNt \tag{143}$$

$$K2_{sNt} = 23.48 - 1.66\ln[10^3(hw + how_{sNt})] \qquad \forall\, sNt \tag{144}$$

$$how_{sNt} = 750 \cdot 10^{-3}\left[\frac{\widehat{Lw}_{sNt}}{\widehat{\rho l}_{sNt}\;lw}\right]^{2/3} \qquad \forall\, sNt \tag{145}$$

- Downcomer Backup

$$hb_{sNt} \leq \frac{1}{2}(lt + hw) \qquad \forall\, sNt \tag{146}$$

$$hb_{sNt} = hw + how_{sNt} + ht_{sNt} + hdc_{sNt} \qquad \forall\, sNt \tag{147}$$

$$ht_{sNt} = hw + how_{sNt} + hd_{sNt} + \widehat{hr}_{sNt} \qquad \forall\, sNt \tag{148}$$

$$\widehat{hr}_{sNt} = \frac{12.5}{\widehat{\rho l}_{sNt}} \qquad \forall\, sNt \tag{149}$$

$$hd_{sNt} = 51 \cdot 10^{-3}\left(\frac{uh_{sNt}}{Co}\right)^2 \frac{\widehat{\rho v}_{sNt}}{\widehat{\rho l}_{sNt}} \qquad \forall\, sNt \tag{150}$$

$$Co = 0.6323 - 0.0255\frac{tt}{dh} + 0.1495\left(\frac{tt}{dh}\right)^2 + 0.777\frac{Ah}{Aa} \tag{151}$$

$$hdc_{sNt} = 166 \cdot 10^{-3}\left(\frac{\widehat{Lw}_{sNt}}{\widehat{\rho l}_{sNt}\;Aap}\right) \qquad \forall\, sNt \tag{152}$$

$$Aap = hap\;lw \tag{153}$$

$$hap = hw - hdwap \tag{154}$$

- Residence time:

$$time_{sNt} \geq 3\;s \qquad \forall\, sNt \tag{155}$$

$$time_{sNt} = \frac{Adc\;hb_{sNt}\,\widehat{\rho l}_{sNt}}{\widehat{Lw}_{sNt}} \qquad \forall\, sNt \tag{156}$$

2.4 Objective function

The optimization proposal consists in minimizing the costs associated with the sieve tray design of a distillation column. Two alternative objective functions are explored: a capital cost equation and an expression of the mass of the distillation column.

The cost equation is given by (assuming a carbon steel column) (Towler; Sinnott, 2013):

$$Min\;Ctotal = (130 + 440Dc^{1.8})\widehat{Nt} + 11600 + 34\;Wshell^{0.85} \tag{157}$$

where $\widehat{Nt}$ is the number of trays and $Wshell$ is the mass of the column shell. The equation is validated from 0.5 < *Dc* < 5.0 m and 160 < *Wshell* < 250,000 kg. The mass of the column shell is given by:

$$Wshell = \pi\, \widehat{\rho shell}\, Dc\, Hc\, twall \tag{158}$$

where $\widehat{\rho shell}$ is the density of the shell material, $twall$ is the column wall thickness and *Hc* is the height of the column between tangent lines, given by:

$$Hc = \widehat{Nt}\, lt \tag{159}$$

Another alternative objective function consists in minimizing the mass of the distillation column and its trays (*Wtotal*):

$$Min\, Wtotal = Wcolumn + Wt\, \widehat{Nt} \tag{160}$$

The mass of the column is given by:(2013)

$$Wcolumn = \widehat{Cw}\, \pi\, \widehat{\rho shell}\, Dm(Hc + 0.8Dm)twall \tag{161}$$

where $\widehat{Cw}$ is a factor responsible by the mass of nozzles, manways, internal supports, etc., to distillation columns is 1.15 and *Dm* is the mean diameter of the column, given by:

$$Dm = Dc + twall \tag{162}$$

The mass of the tray is determined by the volume of the tray (*Vt*) and the volume of the weir together with the downcomer (*Vwdc*).

$$Wt = (Vt + Vwdc)\widehat{\rho t} \tag{163}$$

where $\widehat{\rho t}$ is the specific mass of tray material. The volume of the tray (*Vt*) is given by the area of the column minus the areas of the downcomer and holes, and the volume of the combination weir/downcomer (*Vwdc*) is given by a rectangular plate:

$$Vt = (Ac - Adc - Ah)tt \tag{164}$$

$$Vwdc = [hw + tt + Hdc]tt\, lw \tag{165}$$

where *Hdc* is the height of downcomer:

$$Hdc = lt - hap = lt - (hw - hdwap) \tag{166}$$

2.5 Set Trimming

The Set Trimming technique was initially proposed by Gut and Pinto (2004) for the specific case of the design of plate heat exchangers. Costa and Bagajewicz (2019) generalized it conceptually to apply to any optimization problem with discrete independent variables. The same technique was successfully applied by Lemos *et al.* (2020) and Nahes *et al.* (2021) to the design optimization of shell and tube heat exchangers and plate heat exchangers, respectively.

The Set Trimming technique is applied to problems with a combinatorial representation of the search space, where each candidate solution corresponds to a set of discrete values of the decision variables. The technique consists of applying the inequality constraints sequentially to the set of candidates so that after testing each constraint, the number of candidates decreases. Thus, in the end, if all constraints are applied, only feasible candidates remain, that is, the candidates that respected all the constraints of the model. Consequently, after Set Trimming, the global optimum can be obtained through a simple sorting procedure applied to the objective function of the feasible candidates. This technique is a global optimization technique because only the infeasible candidates are eliminated and, in the end, there is a selection, to obtain the best alternative among feasible candidates (Costa; Bagajewicz, 2019).

Figure 7 – Set Trimming structure

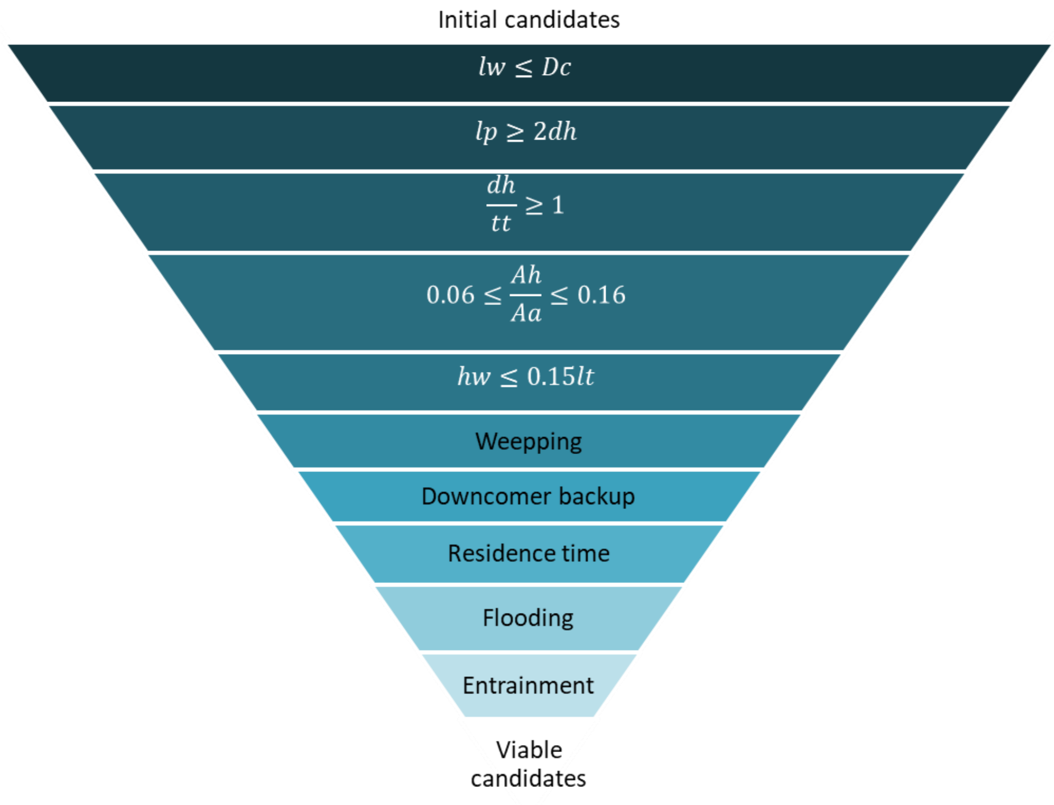

Source: The author, 2022.

The steps of each trim of Set Trimming method, using the model of the sieve tray design are shown below, according to the representation depicted in Figure 7. In these steps, each set is defined as a subset of the previous one, thus eliminating the infeasible candidates from each step. The initial candidate set is the set of all combinations of the independent geometric variables of the problem (Table 5).

The Set Trimming starts with the geometrical constraints, that is, using the inequalities Eqs. (127)-(131). This set of constraints trims the majority of candidates for which some of the operational limits do not even make sense. The application of all the other operational inequalities follows. The order of the trims was selected through an analysis of the computational efficiency of the elimination of candidates provided by each constraint (see Section 2.6). After Set Trimming, the optimal solution is identified through a simple sorting procedure of the values of the objective function of the feasible candidates.

2.6 Power Analysis

The order of the constraints in the Set Trimming is very important for its computational performance. Because the time used to trim a set depends on its size, one wants to identify what are the constraints that trim the largest amount of candidates. However, the time to evaluate each constraint also matters. Therefore, both need to be taken into account.

Aiming at identifying the effectiveness of the trim action associated with each constraint, we use the following procedure. Using the first set of candidates obtained after geometric Set Trimming as a starting point, we apply each constraint separately. Thus, based on the number of candidates eliminated and the computational time spent on each constraint, it is possible to determine the fraction of candidates eliminated and the number of candidates eliminated per second by each trim action. The power of each constraint is in eliminating more candidates in less time.

After that, the appropriate ordering of the constraints is determined by picking the constraints in descending order of power (number of candidates eliminated/second). Therefore the trimmings of the constraints that are slower and eliminate fewer candidates will be applied later, which will provide a reduction in the computational time. While this ordering is not guaranteed to render the smallest computational time in all cases (it still depends on the particular problem), it is a step in the right direction.

2.7 Results

We use an example taken from Towler and Sinnott (2013), where acetone is recovered from a 10% mol of acetone aqueous waste. The top stream of the distillation column must contain 95% mol of acetone and the bottom stream must not contain more than 1% mol of acetone. The number of real stages is 15, considering a column efficiency of 60% and excluding the reboiler. The column material was carbon steel ($\widehat{\rho shell} = \widehat{\rho t}$ = 7900 kg/m^3).

Table 1 presents the operational parameters of the nine ideal stages, with stage 8 as the feed tray. These were obtained by a simulation in the Aspen Plus software using the property package UNIQ-RK, which employs the Redlich-Kwong equation of state (Redlich; Kwong, 1979) and the UNIQUAC activity coefficient model (Abrams; Prausnitz, 1975). The reflux ratio is 1.24.

Table 2 presents the standard alternatives of the geometric variables. The column diameters vary between 0.6096 m (2 ft – 24 in) and 4.826 m (15.8 ft – 190 in), the lower limit is the diameter needed to avoid installation difficulties, and the upper limit is the largest diameter for which the cost equation is valid (Towler; Sinnott, 2013). This set of diameters is selected in such a way that the differences between the diameter values increases as the diameter increases. Table 3 shows the values of the column shell thickness related to each column diameter alternative, according to Towler and Sinnott (2013). Further details of the selection of the possible values for the other design variables can be found in Souza *et al.* (2022). All the computational results presented here were obtained using a computer with Intel Core i7 (8th Gen) processor with 8 Gb of RAM, using GAMS version 24.7.1 (it is important to mention that none of the GAMS solvers was used to implement the Set Trimming algorithm, only the manipulation resources of sets were employed) (Bussieck; Meeraus, 2004).

Table 1 – Operational parameters of the investigated example

Parameter	1	2	3	4	5	6	7	8	9
$\widehat{Lw}$ (kg/s)	0.82	0.80	0.78	0.76	0.72	0.66	0.51	3.12	2.78
$\widehat{Vw}$ (kg/s)	1.50	1.48	1.46	1.43	1.40	1.34	1.18	1.02	0.68
$\widehat{\rho l}$ (kg/m^3)	753.76	754.64	755.64	756.92	758.84	762.57	776.27	873.01	900.73
$\widehat{\rho v}$ (kg/m^3)	2.10	2.09	2.07	2.04	2.01	1.95	1.78	1.61	1.02
$\hat{\sigma}$ (N/m)×10^3	22.28	23.20	24.21	25.45	27.21	30.28	38.60	59.14	60.79

Source: The author, 2022.

Table 2 – Candidate dimensions for the design variables

Variables	1	2	3	4	5	6	7	8	9	10	11	12	13	14	15	16	17
Dc	0.61	0.76	0.91	1.07	1.27	1.47	1.68	1.93	2.18	2.44	2.74	3.05	3.35	3.71	4.06	4.42	4.83
(m - in)	24	30	36	42	50	58	66	76	86	96	108	120	132	146	160	174	190
dh	3.60	4.00	4.40	4.80	5.20	5.60	6.00	6.40									
(mm - in)	9/64	5/32	11/64	3/16	13/64	7/32	15/64	1/4									
hdwap (mm)	5.00	6.00	7.00	8.00	9.00	10.0											
hw	3.81	4.44	5.08	5.71	6.35	6.98	7.62	8.25	8.89								
(cm - in)	1 1/2	1 3/4	2	2 1/4	2 1/2	2 3/4	3	3 1/4	3 1/2								
lt (m - in)	0.15	0.23	0.31	0.47	0.62	0.91											
	6	9	12	18	24	36											
lw	0.41	0.66	0.91	1.17	1.42	1.68	1.93	2.18	2.44	2.69	2.95	3.20	3.45	3.71	3.96		
(m - in)	16	26	36	46	56	66	76	86	96	106	116	126	136	146	156		
lp (mm)	9.00	12.0	15.0	18.0	21.0	24.0											
tt (mm)	3.40																
lay	square		triangular														

Source: The author, 2022.

Table 3 – Shell thickness for each column diameter

Dc (m)	0.61	0.76	0.91	1.07	1.27	1.47	1.68	1.93	2.18	2.44	2.74	3.05	3.35	3.71	4.06	4.42	4.83
twall (mm)	5	5	5	7	7	7	7	7	9	9	10	12	12	12	12	12	12

Source: The author, 2022.

The result of the power analysis is shown in Table 6. The initial number of candidates where those constraints are applied corresponds to 738,900. We conclude that the weeping and residence time are the sets that quickly eliminate a large number of candidates, and for this reason, they should be applied first. Downcomer backup calculations are needed for the evaluation of the residence time so this precedence order is preserved. The sets of flooding and entrainment are the last conditions because they eliminate few candidates per unit time.

Table 6 – Power analysis of Set Trimming

Constraint	Candidates eliminated	Fraction of candidates eliminated	Computational time (s)	Candidates eliminated per second
Flooding	13680	1.75%	49.77	274.86
Entrainment	13716	1.75%	49.52	276.98
Weeping	739032	94.28%	48.25	15316.73
Downcomer backup	26384	3.37%	63.08	418.26
Residence time	233160	29.74%	59.52	3917.34

Source: The author, 2022.

The computational time employed by Set Trimming using the sequence determined by the power analysis is shown in Table 7. Table 7 also shows the computational time of a different arbitrary sequence. We observe that this sequence is associated with a computational time that is almost double the one obtained using the sequence determined by the power analysis, which illustrates the importance of a proper ordering of the constraints in the Set Trimming procedure and the effectiveness of the power analysis to provide a good sequence. We remark that this choice is not universal. A study analyzing several different columns with different vapor and liquid traffic might reveal different sequences to be more efficient under specific flowrate traffic conditions.

Table 7 – Set Trimming computational time using two different sequences of constraints

Constraint order	Time (s)
Power analysis: Weeping / Downcomer backup / Residence time / Flooding / Entrainment	43.66
Arbitrary: Flooding / Entrainment / Weeping / Downcomer backup / Residence time	84.14

Source: The author, 2022.

The results of the application of the technique of Set Trimming with the objective function column cost (Eq. (157)) are shown in Table 8, where the number of candidates after the trim using each constraint is shown.

Table 8 – Number of active candidates after the trim related to each constraint

Constraint	Number of active candidates
Starting set	7,931,520
Geometric 1 – max *lw*	4,167,936
Geometric 2 – min *lp*	3,560,112
Geometric 3 – max *hw*	1,648,200
Geometric 4 – min *Ah*/*Aa*	924,600
Geometric 5 – max *Ah*/*Aa*	738,900
Weeping	44,868
Downcomer backup	27,286
Residence time	18,587
Flooding	18,301
Entrainment	18,097

Source: The author, 2022.

According to Table 8, the search space of the optimization problem is composed of 7,931,520 candidates. The Set Trimming procedure identifies only 18,097 (0.22 %) feasible design alternatives. We observe that the operational constraints (Eqs. (132-156)) are applied to a considerably lower number of candidates, which is a fundamental aspect of the computational efficiency of the Set Trimming procedure.

After the Set Trimming procedure, the optimal solution can be identified through the application of a simple sorting procedure. The results of the sorting procedure are presented in Table 9, which shows the number of feasible candidates identified by the Set Trimming and the number of candidates sharing the lowest value of the objective function. Two alternative objective functions are considered: cost (Eq. (157)) and mass (Eq. (160)). The optimal values obtained for both objective functions, $ 28,915.69 and 1335.52 kg, respectively, are the same as the ones found by Souza et al. (2022)

Because there are multiple candidates with the same value of the objective function, it is possible to apply a second criterion to the optimal set. This feature of Set Trimming allows the user to analyze the final set of solutions with the lowest value of the objective function to consider other aspects of the problem. In our case, we use a second sorting to identify the subset of optimal candidates with the lowest pressure drop (ΔP):

$$\Delta P = \hat{g} \sum_{sNt} ht_{sNt} \widehat{\rho l}_{sNt} \tag{167}$$

where $\hat{g}$ is the gravity acceleration. According to Table 9, there are 6 candidates with the lowest pressure drop with optimal cost and a single candidate with the lowest pressure drop with minimal mass. In both cases, the smallest value of pressure drop is 6,254.94 N/m² (0.907 psi), which is relatively low.

Table 9 – Candidates sharing the same optimal objective function values

Sorting	Objective function	
	Cost	Mass
Number of feasible candidates	18,097	18,097
Candidates with the minimum objective function	354	5
Candidates in the subset featuring minimum ΔP	6	1

Source: The author, 2022.

The optimal values of the design variables with the smallest pressure drop are presented in Table 10. Among the 6 candidates of optimal cost and smallest pressure drop, the *hdwap* is the only variable that changes among all candidates. We remark that this variable has no effect on pressure drop, which explains the multiplicity of results. The results correspond to the lowest height of the liquid in the downcomer backup.

Table 10 – Optimal design variables

Variable	Objective function	
	Cost	Mass
Dc (m)	0.9144	0.9144
dh (m)	0.0036	0.0036
hdwap (m)	0.005	0.005
hw (m)	0.0381	0.0381
lt (m)	0.4572	0.4572
lw (m)	0.6604	0.6604
lp (m)	0.009	0.009
lay	triangular	triangular
Cost ($)	28915.69	28915.69
Mass (kg)	1335.52	1335.52
ΔP (N/m²)	6254.94	6254.94

Source: The author, 2022.

The histogram in Figure 8 shows the distribution of column costs for the 18,097 feasible candidates identified by the Set Trimming technique. In this histogram, the minimum cost of $ 28,915.69, associated with only 354 candidates, corresponds to less than 2% of the total of feasible candidates. Among the objective function values of the feasible candidates, there are several alternatives with objective function values much higher than the optimum value, some up to 115% more expensive. These data indicate that just guaranteeing a feasible solution as a result of the design can imply high costs, thus questioning the value of trial-and-verification procedures.

Figure 8 – Histogram of the column cost of the feasible alternatives

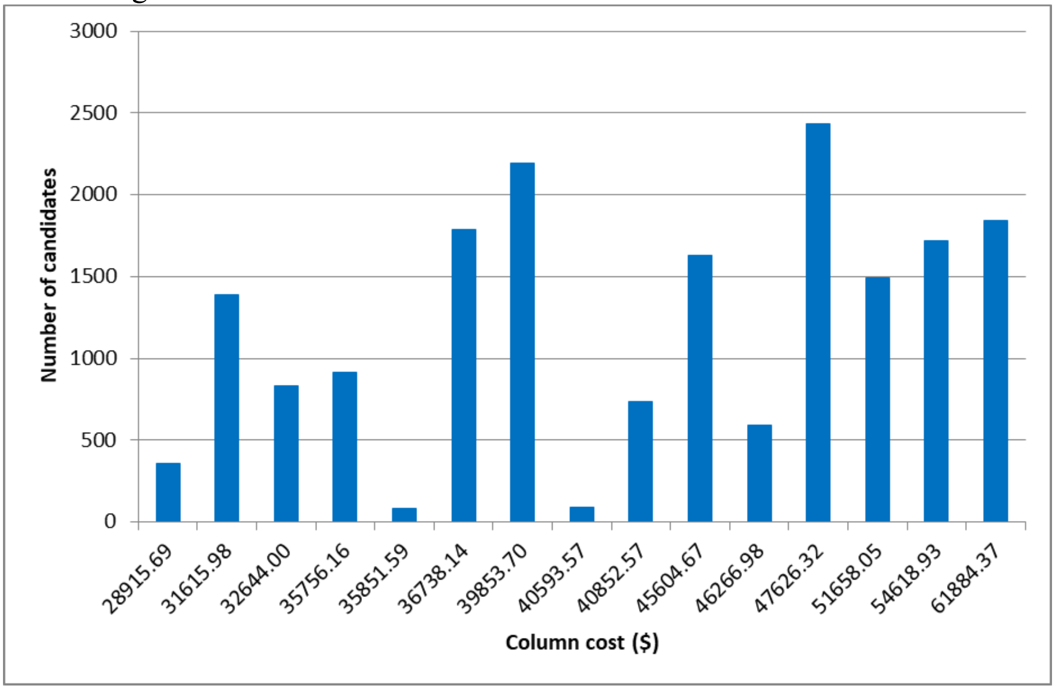

Source: The author, 2022.

Design textbooks present heuristics that aim to guide the designer to a "good" solution. Towler and Sinnott (2013) suggested the following values for the ratios *Adc*/*Ac* and *Ah*/*Aa*: 0.12 and 0.10, respectively. Therefore, one can identify which solution candidates present similar ratios of this type, within the bounds:

$$0.09 \leq \frac{Adc}{Ac} \leq 0.15 \tag{168}$$

$$0.08 \leq \frac{Ah}{Aa} \leq 0.12 \tag{169}$$

The histogram of all feasible options, which comply with the heuristics conditions according to Eqs. (168)-(169), is given in Figure 9. We observe that the heuristics are useful to eliminate a large number of expensive candidates. However, the number of optimal candidates is still a small fraction of the set of candidates: the optimal candidates are only 10% of the total number of candidates that follows the heuristics, i.e. from the histogram, we conclude that there is only 10% chance that a designer that follows the heuristics picks a column of minimum cost. Likewise, there is a 45% chance that the designer can pick a solution with a 27% higher cost. We also note that among the set of columns of minimum cost, only 180 of the 354 feasible columns follow the guidelines. Incidentally, among the 6 columns with minimum pressure drop, all follow the heuristic condition of *Adc*/*Ac* and none follow the heuristic condition of *Ah*/*Aa*.

Figure 9 – Histogram of the column cost, heuristic results

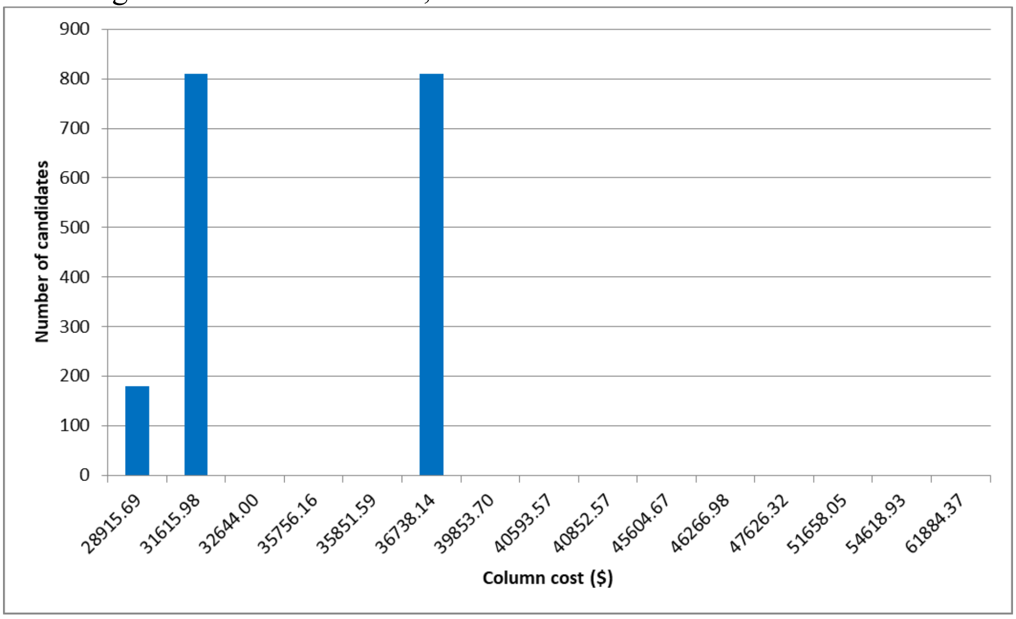

Source: The author, 2022.

Figure 10 shows the histogram with the distribution of column mass for the 18,097 feasible candidates identified by the Set Trimming technique. We observe that 20 of 18,097 candidates (0.11%) present a mass of 1336 kg, close to the optimum shown in Table 10. Without an optimization tool, an inexperienced designer could find a feasible column up to 4 times heavier than the optimum. Roughly, the probability of this event is 10%.

Figure 10 – Histogram of the column mass of the feasible alternatives

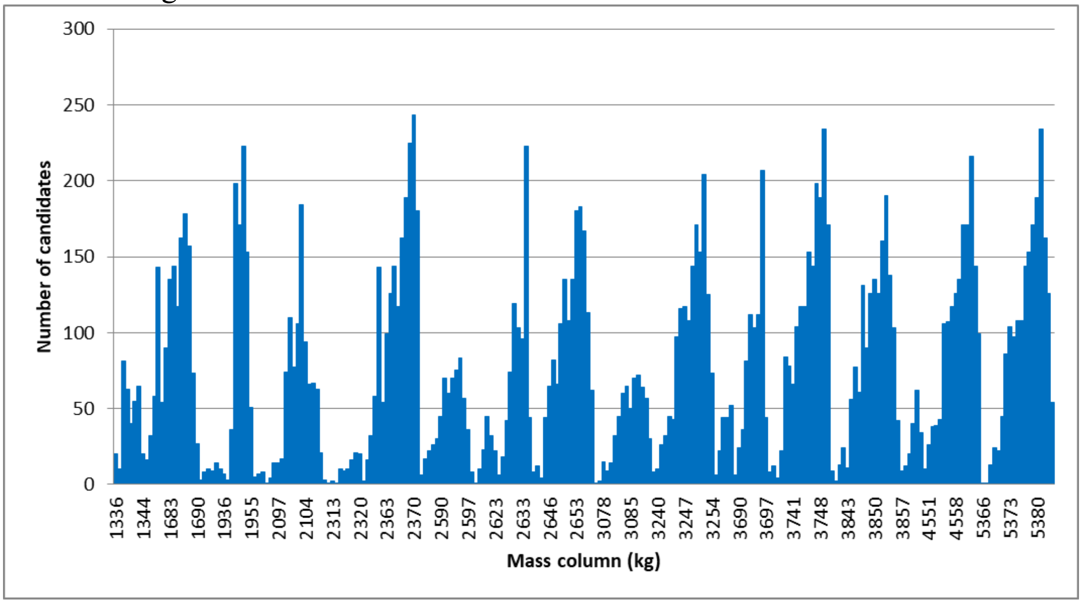

Source: The author, 2022.

The histogram based on mass, presented in Figure 11, shows all the feasible options which comply with the heuristics conditions. In this histogram, there is only 10% of the solutions that follow the heuristics close to the optimum (1340-1344 kg) and 45% of the heuristic-based solutions have a mass around 77% heavier than the optimum. Therefore, there is a considerable chance that a designer that follows the heuristics get a poor solution.

Figure 11 – Histogram of the column mass, heuristic results

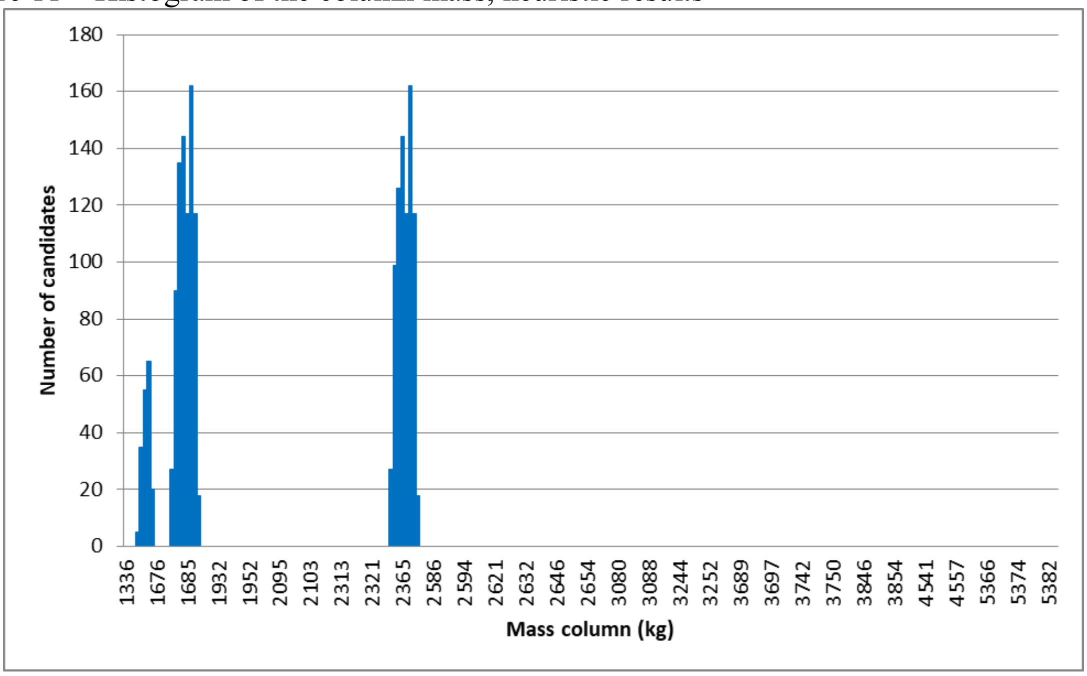

Source: The author, 2022.

The sieve tray performance diagram is illustrated in Figure 12. This figure shows the operating point (vapor and liquid flow rates, for tray 5) and the area of the satisfactory operation, bounded by tray stability limits: entrainment, flooding, downcomer backup, and weeping. The operational point must be inside the area of satisfactory operation.

Figure 12a shows the results for the minimum cost solution ($ 28,915.69) and Figure 12b shows the results of a tray with a $ 61,884.37 cost. The satisfactory operating area depends on the geometric variables of the trays. For each different tray, the curves of the operating limits change, but the operating point remains the same. The comparison of Figures 12a and 12b indicates that the large cost of the latter is associated with oversizing. The expensive tray can be used for other operating points with different liquid and vapor flows, while the optimal tray, should only be used for operating points close to the ones in the example because it has a smaller operating area.

Figure 12 – Sieve tray performance diagram

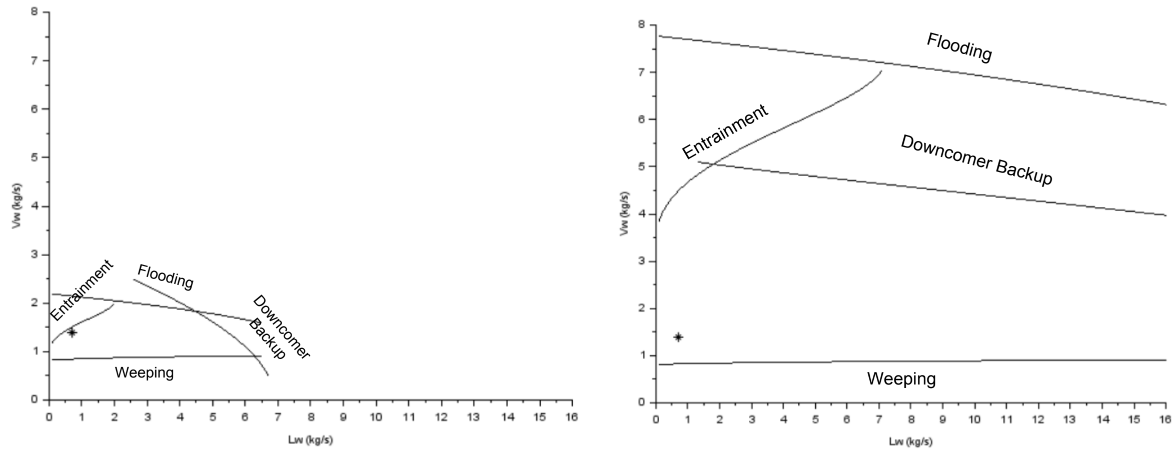

(a) (b)

Subtitle: (a) optimal tray: $Dc = 0.9144$ m, $dh = 0.0036$ m, $hdwap = 0.005$ m, $hw = 0.0381$ m, $lt = 0.4572$ m, $lw = 0.6604$ m, $lp = 0.009$ m, lay = triangular - (b) expensive tray: $Dc = 1.4732$ m, $dh = 0.0036$, $hdwap = 0.005$ m, $hw = 0.0381$ m, $lt = 0.9144$ m, $lw = 1.4224$ m, $lp = 0.009$ m, lay = triangular.

Source: The author, 2022.

2.8 Computational comparison with the MINLP approach

The computational performance of the proposed Set Trimming procedure for column tray design is compared with the mathematical programming of the Mixed-Integer Nonlinear Model (MINLM) described in Souza *et al.* (2022), using different solvers: ANTIGONE 1.1

(Misener; Floudas, 2014) and BARON 16.3.4 (Sahinidis, 1996). All of the tests involving mathematical programming were conducted using default initial estimates and a stopping criterion of 0% gap between the upper and lower bounds.

To provide a clearer assessment of the comparison of the performance of Set Trimming and mathematical programming, the tests were conducted using 32 different optimization runs. The runs were based on the tray design problem presented above, for both objective functions, and associated with different sets of values of the liquid and vapor flow rates as well as different search spaces. The set of tested distillation column flow rates corresponds to the values reported in Table 1 multiplied by 0.5, 1.0, 2.0, and 3.0. The tested search spaces were generated through an increase of the number of possible values for the column diameters (the search space of the other variables was not modified), therefore, the corresponding tested sample was composed of 7,931,520 candidates, 9,331,200 candidates, 10,730,880 candidates, and 12,130,560 candidates. The details of each run are shown in the Appendix B, where the objective function and the computational time employed by each solution method are reported.

The analysis of the values of the optimal objective function of each run indicates that Set Trimming always finds the lowest cost solution. Despite the global nature of the solvers ANTIGONE and BARON, the lowest-cost solution was not found in a considerable fraction of the test sample. ANTIGONE solutions were trapped in a local optimum in 13 runs (41% of the sample). BARON did not converge in 5 runs (16% of the sample) and was trapped in a local optimum in 8 runs (25% of the sample).

Among the set of runs where the mathematical programming solver attained the lowest value of the objective function (19 ANTIGONE and BARON runs), an analysis of the computational time indicates that Set Trimming was faster than ANTIGONE in 8 runs (42% of this sample) and faster than BARON in 12 runs (63%).

Another comparison was done asking that mathematical programming finds other solutions with the same optimal cost, the same way as Set Trimming. To do this, we added in mathematical programming the following constraints that remove the previously found solution (Floudas, 1995).

$$\sum_i \hat{A}_{i,j} yx_i - (\hat{B}_j - 1) \leq 0 \tag{170}$$

$$\hat{A}_{i,j} = \begin{cases} 1, & if\ yx_i = 1 \\ -1, & if\ yx_i = 0 \end{cases} \tag{171}$$

$$\hat{B}_j = \sum_i \hat{A}_{i,j}\ ,\ \forall\ \hat{A}_{i,j} = 1 \tag{172}$$

where i is a set of binary variables, j is a set of constraints, $\hat{A}_{i,j}$ and $\hat{B}_j$ are parameters. Then, for each new solution, a new constraint is added to the set j. The variable x is related to the corresponding set of binary variables by:

$$x = \sum_i \widehat{px}_i yx_i \tag{173}$$

$$\sum_i yx_i = 1 \tag{174}$$

After adding these equations to the mathematical programming formulations using a recursive algorithm, the solvers ANTIGONE and BARON could identify only 3 least-cost solutions in 121 s and 150 s, respectively. Thus, comparing Set Trimming and mathematical programming, Set Trimming obtained a set of 354 least-cost solutions in 43.66 s, while mathematical programming fails to obtain all and employs three times as much time to obtain only 3 of the 354 solutions.

A similar procedure was applied for the identification of the set of least-cost solutions with minimum pressure drops. In this case, the mathematical programming formulations were modified by substituting the objective function to use the minimization of the pressure drop and the insertion of an additional constraint of an upper bound on the cost, equivalent to the minimum cost already found. The minimization of pressure drop after minimizing the cost using the solver ANTIGONE identified all 6 solutions in 108.44 s. The same procedure using BARON could not identify a solution. The Set Trimming obtained the 6 solutions in 43.66 s.

2.9 Conclusions

This paper presented a method to obtain a globally optimal design of distillation column trays, determining the independent geometrical variables of the tray. Two alternative objective functions were studied: minimization of column cost and mass. The method used is Set Trimming, to sequentially eliminate alternatives that do not follow the inequality constraints.

The analysis of the optimization results indicates that the results found for Set Trimming, after the sorting step, would unlikely be found by a designer guided by heuristic rules. However, the sorting step depends on a designer to select the best candidate.

Another important aspect of the Set Trimming procedure is its capacity to identify all of the global optima of the problem. Therefore, the user can analyze the different optimal solutions, considering other aspects of the problem to choose the more adequate alternative. A similar result using mathematical programming demands a set of recursive runs, which is computationally expensive.

A comparison with two different global solvers (ANTIGONE and BARON) indicates that Set Trimming is more robust than MINLP approaches. For a given sample of optimization problems, Set Trimming always attained the lowest value of the objective function, but mathematical programming approaches were trapped in a local optimum or did not converge in a considerable number of runs (41% of the sample). The computational time of the Set Trimming runs was competitive when compared with the mathematical programming runs.

Therefore, because of its robustness and computational efficiency, the proposed procedure can be a useful tool for the design of distillation columns, especially in situations where its recursive use is needed, such as in design under uncertainty.

3 IMPROVED CORRELATIONS FOR THRESHOLD FLOODING AND ENTRAINMENT IN SIEVE TRAYS IN DISTILLATION/ABSORPTION COLUMNS

The data available in the literature about flooding and entrainment in distillation/absorption columns were originally reported in graphs. Aiming at the use of these data for computational applications, several algebraic correlations were proposed for evaluation of the Souders-Brown flooding constant (*Csb*) and the fractional entrainment (ψ). In this article, we revisit these correlations, using the graphs presented by Fair (1961) as a source of data and targets to match. We digitized these graphs to obtain a set of points for each reported curve. Comparing these data with the correlations predictions, we show that there are considerable deviations. Therefore, we use the collected dataset to re-estimate the parameters of several correlations, also exploring the scheme of splitting the domain of a correlation in multiple regions and estimate parameters for each region. We found that our results reduce the error of the original correlations significantly. We also conducted a study of how the correlations with their original parameters behave when used for designing trays. We show that the mentioned deviations of these correlations can affect the design problem solution, which emphasizes the importance to use the results presented here.

3.1 Introduction

The design of sieve trays in distillation/absorption columns is usually performed by checking proposed geometries for their performance using several hydraulic extremes, namely flooding, entrainment, weeping, downcomer choking, and residence time (Kister, 1992; Towler; Sinnott, 2013; Wankat, 1988). Some of these tests are based on data that were originally presented in the form of graphs. In this article, we are concerned with two: flooding and entrainment.

With the increased use of computers for process equipment design, the need to rely on equations, instead of manual data extraction from graphs emerged. Thus, several correlations attempting to fit the data from these graphs into different expressions as a function of the independent variables were developed.

Correlations for the flooding graphical information presented by Fair (1961) (also reproduced in Fair (1963), Coulson *et al.* (2005), and Kister *et al.* (2008)) were proposed by Economopoulos (1978), Lygeros e Magoulas (1986), Kessler and Wankat (1988), and Ogboja and Kuye (1990). In turn, correlations for entrainment were proposed by Economopoulos (1978), Lygeros and Magoulas (1986), and Ogboja and Kuye (1990). Later, these correlations were employed by many authors involving different separation systems and problems.

The correlations proposed by Economopoulos (1978) were employed for the hydraulic design of CO_2 and H_2S absorbers (Al-Baghli *et al.*, 2001). The correlations proposed by Lygeros e Magoulas (1986) were employed in investigations of the interactions between optimal design and control, involving double-effect distillation (Bansal *et al.*, 2000), reactive distillation (Georgiadis *et al.*, 2002; Miranda *et al.*, 2008), and multicomponent distillation (Bansal; Perkins; Pistikopoulos, 2002). These correlations were also used for the analysis of other separation systems, such as: supercritical fluid extraction (Boukouvalas; Magoulas; Tassios, 1998), high pressure separation of carbon dioxide and methane (Pereira *et al.*, 2011), dehydration of natural gas using triethylene glycol (Jaćimović *et al.*, 2011), and azeotropic separation processes with ionic liquids (Chen *et al.*, 2019). The correlation of Kessler and Wankat (1988) for flooding was used for modelling an ammonia absorber of an ammonia-water refrigeration cycle (Chávez-Islas; Heard, 2009). The liquid entrainment correlation of Ogboja and Kuye (1990) was employed for the nonequilibrium modelling of multicomponent separation processes (Taylor; Kooijman; Hung, 1994). More recently, the correlations of Ogboja and Kuye (1990) were employed in the optimal design of sieve plates using mixed-integer nonlinear programming (Souza; Bagajewicz; Costa, 2022).

The accuracy of the results from the papers mentioned above depends on the accuracy of the employed correlations. Therefore, it is important to evaluate how close the correlations predictions are from the original Fair's data and try to reduce the corresponding errors. The availability of more accurate predictions is important for future works about analysis and optimization of distillation/absortion columns using computational tools.

According to these needs, we compare in this article the correlations predictions with the Fair's dataset, identifying the errors associated with each alternative and providing more accurate options based on the same correlations. The reduction of the errors associated with these correlations was attained by a reevaluation of the correlation parameters through the solution of parameter estimation problems using modern optimization algorithms. The split of the correlations domain and the estimation of the parameters for each resultant region was also employed to provide more accurate results. It is important to observe that the original correlations were published from 1978 until 1990, i.e. the original parameters were determined using older optimization tools, which can explain the accuracy problems shown in this paper (according to our knowledge, there are not newer alternatives of correlations available in the literature).

The current article is organized as follows. Section 3.2 presents the published correlations of flooding and entrainment associated with an analysis of the corresponding errors in relation to the original data from Fair (1961). Section 3.3 presents the objective function for the estimation of the parameters. Section 3.4 presents the results of the parameter estimation of the correlations applied in this paper. Section 3.5 illustrates the application of the correlations with the original and new parameters for the design of distillation columns. The conclusions are finally presented in Section 3.6.

3.2 Accuracy of the correlations available in the literature

To determine the accuracy of the models found in the literature, we obtained numerical values of Fair's curves using the Engauge Digitizer software version 4.1 (Mitchell *et al.*, 2002) and calculated the errors of the correlations proposed to fit the original curves. The data collection corresponds to 328 points about flooding and 379 points about entrainment, individually reported in the Appendix C.

3.2.1 Flooding correlations

A flooding correlation usually determines the limiting velocity of the vapor ($uflood$) in the active zone. In tray rating/design, the following constraint is used (Towler; Sinnott, 2013):

$$un \leq 0.85\, uflood \tag{175}$$

This correlation states that the velocity (un) of the vapor in the active zone must be below 85% of the flooding velocity ($uflood$). In turn, the flooding velocity is given by:

$$uflood = K\, Csb \sqrt{\frac{\rho l - \rho v}{\rho v}} \left(\frac{\sigma}{0.02}\right)^{0.2} \tag{176}$$

where ρl and ρv are the liquid and vapor densities, respectively, σ is the surface tension, K is a constant depending exclusively on the tray geometry and Csb is the Souders-Brown constant. The Souders-Brown constant depends on the tray spacing (*lt*) and the liquid-vapor flow factor (*Flv*):

$$Flv = \frac{L}{V}\sqrt{\frac{\rho v}{\rho l}} \tag{177}$$

where L and V are the liquid and vapor flow rates, respectively.

Fair (1961) presented graphs from which one is supposed to extract the value of Csb. Several correlations were proposed to obtain Csb algebraically, where the parameter values were obtained by undisclosed methods (maybe nonlinear fitting): Economopoulos (1978), Lygeros e Magoulas (1986), Kessler and Wankat (1988), and Ogboja and Kuye (1990). These correlations are shown next, according to the original units of *lt* presented in the respective papers:

Economopoulos (1978):

$$Csb = \min\left[\theta_{Csb,1}\exp\left(\theta_{Csb,2}\, lt(\text{in})\right), \theta_{Csb,3}\exp\left(\theta_{Csb,4} lt(\text{in})\right)\left(\theta_{Csb,5} + \theta_{Csb,6}\ln Flv\right)\right] \tag{178}$$

Lygeros e Magoulas (1986):

$$Csb = \theta_{Csb,1} + \theta_{Csb,2}\,[lt(\text{m})]^{\theta_{Csb,3}}\exp\left(-\theta_{Csb,4}\, Flv^{\theta_{Csb,5}}\right) \tag{179}$$

Ogboja and Kuye (1990):

$$Csb = \theta_{Csb,1} + \theta_{Csb,2}\, lt(\text{m}) + \theta_{Csb,3}\, Flv + \theta_{Csb,4} lt(\text{m})\, Flv + \theta_{Csb,5} Flv^2 + \theta_{Csb,6}\, lt(\text{m})\, Flv^2 \tag{180}$$

Kessler and Wankat (1988), quadratic expressions:

$$\log_{10} Csb = -\theta_{Csb,1} - \theta_{Csb,2}\log_{10} Flv - \theta_{Csb,3}(\log_{10} Flv)^2 \tag{181}$$

Kessler and Wankat (1988), cubic spline expressions:

For $Flv \le 0.1$:

$$\log_{10} Csb = -\theta_{Csb,1} - \theta_{Csb,2}\,(\log_{10} Flv + 2) + \theta_{Csb,3}(\log_{10} Flv + 2)^2 - \theta_{Csb,4}(\log_{10} Flv + 2)^3 \tag{182}$$

For $Flv > 0.1$:

$$\log_{10} Csb = -\theta_{Csb,1} - \theta_{Csb,2}\,(\log_{10} Flv + 1) + \theta_{Csb,3}(\log_{10} Flv + 1)^2 - \theta_{Csb,4}(\log_{10} Flv + 1)^3 \tag{183}$$

where $\theta_{Csb,k}$, for k = 1,…, 6, are correlation parameters, displayed in Tables 11-13 (the parameters of the quadratic and cubic correlations of Kessler and Wankat (1988) depend on the tray spacing and the parameters of the cubic correlation also depend on the *Flv* range).

Table 11 – Parameters of the correlations of Economopoulos (1978), Lygeros e Magoulas (1986), and Ogboja and Kuye (1990)

Correlation	$\theta_{Csb,1}$	$\theta_{Csb,2}$	$\theta_{Csb,3}$	$\theta_{Csb,4}$	$\theta_{Csb,5}$	$\theta_{Csb,6}$
Economopoulos (1978)	0.118	0.0479	0.425	0.0479	0.1092	-0.058
Lygeros e Magoulas (1986)	0.0105	0.1496	0.755	1.463	0.842	-
Ogboja and Kuye (1990)	0.0129	0.1674	0.0063	-0.2686	-0.008	0.1448

Source: Economopoulos, 1978; Lygeros; Magoulas, 1986; Ogboja; Kuye, 1990.

Table 12 – Parameters of the correlation of Kessler and Wankat (1988), quadratic expression

Tray spacing (in)	$\theta_{Csb,1}$	$\theta_{Csb,2}$	$\theta_{Csb,3}$
6	1.1977	0.53143	0.18760
9	1.1622	0.56014	0.18168
12	1.1175	0.61567	0.19510
18	1.0262	0.63513	0.20097
24	0.94506	0.70234	0.22618
36	0.85984	0.73980	0.23735

Source: Kessler; Wankat, 1987.

Table 13 – Parameters of the correlation of Kessler and Wankat (1988), cubic expression

Tray spacing (in)	Flv	$\theta_{Csb,1}$	$\theta_{Csb,2}$	$\theta_{Csb,3}$	$\theta_{Csb,4}$
6	≤ 0.1	0.858	0.0398	0.148	0.112
9		0.744	0.0598	0.100	0.0891
12		0.646	0.00908	0.00179	0.0509
18		0.538	0.0281	0.0319	0.0681
24		0.420	0.0294	0.0636	0.0918
36		0.301	0.0340	0.0389	0.0751
6	> 0.1	0.862	0.0808	0.189	0.0515
9		0.793	0.127	0.167	0.0605
12		0.708	0.165	0.155	0.0729
18		0.602	0.169	0.172	0.0673
24		0.478	0.178	0.212	0.0623
36		0.371	0.181	0.186	0.0985

Source: Kessler; Wankat, 1987.

Tables 14-18 present the errors of the correlations proposed by Economopoulos (1978), Lygeros e Magoulas (1986), Ogboja and Kuye (1990), and Kessler and Wankat (1988), respectively, as compared to the data extracted from the original Fair's graph (Fair (1961)) (the values of tray spacing are depicted in these tables according to the original units of the correlation):

Table 14 – Errors of the flooding correlation by Economopoulos (1978)

Tray spacing (in)	Average error (%)	Maximum error (%)
6	9.09	21.98
9	5.44	15.76
12	4.32	18.48
18	5.56	37.99
24	8.38	53.82
36	52.33	85.06

Source: The author, 2022.

Table 15 – Errors of the flooding correlation by Lygeros and Magoulas (1986)

Tray spacing (m)	Average error (%)	Maximum error (%)
0.1524	5.02	15.90
0.2286	5.05	21.52
0.3048	4.24	13.26
0.4572	4.56	15.09
0.6096	3.12	6.67
0.9144	2.51	4.57

Source: The author, 2022.

Table 16 – Errors of the flooding correlation by Ogboja and Kuye (1990).

Tray spacing (m)	Average error (%)	Maximum error (%)
0.1524	12.78	15.17
0.2286	10.76	208.61
0.3048	11.48	290.24
0.4572	16.39	433.40
0.6096	17.40	504.05
0.9144	14.97	20.71

Source: The author, 2022.

Table 17 – Errors of the flooding quadratic correlation by Kessler and Wankat (1988)

Tray spacing (in)	Average error (%)	Maximum error (%)
6	4.47	7.81
9	5.10	9.79
12	7.43	25.59
18	5.06	15.27
24	5.16	10.55
36	6.67	15.63

Source: The author, 2022.

Table 18 – Errors of the cubic flooding correlation by Kessler and Wankat (1988)

Tray spacing (in)	Average error (%)	Maximum error (%)
6	1.24	7.47
9	1.70	14.81
12	2.99	11.96
18	2.42	11.82
24	2.60	9.83
36	5.53	7.84

Source: The author, 2022.

Figures 13-17 show the points of the data extracted from the original curve and the curves of the correlations of Economopoulos (1978), Lygeros and Magoulas (1986), Ogboja and Kuye (1990), and Kessler and Wankat (1988). The original set of points were reduced from 328 to 45 in these figures for better visualization. The points associated with the maximum errors of each correlation are marked in the graph to provide an identification of the regions with higher deviations between the correlation and the original data.

Figure 13 – Comparison of the original data of the Souders-Brown constant with the correlation proposed by Economopoulos (1978).

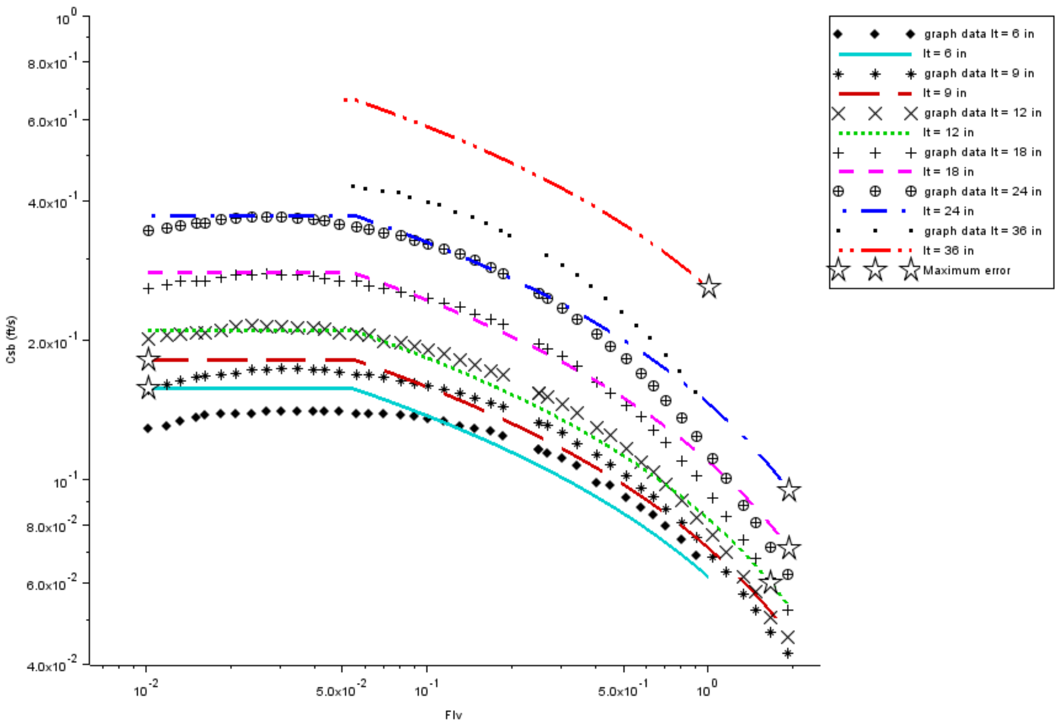

Source: The author, 2022.

Figure 14 - Comparison of the original data of the Souders-Brown constant with the correlation proposed by Lygeros and Magoulas (1986).

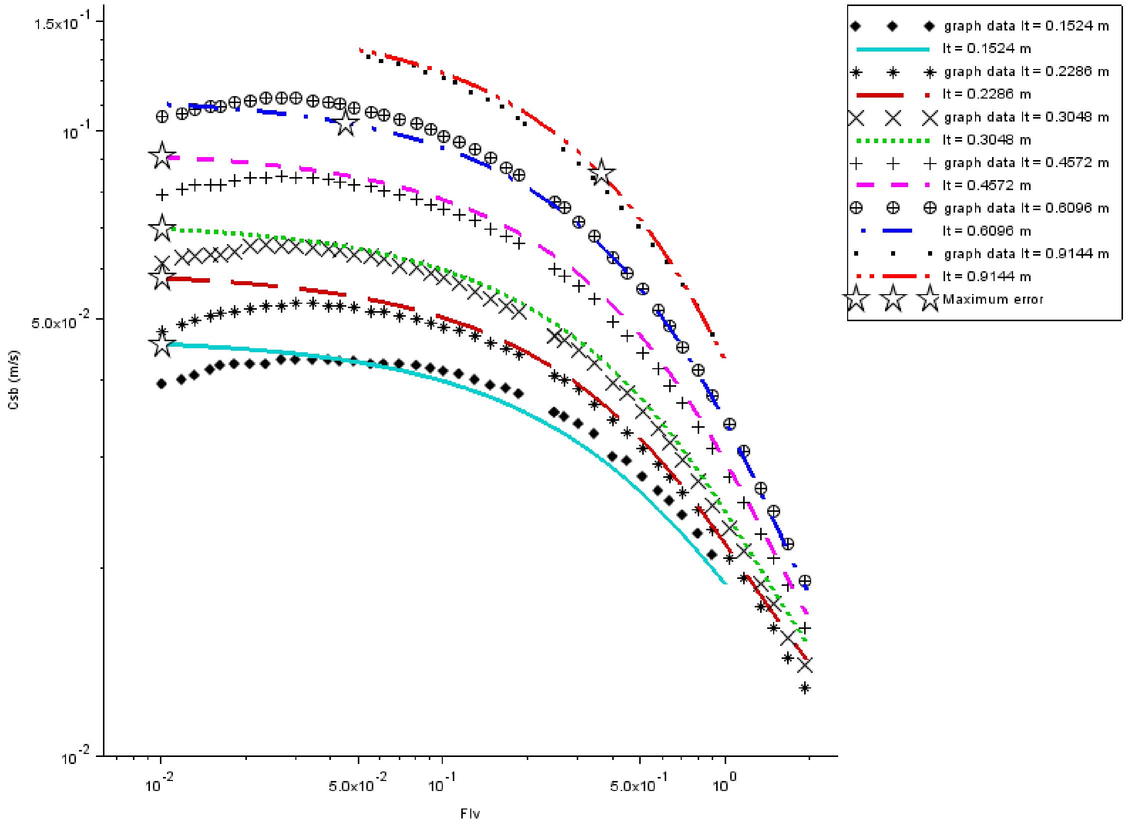

Source: The author, 2022.

Figure 15 – Comparison of the original data of the Souders-Brown constant with the correlation proposed by Ogboja and Kuye (1990).

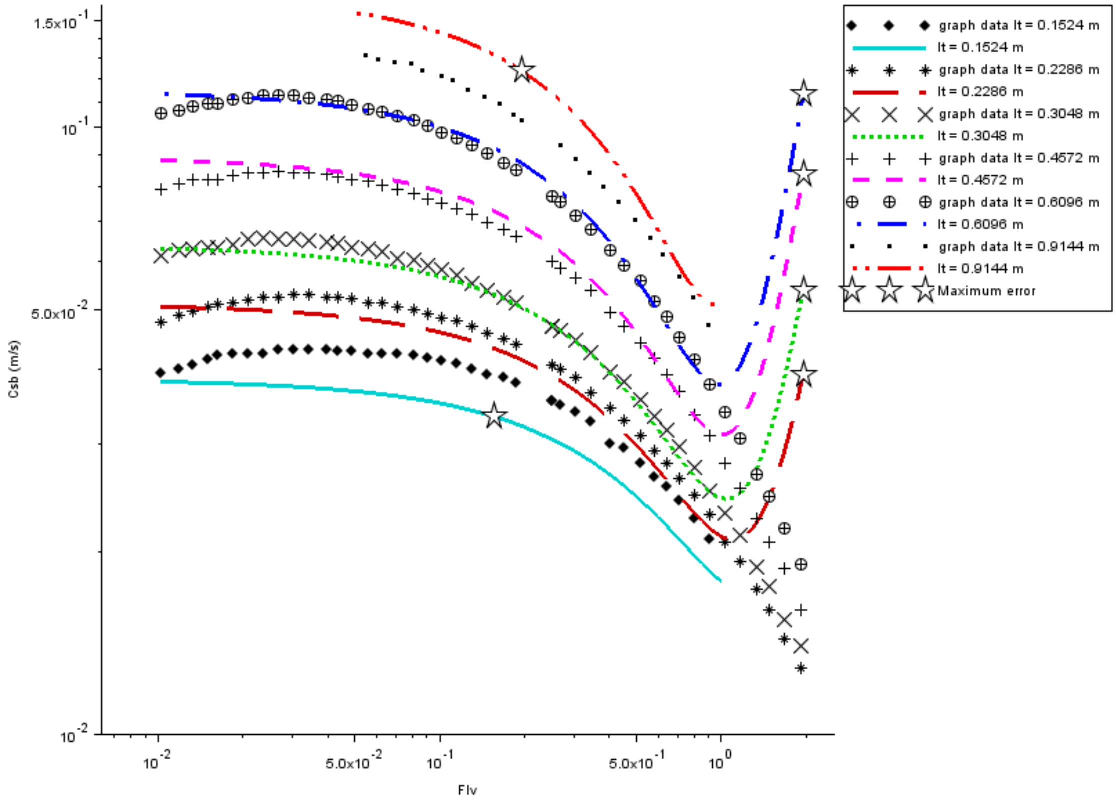

Source: The author, 2022.

Figure 16 – Comparison of the original data of the Souders-Brown constant with the quadratic correlation proposed by Kessler and Wankat (1988).

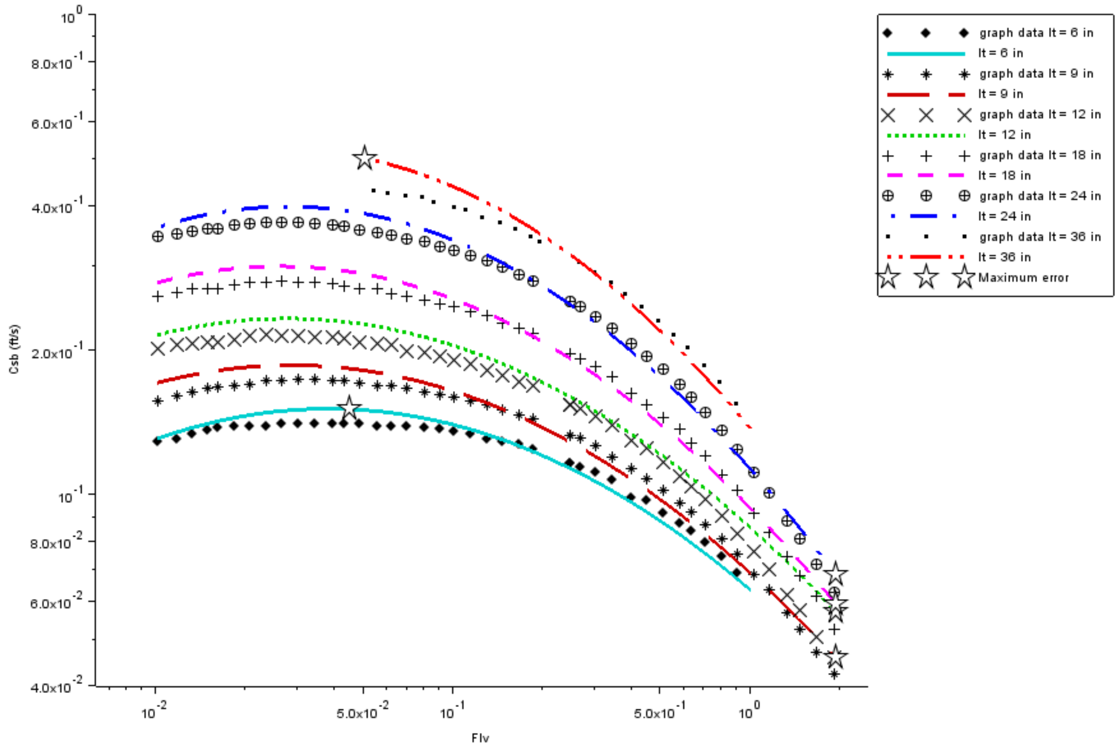

Source: The author, 2022.

Figure 17 - Comparison of the original data of the Souders-Brown constant with the cubic correlation proposed by Kessler and Wankat (1988).

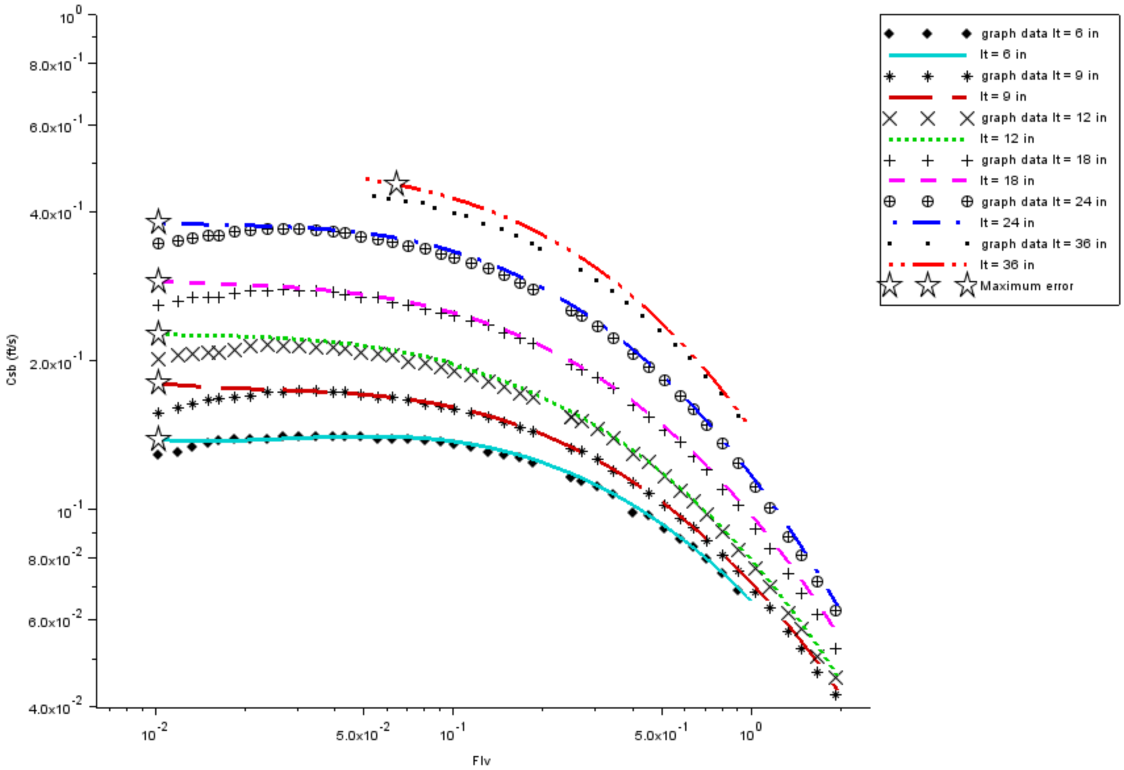

Source: The author, 2022.

The analysis of the accuracy of each correlation indicates the presence of large errors, which can compromise the results of the computational applications that use these correlations.

The correlation of Economopoulos (1978) presents lower accuracy for larger values of tray spacing. It is possible to observe in Figure 13 that the results of this correlation are far from the Fair's data along the entire dataset of the 36 in tray spacing (the maximum error here is 85.06%).

The correlation of Lygeros and Magoulas (1986) is more accurate, with a maximum error of 21.52% (but it is still considerably large). Figure 14 indicates that the higher deviations are concentrated in the data with smaller values of *Flv*.

The correlation of Ogboja and Kuye (1990) presents average errors higher than the correlations of Economopoulos (1978) and Lygeros and Magoulas (1986). The maximum errors are particularly high because the profile of the curves for large values of *Flv* are in an opposite trend when compared with the Fair's data, as it can be observed in Figure 15.

The correlation of Kessler and Wankat (1988) based on a cubic expression presents a better performance than the quadratic expression. The average errors are the smallest ones, compared with the other correlations, but there are errors up to 14.81%. The best performance of this correlation can be explained by the separation of the domain in different regions of tray spacing and *Flv*. Additionally, Kessler and Wankat (1988) correlation are only available for the discrete values of tray spacing reported in Fair (1961) (the dependency with the tray spacing in the other correlations are explicitly include in the mathematical expression).

3.2.2 Entrainment correlations

Entrainment in sieve trays is controlled by limiting the fractional entrainment (ψ), which is defined as the fraction of liquid carried to the tray above by the vapor. Typically, this limit corresponds to the following constraint, employed in rating/design procedures (Towler; Sinnott, 2013):

$$\psi(Fflood) \leq 0.1 \tag{184}$$

where $Fflood$ is the fractional flooding, in turn, defined by:

$$Fflood = \frac{un}{uflood} \tag{185}$$

Ogboja and Kuye (1990), Lygeros and Magoulas (1986), and Economopoulos (1978) proposed the following correlations:

Ogboja and Kuye (1990):

$$\psi = \exp\left[\theta_{\psi,1} + \theta_{\psi,2}\, Fflood - \left(\theta_{\psi,3} + \theta_{\psi,4}\, Fflood\right)\ln(Flv) + \left(\theta_{\psi,5} + \theta_{\psi,6}\, Fflood + \theta_{\psi,7}\, Fflood^2 + \theta_{\psi,8}\, Fflood^3\right)(\ln(Flv))^2\right] \tag{186}$$

Economopoulos (1978):

$$\psi = \exp\left[-\left(\theta_{\psi,1} + \theta_{\psi,2}\, Fflood\right)Flv^{\left(\theta_{\psi,3}+\theta_{\psi,4}Fflood\right)}\right] \tag{187}$$

Lygeros and Magoulas (1986):

$$\psi = \theta_{\psi,1} + \theta_{\psi,2}\exp\left[-\theta_{\psi,3}Flv^{\left(\theta_{\psi,4}\right)}\right] \tag{188}$$

where $\theta_{\psi,k}$, for *k* = 1, …, 8, are correlation parameters (the parameters of the correlation of Lygeros and Magoulas (1986) depend on discrete values of fractional flooding), as depicted in Tables 19 and 20.

Table 19 – Parameters of the correlations of Ogboja and Kuye (1990) and Economopoulos (1978) for evaluation of the fractional entrainment

Correlation	$\theta_{\psi,1}$	$\theta_{\psi,2}$	$\theta_{\psi,3}$	$\theta_{\psi,4}$	$\theta_{\psi,5}$	$\theta_{\psi,6}$	$\theta_{\psi,7}$	$\theta_{\psi,8}$
Ogboja and Kuye (1990)	-7.9196	1.0891	0.0705	2.1916	0.046	-0.605	1.2699	-0.9563
Economopoulos (1978)	6.692	1.956	-0.132	0.654	-	-	-	-

Source: Economopoulos, 1978; Ogboja; Kuye, 1990

Table 20 – Parameters of the correlation of Lygeros and Magoulas (1986) for evaluation of the fractional entrainment

Fractional flooding	$\theta_{\psi,1}$	$\theta_{\psi,2}$	$\theta_{\psi,3}$	$\theta_{\psi,4}$
90%	$0.517 \cdot 10^{-2}$	1.050	10.837	0.511
80%	$0.224 \cdot 10^{-2}$	2.377	9.394	0.314
70%	$-0.509 \cdot 10^{-3}$	81.82	11.389	0.1317
60%	$-0.868 \cdot 10^{-3}$	1537.05	14.205	0.0828

Source: Lygeros; Magoulas, 1986

Tables 21 – 23 present the errors of the models of Economopoulos (1978), Ogboja and Kuye (1990) and Lygeros e Magoulas (1986) as compared to the data extracted from the original Fair's graph.

Table 21 – Errors of the entrainment correlations by Economopoulos (1978).

Fflood (%)	Average error (%)	Maximum error (%)
90	20.73	42.68
80	26.99	48.38
70	28.94	50.60
60	22.88	32.24
50	6.23	13.61
45	5.48	8.34
40	2.95	5.79
35	3.87	15.35
30	9.49	31.56

Source: The author, 2022.

Table 22 – Errors of the entrainment correlations by Ogboja and Kuye (1990).

Fflood (%)	Average error (%)	Maximum error (%)
90	9.02	23.69
80	34.37	75.84
70	36.24	82.41
60	19.27	29.17
50	7.18	24.22
45	8.26	26.15
40	5.69	16.22
35	1.54	4.73
30	23.63	47.92

Source: The author, 2022.

Table 23 – Errors of the entrainment correlations by Lygeros and Magoulas (1986)

Fractional flooding	Average error (%)	Maximum error (%)
90%	15.26	42.88
80%	14.61	37.60
70%	14.54	44.68
60%	12.88	27.52

Source: The author, 2022.

Figures 18 – 20 show the points of the data extracted from the original Fair's graph and the curves of the models of Economopoulos (1978), Ogboja and Kuye (1990), and Lygeros and Magoulas (1986). The original points in these figures were reduced from 380 to 50 points for better visualization. The points associated with the maximum errors of each correlation are marked in the graph to provide an identification of the regions with higher deviations between the correlations and the original data.

Figure 18 - Comparison of the original data of entrainment fraction with the correlation proposed by Economopoulos (1978).

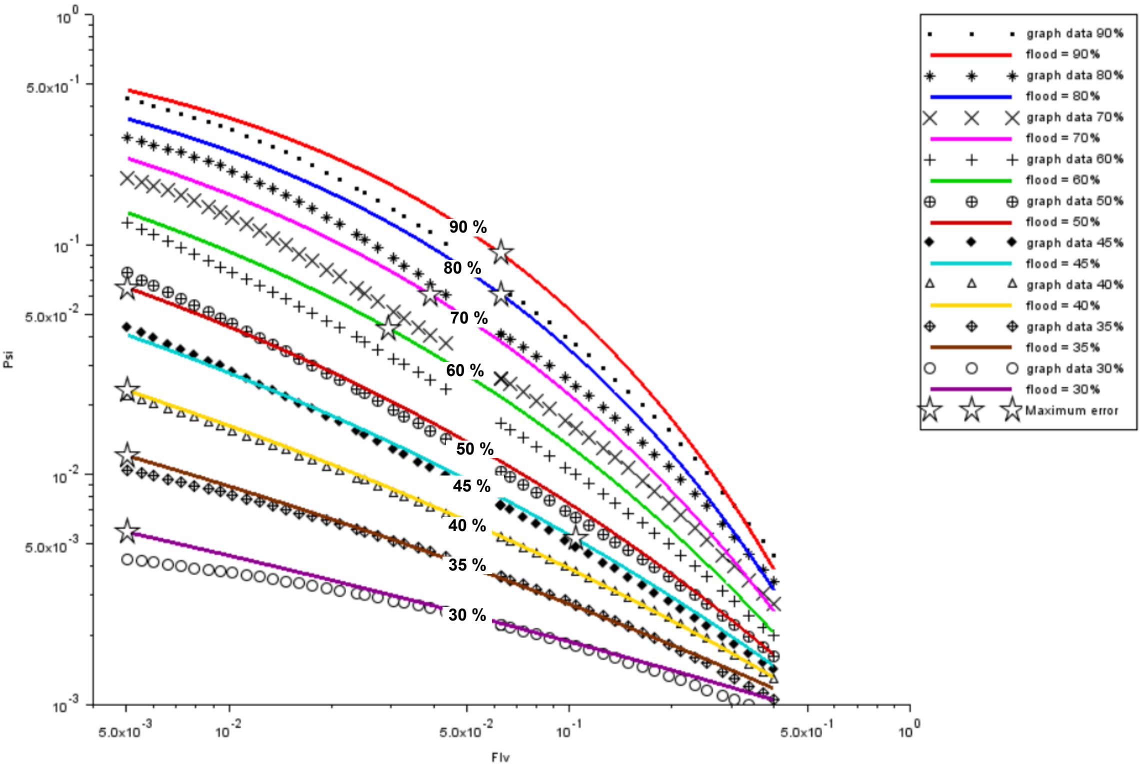

Source: The author, 2022.

Figure 19 - Comparison of the original data of entrainment fraction with the correlation proposed by Ogboja and Kuye (1990)

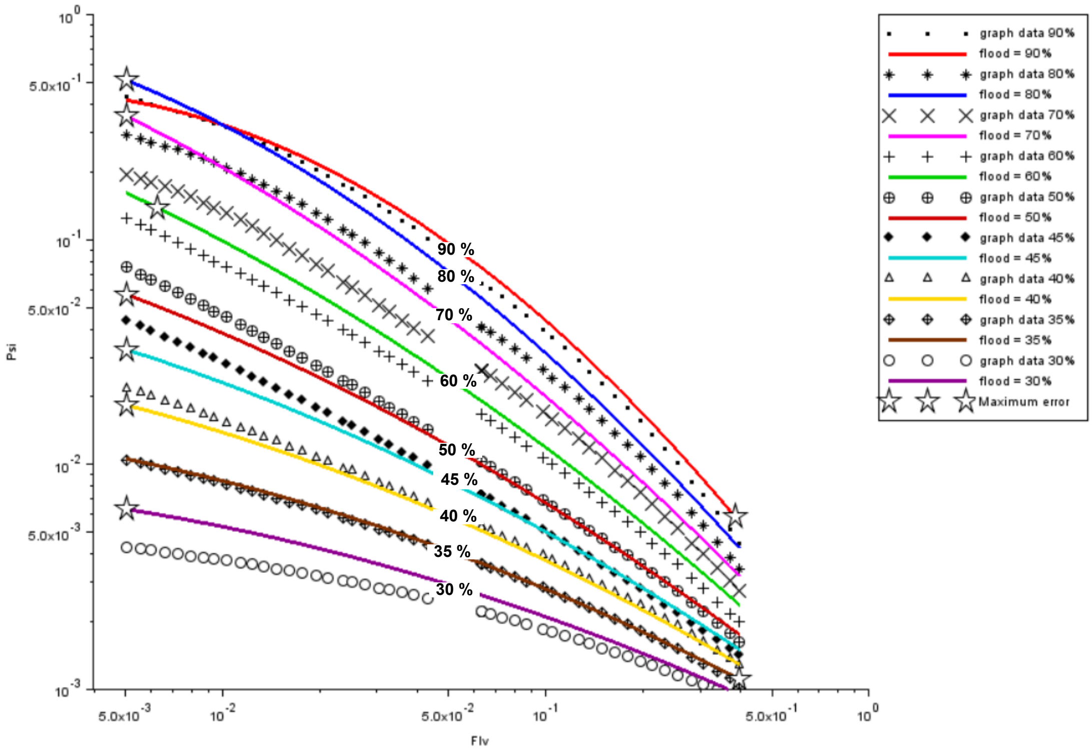

Source: The author, 2022.

Figure 20 - Comparison of the original data of entrainment fraction with the correlation proposed by Lygeros and Magoulas (1986)

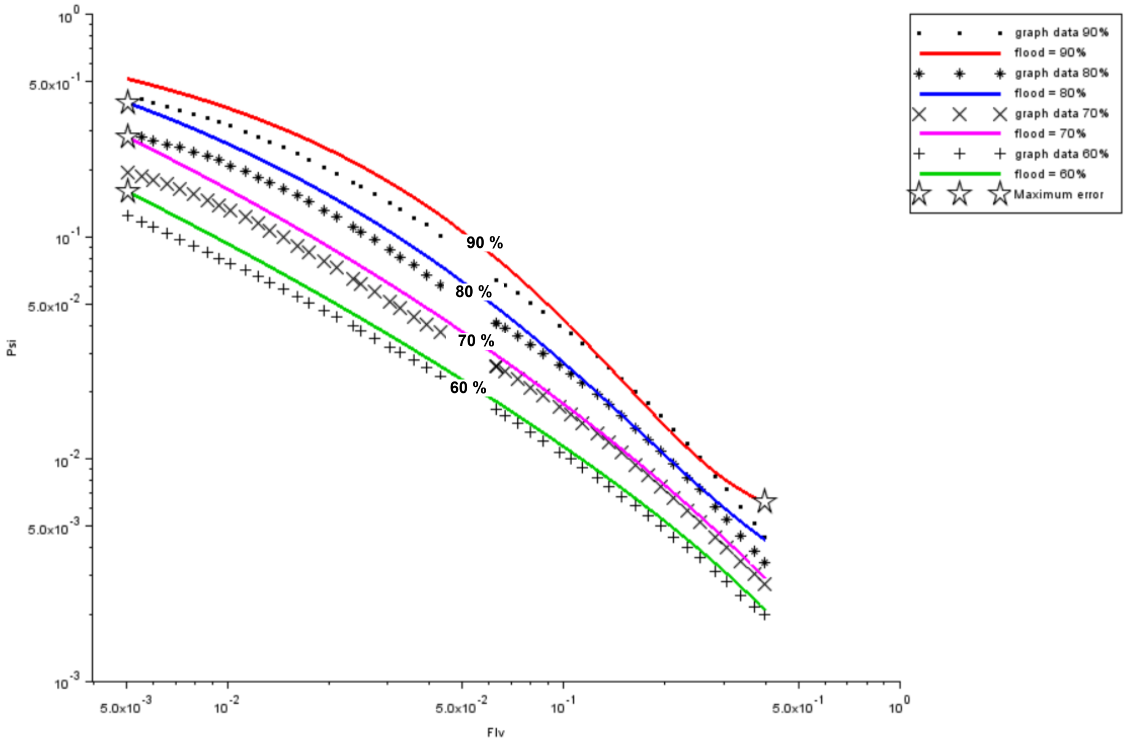

Source: The author, 2022.

The analysis of the performance of each correlation does not indicate clearly the most accurate alternative. The lowest average errors related to different values of fractional flooding are associated with different correlations (e.g. the lowest average error for the values of fractional flooding 35%, 40%, and 60% are associated with the correlations of Ogboja and Kuye (1990), Economopoulos (1978), and Lygeros and Magoulas (1986), respectively).

The maximum errors associated with the correlations of Ogboja and Kuye (1990) and Lygeros and Magoulas (1986) are located at the lowest or at the highest values of *Flv*. The maximum errors of the correlation Economopoulos (1978) are located at the lowest or intermediate values of *Flv*.

3.2.3 Critical analysis

The investigated correlations present different performances, from good adherence to the original data to very poor fittings. The main question to be made is if these errors are tolerable, that is, if the design solutions obtained using these correlations would later violate the operational limits established. Additionally, considering optimization design problems, there is also the issue if the correlations will lead to suboptimal designs.

In the rest of our article, we recalculate the parameters of the above presented correlations. In addition, we study situations in the design procedure where the correlation predictions indicate the acceptance of a distillation column that is, in reality, infeasible (i.e. a "false positive" result) and other situations where the correlation indicates that a certain distillation column is infeasible, but it is actually feasible (i.e. a "false negative" result).

3.3 Parameter estimation procedure

The previous section showed that the errors associated with the correlations available in the literature for the evaluation of flooding and entrainment can be significant. Therefore, aiming at reducing these errors, we applied a parameter estimation procedure to reevaluate the correlations parameters.

The objective function employed for the estimation of the parameters was the weighted least squares:

$$Fobj = \text{Min}_{\theta} \sum_{i=1}^{NP} \frac{\left(y_i^{graph}(x_i) - y_i^{model}(x_i,\boldsymbol{\theta})\right)^2}{\sigma_{y,i}^2} \tag{189}$$

where i is the index of each data point collected from the Fair's graphs (i = 1,…,*NP*), $\boldsymbol{x}_i$ is the vector of the independent variable values at the data point i, $\boldsymbol{\theta}$ is the vector of parameters to be estimated, $y_i^{graph}(\boldsymbol{x_i})$ is the data obtained from the Fair's graph (*Csb* or ψ) for each set of independent variables $\boldsymbol{x_i}$ (*Flv* and *lt* or only *Flv* for flooding correlations, *Flv* and *Fflood* or only *Flv* for the entrainment correlations) and $y_i^{model}(\boldsymbol{x_i},\boldsymbol{\theta})$ is the correlation prediction of the corresponding dependent variable associated with the set of independent variables $\boldsymbol{x}_i$ and parameters $\boldsymbol{\theta}$, and $\sigma_{y,i}^2$ is the variance of the data points. The values of the variance of the data points are unknown, but we use $\sigma_{y,i}^2$ to avoid a bias of the models output towards larger values of the dependent variables. Therefore, the value adopted for $\sigma_{y,i}^2$ is $0.1 y_i^{graph}(\boldsymbol{x}_i)$. This aspect is particularly important due to the large variations of the values of *Csb* and ψ in the dataset collected from the Fair´s graphs.

3.4 Parameter estimation results

The estimation of the parameters for the correlations of flooding and entrainment was conducted without any linearization procedure previously applied to the models. The parameter estimation procedures employed global optimization solvers initialized by the solutions obtained by local solvers, using the GAMS software (version 24.7.1). The unique exception was the parameter estimation of the flooding correlation using the Economopoulos (1978) correlation. In this case, the GAMS solvers failed, then the initialization was provided by a stochastic algorithm and the parameter estimation problem was solved using a local solver from Scilab.

Aiming at providing additional error reductions of the correlation predictions, parameter estimations were also tried using the split of the domain. For each region, different set of parameters were obtained. The corresponding results are shown below. Equivalent results without the domain split of the parameter estimation are available in the Appendix C.

3.4.1 Flooding correlation

In the flooding correlation, the parameters of the models of Lygeros and Magoulas (1986), Kessler and Wankat (1987), Ogboja and Kuye (1990) and Economopoulos (1978) were determined.

The *Flv* domain was split into two regions, followed by the application of the parameter estimation procedure to each region separately (i.e. two sets of parameters were evaluated, each one valid for a given region). The split was made at the median of the values of *Flv*.

3.4.1.1 Lygeros and Magoulas (1986)

The parameters were determined for each discrete value of the tray spacing present in Fair's data using the ANTIGONE solver (Misener; Floudas, 2014) with initial estimates provided by a previous CONOPT solver run (Drud, 1985).

Table 24 shows the new parameters. The errors of the correlation with the new parameters are shown in Table 25. Figure 21 shows the corresponding comparison between the original data and the correlation.

Table 24 – New parameters for the correlation of Lygeros and Magoulas (1986), considering two regions

Tray spacing (m)	Flv	$\theta_{Csb,1}$	$\theta_{Csb,2}$	$\theta_{Csb,3}$	$\theta_{Csb,4}$	$\theta_{Csb,5}$
0.1524		-83.6202	9.02113252	-1.18390552	2.02951064	5.47697064
0.2286		0.04761459	0.70987588	3.51949019	$2.591576 \cdot 10^{+6}$	6.18532635
0.3048	≤ 0.12	0.05633279	0.59564551	3.62416469	$1.367922 \cdot 10^{+4}$	3.92480287
0.4572		0.07300709	0.56207926	5.14476362	$2.253357 \cdot 10^{+4}$	4.09383704
0.6096		0.09482061	0.83479308	8.02227176	$1.022961 \cdot 10^{+4}$	3.78047576
0.9144		0.14942903	-0.00867470	0.63306988	-5.75281342	0.67489572
0.1524		0.00976870	0.15259236	0.75500000	1.29662151	0.92188085
0.2286		0.00514023	0.16754077	0.75499476	1.21933126	0.73465549
0.3048	> 0.12	0.00701328	0.15604655	0.75500000	1.34131675	0.77460268
0.4572		0.00567572	0.17037018	0.75500000	1.40632291	0.67788468
0.6096		0.00771888	0.17865301	0.75500000	1.50815571	0.69988173
0.9144		-0.01764596	0.23479760	1.94962958	1.17643572	0.53675747

Source: The author, 2022.

Table 25 – Errors of the flooding correlation by Lygeros and Magoulas (1986) with new parameters, considering two regions

Tray spacing (m)	Average error (%)	Maximum error (%)
0.1524	0.99	7.05
0.2286	0.89	7.82
0.3048	0.71	4.66
0.4572	0.74	5.19
0.6096	0.77	4.84
0.9144	0.25	0.94

Source: The author, 2022.

Figure 21 - Comparison of Fair’s data from Souders-Brown constant with the correlation proposed by Lygeros and Magoulas (1986) with new parameters, considering two regions

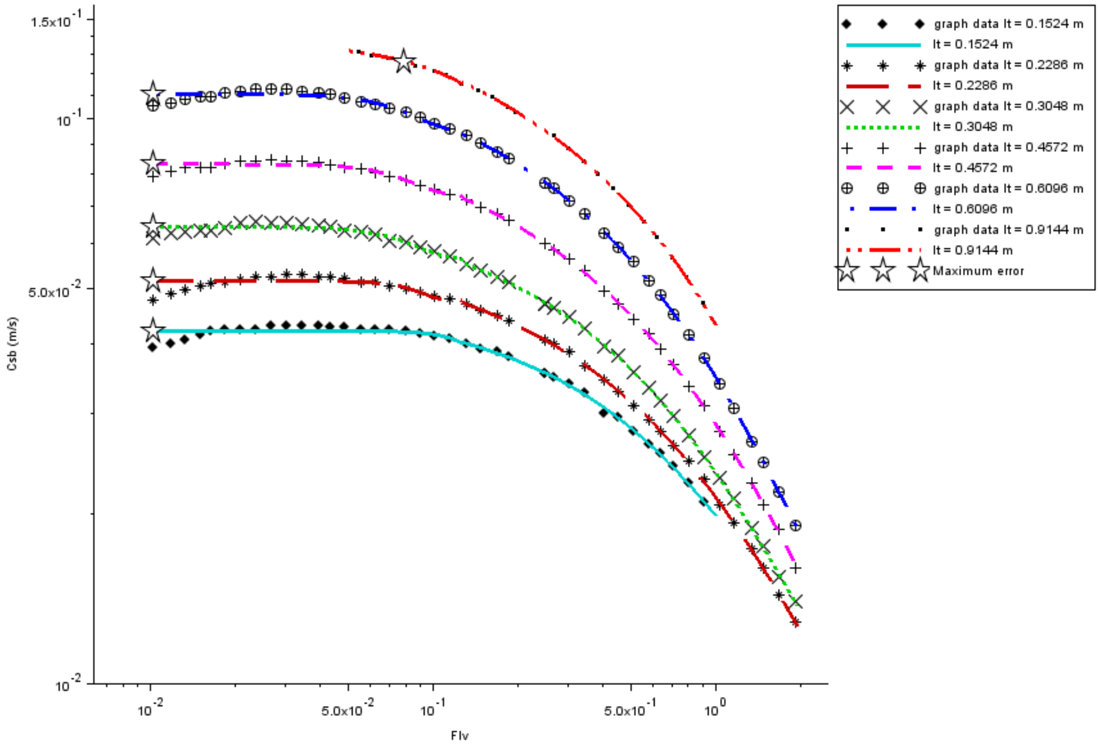

Source: The author, 2022.

3.4.1.2 Kessler and Wankat (1988)

New parameters were estimated for the Kessler and Wankat (1988) correlation for each discrete value of the tray spacing. Only the quadratic equation was employed because it is simpler and provided a good fit. The parameter estimation problem was solved using the BARON solver (Sahinidis, 1996) associated with the CONOPT solver (Drud, 1985) to provide an initial estimate.

Table 26 shows the new parameters after splitting *Flv* into two regions, Table 27 shows the errors of the correlation with new parameters for each region and Figure 22 shows a comparison between the original data and the correlation predictions.

Table 26 – New parameters of the quadratic correlation of Kessler and Wankat (1988), considering two regions

Tray spacing (in)	Flv	$\theta_{Csb,1}$	$\theta_{Csb,2}$	$\theta_{Csb,3}$
6	≤ 0.1263	1.0605	0.2969	0.1054
9		1.0973	0.4533	0.1533
12		1.0454	0.4795	0.1528
18		0.9432	0.4925	0.1576
24		0.8635	0.5450	0.1729
36		0.8152	0.6473	0.2313
6	> 0.1263	1.1837	0.5868	0.2814
9		1.1563	0.6597	0.3127
12		1.1110	0.7059	0.3320
18		1.0270	0.7434	0.3360
24		0.9423	0.7964	0.3596
36		0.8393	0.7543	0.3245

Source: The author, 2022.

Table 27 - Errors of the flooding quadratic correlation by Kessler and Wankat (1988) with new parameters, considering two regions

Tray Spacing (in)	Average error (%)	Maximum error (%)
6	0.46	2.47
9	0.44	2.07
12	0.45	2.48
18	0.50	4.27
24	0.52	1.82
36	0.45	2.81

Source: The author, 2022.

Figure 22 – Comparison of Fair's data from Souders-Brown constant with the quadratic correlation proposed by Kessler and Wankat (1988) with new parameters, considering two regions

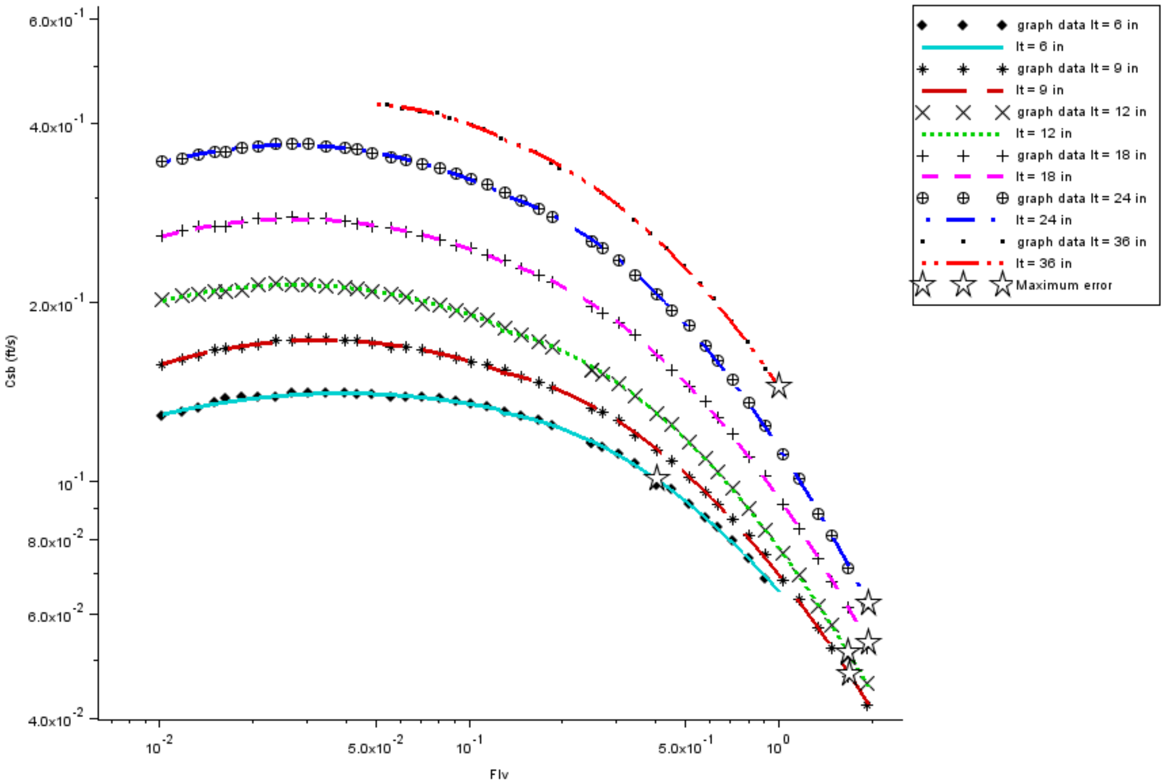

Source: The author, 2022.

3.4.1.3 Ogboja and Kuye (1990)

New parameters were determined for each discrete value of the tray spacing for the Ogboja and Kuye (1990). The parameter estimation problem was solved using the BARON solver (Sahinidis, 1996) associated with the CONOPT solver (Drud, 1985) to provide an initial estimate.

Table 28 shows the new parameters considering the split of the *Flv* range in two regions. The errors of the correlation with the new parameters are shown in Table 29 and Figure 23 shows the corresponding comparison between the original data and the correlation.

Table 28 – New parameters for the correlation of Ogboja and Kuye (1990), considering two regions

Tray spacing (m)	Flv	$\theta_{Csb,1}$	$\theta_{Csb,2}$	$\theta_{Csb,3}$	$\theta_{Csb,4}$	$\theta_{Csb,5}$	$\theta_{Csb,6}$
0.1524	≤ 0.1263	-0.4168	3.0206	-0.3346	1.9667	3.0713	-20.0825
0.2286		0.0525	0	-0.0461	0	0.0138	0
0.3048		0.7902	-2.3816	-0.2686	0.6759	-1.2452	4.1504
0.4572		-1.2979	3.0206	-0.9831	1.9667	-0.3059	0.7279
0.6096		0.1098	0	-0.1174	0	0.03841	0
0.9144		-2.6236	3.0206	-1.9837	1.9667	3.0713	-3.2559
0.1524	> 0.1263	0.0129	0.2011	0.0061	-0.2686	-0.008	0.1229
0.2286		0.0129	0.1731	0.0153	-0.2686	-0.008	0.0954
0.3048		0.0129	0.1688	0.0193	-0.2686	-0.008	0.0914
0.4572		0.0129	0.1535	0.0388	-0.2686	-0.008	0.0763
0.6096		0.0129	0.1589	0.0464	-0.2686	-0.008	0.0761
0.9144		0.0129	0.1373	0.0603	-0.2686	-0.008	0.1116

Source: The author, 2022.

Table 29 – Error the flooding correlation by Ogboja and Kuye (1990) with new parameters, considering two regions

Tray spacing (m)	Average error (%)	Maximum error (%)
0.1524	1.94	9.88
0.2286	3.20	18.81
0.3048	4.16	29.10
0.4572	4.55	37.23
0.6096	5.46	43.77
0.9144	2.01	10.38

Source: The author, 2022.

Figure 23 – Comparison of Fair’s data from Souders-Brown constant with the correlation proposed by Ogboja and Kuye (1990) with new parameters, considering two regions

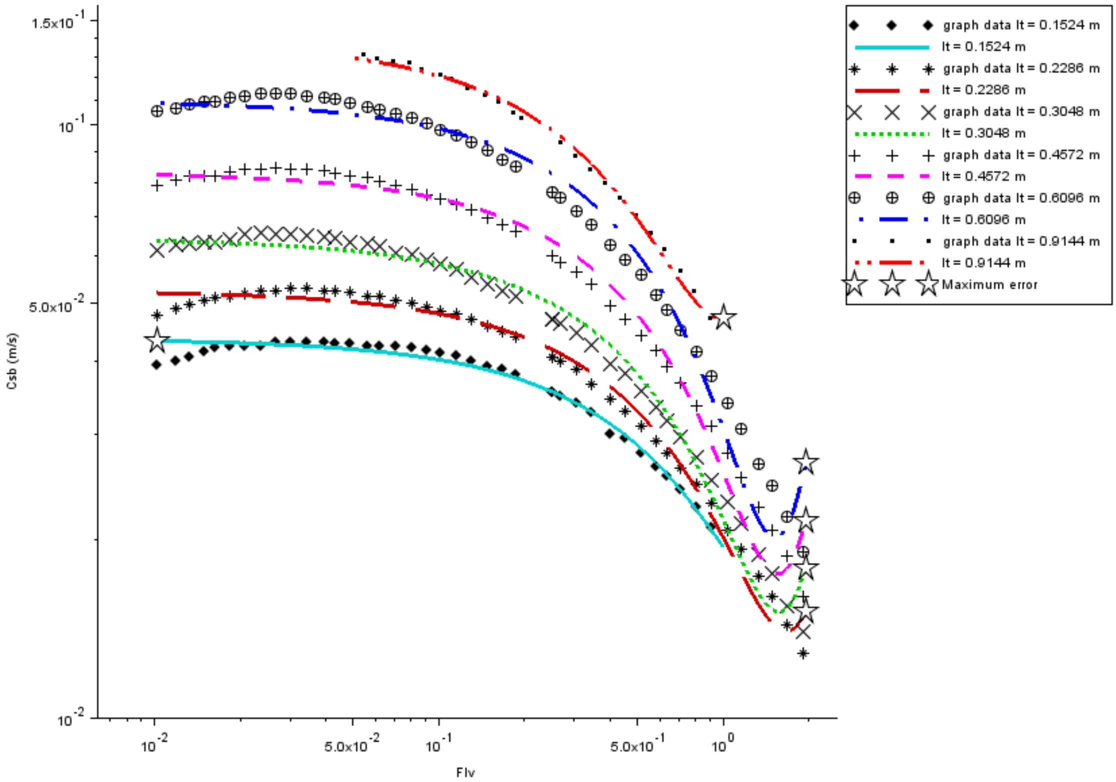

Source: The author, 2022.

3.4.1.4 Economopoulos (1978)

The parameters were determined for each discrete value of the tray spacing present in Fair’s data considering the split of the *Flv* range in two regions. The Simplex optimization method (Nelder; Mead, 1965; Spendley; Hext; Himsworth, 1962) was used with initial estimates provided by the Particle Swarm Optimization (PSO) (Kennedy; Eberhart, 1995). Because of the stochastic nature of PSO, 10 parameter estimation runs were made and the one with the lowest objective function is presented here.

The results are shown in Table 30. Table 31 shows the errors of the correlation with the new values of the parameters and Figure 24 shows the corresponding comparison between the original data and the correlation.

Table 30 – New parameters for the correlation of Economopoulos (1978), considering two regions

Tray Spacing (in)	Flv	$\theta_{Csb,1}$	$\theta_{Csb,2}$	$\theta_{Csb,3}$	$\theta_{Csb,4}$	$\theta_{Csb,5}$	$\theta_{Csb,6}$
6	≤ 0.1263	4.4000697	- 0.5775733	4.8304139	2.6799314	4.4557714	- 3.103613
9		4.7269972	- 0.3699619	- 4.999006	- 0.5977399	- 4.9983493	0.8334274
12		4.7459131	- 0.2593782	- 4.3885062	- 0.4428965	- 5.9949766	1.2393609
18		4.9470236	- 0.1610794	- 4.9915123	- 0.2783693	- 4.9998887	1.0445176
24		4.9999759	- 0.1093138	- 4.1404762	- 0.1918679	- 4.9961433	1.2133206
36		4.1266714	3.1289251	- 3.6024925	- 0.1147729	- 4.6425641	0.9738661
6	> 0.1263	4.5178369	- 0.5942546	4.8414634	- 0.9702420	4.6445794	- 2.557437
9		3.7605707	- 0.3571457	4.6764574	- 0.6410964	4.8750665	- 3.0671162
12		4.3937897	4.667488	4.9192652	- 0.4728603	4.7185437	- 3.1293533
18		3.0470916	3.5050506	4.9563515	- 0.3076338	4.9621191	- 3.6316262
24		3.3388334	3.2393369	4.7410224	- 0.2191914	4.797542	- 3.8619151
36		3.8511541	3.7137044	4.6400848	- 0.1383541	4.6007155	- 3.6763634

Source: The author, 2022.

Table 31 – Error the flooding correlation by Economopoulos (1978) with new parameters, considering two regions

Tray Spacing (in)	Average error (%)	Maximum error (%)
6	1.46	6.67
9	1.45	7.89
12	1.41	4.64
18	1.21	5.17
24	1.38	11.16
36	0.91	4.11

Source: The author, 2022.

Figure 24 – Comparison of Fair’s data from Souders-Brown constant with the correlation proposed by Economopoulos (1978) with new parameters, considering two regions

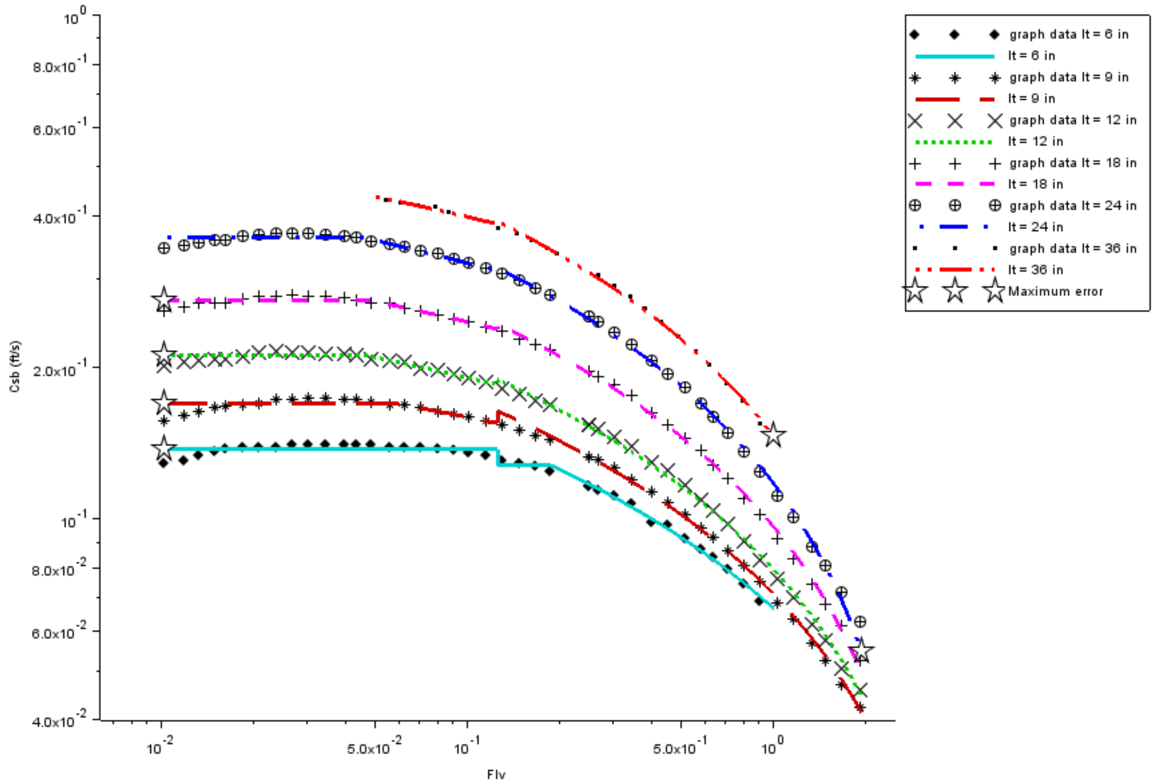

Source: The author, 2022.

3.4.1.5 Performance comparison

Table 32 shows a comparison of the accuracy of the flooding correlations with the original parameters (Tables 14 and 18) and with the parameters obtained in this paper (Tables 25, 27, 29 and 31) for different values of tray spacing. According to these data, there is a considerable reduction of the average and maximum errors (e.g. the upper bounds of the average and maximum error ranges were reduced by more than a half).

Table 32 – Performance comparison of the entrainment correlations with the original parameter and the new ones

Correlation	Original parameters Average error range (%)	Original parameters Maximum error range (%)	Parameters from this paper Average error range (%)	Parameters from this paper Maximum error range (%)
Lygeros and Magoulas (1986)	2.51 - 5.05	4.57 - 21.52	0.25 - 0.99	0.94 – 7.82
Kessler and Wankat (1988)	1.24 - 5.53	7.47 - 14.81	0.44 – 0.52	1.82 – 4.27
Ogboja and Kuye (1990)	10.76 - 17.40	15.17 - 504.05	1.94 – 5.46	9.88 – 43.77
Economopoulos (1978)	4.32 - 52.33	15.76 - 85.06	0.91 – 1.46	4.11 – 11.16

Source: The author, 2022.

3.4.2 Entrainment correlation

The parameters of the correlations of Economopoulos (1978), Ogboja and Kuye (1990), and Lygeros and Magoulas (1986) were reevaluated using the parameter estimation procedure discussed in the previous section. Considering the reduction of the error shown above through the split of the correlation domain, the same procedure was applied here. Instead of using a single set of parameters for the entire domain of the independent variables, the domain was split in a certain number of regions and the parameter estimation was applied for each region.

3.4.2.1 Economopoulos (1978)

The parameter estimation of the Economopoulos (1978) correlation model was done by splitting the domain of *Flv* and *Fflood* in 6 regions. The parameter estimation problem was solved using the ANTIGONE solver (Misener; Floudas, 2014) with initial estimates provided by a previous CONOPT solver run (Drud, 1985). The results are displayed in Table 33. Table 34 shows the errors of the correlation with new parameters. Figure 25 shows the comparison between the Fair's data and the correlation with new parameters.

Table 33 – New parameters of the correlation of Economopoulos (1978) for evaluation of the fractional entrainment

Flv	$Fflood$	$\theta_{\psi,1}$	$\theta_{\psi,2}$	$\theta_{\psi,3}$	$\theta_{\psi,4}$
$Flv \leq 0.05$	$Fflood \geq 0.6$	3.377	8.327	-0.211	0.773
$0.05 < Flv \leq 0.1$	$Fflood \geq 0.6$	3.896	4.551	-0.273	0.734
$Flv > 0.1$	$Fflood \geq 0.6$	7.758	-0.175	-0.062	0.478
$Flv \leq 0.05$	$Fflood < 0.6$	3.862	9.567	-0.233	0.916
$0.05 < Flv \leq 0.1$	$Fflood < 0.6$	7.028	1.145	-0.098	0.563
$Flv > 0.1$	$Fflood < 0.6$	7.434	0.267	-0.071	0.503

Source: The author, 2022.

Table 34 – Errors of entrainment correlations by Economopoulos (1978) with new parameters, considering multiple regions

Fflood (%)	Average error (%)	Maximum error (%)
90	1.95	7.91
80	1.56	7.10
70	2.01	7.23
60	2.72	11.40
50	1.26	4.08
45	1.42	3.75
40	2.72	5.25
35	2.96	4.92
30	3.85	8.24

Source: The author, 2022.

Figure 25 – Comparison of Fair’s data from entrainment fraction with the correlation proposed by Economopoulos (1978) with new parameters, considering multiple regions

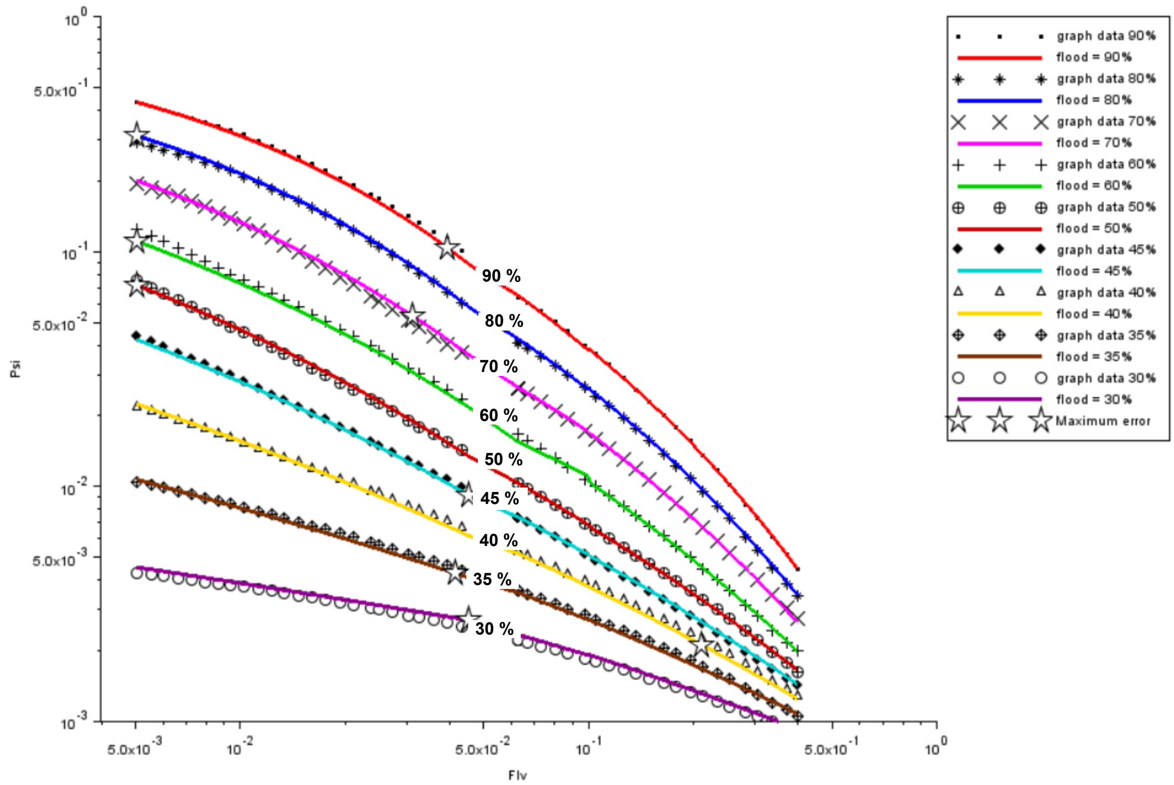

Source: The author, 2022.

3.4.2.2 Ogboja and Kuye (1990)

The parameter estimation of the correlation of Ogboja and Kuye (1990) was done by splitting the domain of *Flv* and *Fflood* in 3 regions using the solver CONOPT (Drud, 1985). The results are displayed in Table 35. Table 36 shows the errors and the corresponding standard deviation of the correlation with the new parameters. Figure 26 shows the comparison between the Fair’s data and the correlation prediction.

Table 35 – New parameters of the correlation of Ogboja and Kuye (1990) for evaluation of the fractional entrainment, considering multiple regions

Flv	$Fflood$	$\theta_{\psi,1}$	$\theta_{\psi,2}$	$\theta_{\psi,3}$	$\theta_{\psi,4}$	$\theta_{\psi,5}$	$\theta_{\psi,6}$	$\theta_{\psi,7}$	$\theta_{\psi,8}$
$Flv \leq 0.15$	$Fflood \geq 0.5$	-7.395	0.324	-0.222	2.516	0.146	-0.430	0.234	-0.153
$Flv > 0.15$	$Fflood \geq 0.5$	-7.743	0.270	-0.170	3.001	0.927	-3.806	4.706	-2.217
$\forall Flv$	$Fflood < 0.5$	-7.903	1.135	-0.073	2.066	-0.647	4.309	-10.301	8.308

Source: The author, 2022.

Table 36 – Errors of the entrainment correlations of Ogboja and Kuye (1990) with new parameters, considering multiple regions

Fflood (%)	Average error (%)	Maximum error (%)
90	1.17	4.58
80	1.56	4.84
70	2.54	6.09
60	0.69	3.94
50	1.51	3.57
45	1.64	5.62
40	2.03	4.25
35	1.59	4.78
30	2.69	4.44

Source: The author, 2022.

Figure 26 – Comparison of the original data from entrainment fraction with the correlation proposed by Ogboja and Kuye (1990) with new parameters

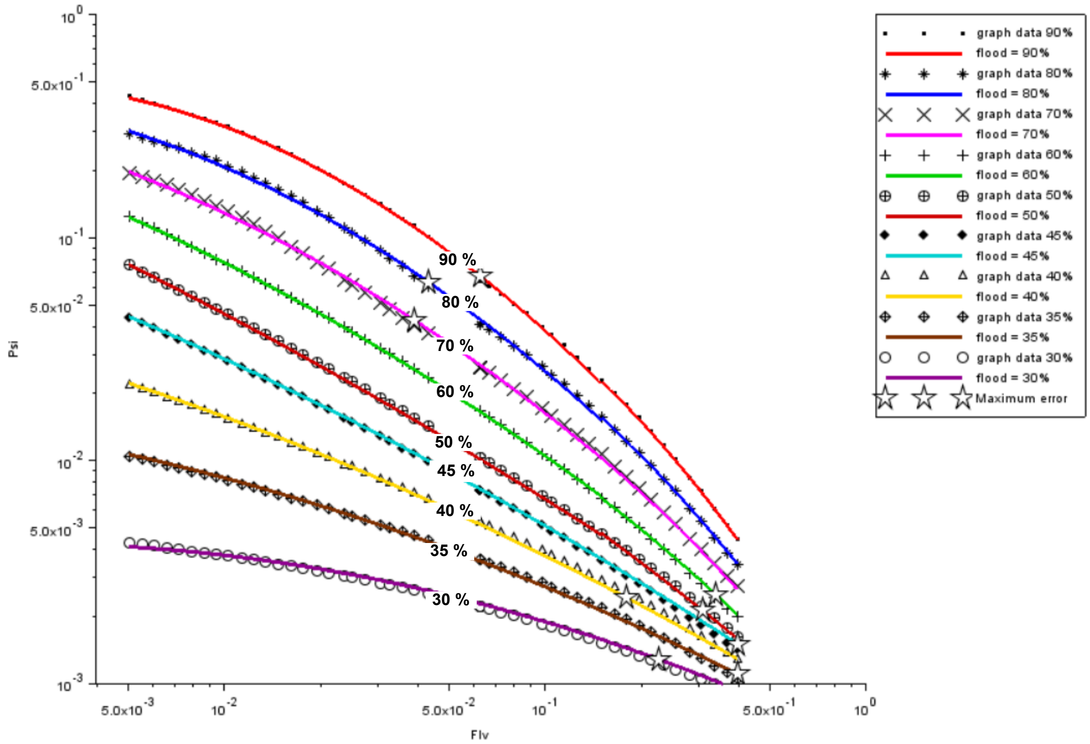

Source: The author, 2022.

3.4.2.3 Lygeros and Magoulas (1986)

The parameter estimation of the Lygeros and Magoulas (1986) correlation was done for each discrete value of the flooding fraction present in Fair's graph using the solver CONOPT (Drud, 1985).

The estimated parameters are shown in Table 37. Table 38 shows the errors of the correlation with the new parameters and Figure 27 shows the comparison between the Fair's data and the correlation prediction.

Table 37 – New parameters of the correlation of Lygeros and Magoulas (1986) for evaluation of the fractional entrainment for each *Fflood* value

Fflood (%)	$\theta_{\psi,1}$	$\theta_{\psi,2}$	$\theta_{\psi,3}$	$\theta_{\psi,4}$
90	$3.178{\cdot}10^{-3}$	1.262	9.116	0.4071
80	$2.067{\cdot}10^{-3}$	1.381	8.794	0.3322
70	$4.499{\cdot}10^{-4}$	4.741	9.054	0.2003
60	$-6.575{\cdot}10^{-4}$	23.761	10.264	0.1270
50	$-2.475{\cdot}10^{-4}$	531.301	13.484	0.0794
45	$-1.377{\cdot}10^{-4}$	38.812	11.025	0.0919
40	$-4.035{\cdot}10^{-4}$	6.598	8.946	0.0857
35	$-3.152{\cdot}10^{-4}$	0.0742	4.658	0.1666
30	$2.677{\cdot}10^{-4}$	0.0066	3.242	0.3532

Source: The author, 2022.

Table 38 – Errors of entrainment correlations by Lygeros and Magoulas (1986) with new parameters for each *Fflood* value

Fflood (%)	Average error (%)	Maximum error (%)
90	2.35	25.01
80	3.01	22.32
70	2.72	9.10
60	0.24	3.40
50	0.36	2.77
45	0.19	1.02
40	0.26	1.61
35	0.18	0.56
30	0.23	1.22

Source: The author, 2022.

Figure 27 – Comparison of experimental data from entrainment fraction with the correlation proposed by Lygeros and Magoulas (1986) with new parameters

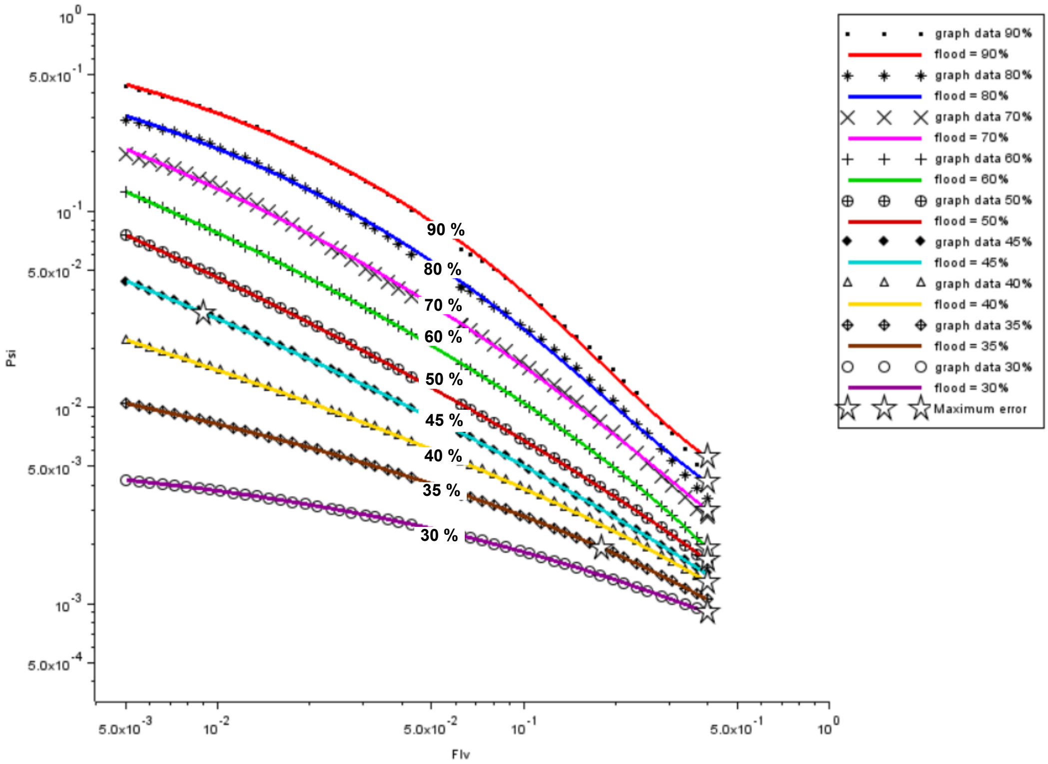

Source: The author, 2022.

3.4.2.4 Performance comparison

Table 39 shows a comparison of the accuracy of the entrainment correlations with the original parameters (Tables 21 - 23) and with the parameters obtained in this paper (Tables 34, 36 and 38) for different values of fractional flooding. It is possible to observe that a large improvement of the model predictions was attained.

Table 39 – Performance comparison of the entrainment correlations with the original parameter and the new ones

Correlation	Original parameters: Average error range (%)	Original parameters: Maximum error range (%)	Parameters from this paper: Average error range (%)	Parameters from this paper: Maximum error range (%)
Economopoulos (1978)	2.95 - 28.94	5.79 - 50.60	1.26 - 3.85	3.75 – 11.40
Ogboja and Kuye (1990)	1.54 - 36.24	4.73 - 82.41	0.69- 2.69	3.57 – 6.09
Lygeros and Magoulas (1986)	12.88 - 15.26	27.52 - 44.68	0.18 – 3.01	0.56 – 25.01

Source: The author, 2022.

3.5 Performance of the correlations

This paper has shown that the correlations available in the literature for sieve tray performance may present considerable deviations in relation to the original Fair's data and the application of a new procedure for parameter estimation can reduce these errors significantly.

Therefore, considering that the original correlations were employed in several other papers, this section presents an analysis of how the corresponding deviations can affect the design of a distillation column, comparing the design solutions obtained using these correlations with the design solutions using the improved predictions developed in this paper.

Three design optimization problems of distillation columns were considered. Example 1 is the design of a depropanizer column and was taken from Kister (1992), with larger flow rates (the original values of the flow rates were multiplied by 2.0). Example 2 is the design of a distillation column for acetone recovery from a waste stream and was taken from Towler and Sinnott (2013), also with larger flow rates (the original values were multiplied by 2.0). Example 3 consists of a methanol purification column and was taken from Kiss and Ignat (2012), with lower flow rates (the original values were multiplied by 0.5). The optimization search space and the details of each example are described in the Appendix C.

The distillation column of each example was optimally designed using the Set Trimming procedure described by Costa and Bagajewicz (2019), applied to sieve tray design (Souza; Bagajewicz; Costa, 2023). This procedure guarantees global optimality of the design problem and is robust.

The design problems were solved using two different alternatives of flooding and entrainment correlations from the literature, with their original parameters: Economopoulos (1978) and Ogboja and Kuye (1990). The same problems were also solved using the best results developed in this paper, represented by the correlations of Kessler and Wankat (1988) for flooding and Ogboja and Kuye (1990) for entrainment, with the new parameters calculated here. The optimal design solutions are depicted in Table 40. The geometric details of each optimal solution are described in the Appendix C.

Table 40 – Design Results

Example	Result	Economopoulos (1978)	Ogboja and Kuye (1990)	New correlations parameters
1	Cost total ($)	316,361.07	352,484.38	441,644.54
	Column diameter (m)	3.0480	3.3528	4.064
	Tray spacing (m)	0.9144	0.9144	0.9144
2	Cost total ($)	36,738.14	45,604.67	40,852.56
	Column diameter (m)	0.9144	1.2700	1.2700
	Tray spacing (m)	0.9144	0.6096	0.4572
3	Cost total ($)	31,955.10	31,955.10	30,643.87
	Column diameter (m)	0.7620	0.7620	0.6096
	Tray spacing (m)	0.4572	0.4572	0.6096

Source: The author, 2022.

The results displayed in Table 40 indicate that the deviations of the literature correlations predictions have a direct impact in the design results. In Example 1, the original literature correlations are associated with distillation columns with smaller diameters. However, considering that the correlations with the new parameters proposed in the current paper provide the most accurate predictions, the distillation columns designed with the original correlations may not operate adequately. The opposite situation occurs in Example 3, the distillation columns designed with the original correlations are associated with a larger diameter, i.e. the literature correlations excluded from the search feasible distillation column associated with a smaller capital cost. The results of Example 2 contain both problems: one column designed using the literature correlations is infeasible and the other is unnecessarily expensive.

Aiming at providing a better comprehension of the detachments indicated in Table 40, the analysis of the correlations was also conducted through the evaluation of each solution candidate of the search space of the design problem. This analysis is based on 783,900 different candidate solutions composed of different plate dimensions.

Considering the constraints of flooding (Eq. (175)) and entrainment (Eq. (184)), the results are classified in four different classes, based on the comparison of the plates that did or did not abide by the restrictions of flooding and entrainment.

- Feasible: feasible design under the correlation from the literature and the predictions developed in this paper.
- Infeasible: infeasible design under the correlation from the literature and the predictions developed in this paper.
- False positive: the correlation of the literature indicates that the design is feasible, but the prediction developed in this paper indicates that the design is not feasible.
- False negative: the correlation of the literature indicates that the design is infeasible, but the prediction developed in this paper indicates that the design is feasible.

The main deviations are associated with the design problem of Example 1, as discussed below. The comparison of the performance of the correlations of Economopoulos (1978) with our predictions is shown in Figure 28. False positives are associated with the flooding constraint and false negatives are associated in the entrainment constraint, as shown in Figure 28a and 28b, respectively. These deviations are relevant because they affect the solution of the optimal design problem, as shown in Table 40. The solution of the optimal design problem using the correlation of Economopoulos (1978) is a distillation column with a cost of $316,361.07. However, this solution is a false positive, i.e. testing this optimal design with the more accurate predictions developed in this paper, it is verified that this column is not feasible.

Figure 28 – Example 1: Comparison between correlations of the Economopoulos (1978) and our predictions

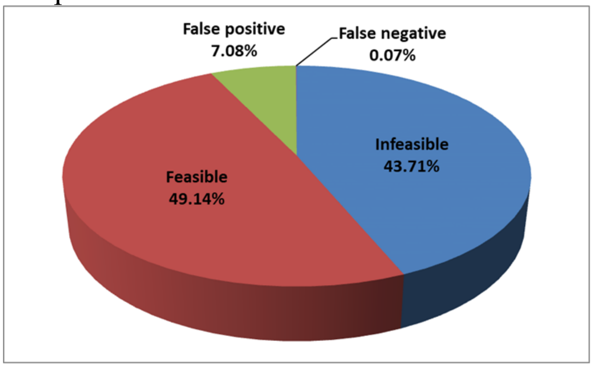

(a)

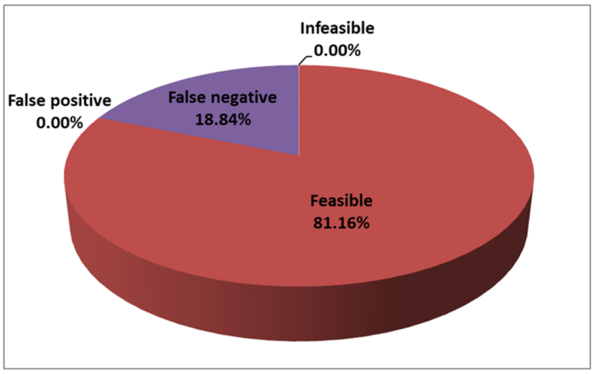

(b)

Subtitle: (a) Flooding, (b) Entrainment

Source: The author, 2022.

The correlation of Ogboja and Kuye (1990) present a smaller number of false positives and negatives, as depicted in Figure 29. However, these deviations also affects the solution of the optimal design problem, i.e. another false positive is associated with the design optimization.

Figure 29 - Example 1: Comparison between correlations of the Ogboja and Kuye (1990) and our readjusted correlations

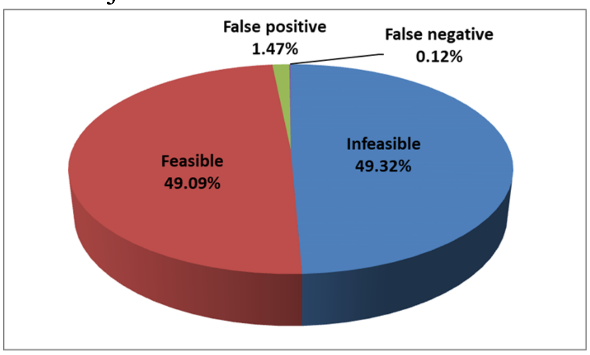

(a)

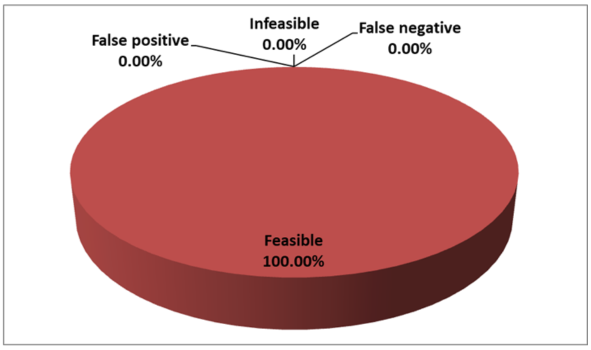

(b)

Subtitle: (a) Flooding, (b) Entrainment

Source: The author, 2022.

Similar analysis are available in the Appendix C for Examples 2 and 3. The number of deviations is smaller, but, as shown in Table 40, they can affect the result of the optimal design.

3.6 Conclusions

This paper presented an update of the flooding and entrainment correlation parameters from the literature for sieve trays. First, the errors in the literature correlations compared to the original data were analyzed. To reduce errors and improve the fit of the curves, several attempts were made, the best parameter updates obtained were with the flooding correlation of Kessler and Wankat (1988) and the entrainment correlation of Ogboja and Kuye (1990).

The readjustment of correlations was applied in three examples from the literature on globally optimal design procedures, the result was compared with the literature correlations Economopoulos (1978) and Ogboja and Kuye (1990). In all three examples, the optimal tray found is a false positive or a false negative, thus they are infeasible results for our readjustment (false positive) or results that eliminate feasible designs that should be considered at lower cost (false negative).

CONCLUSIONS AND SUGGESTIONS

This chapter is intended to present the conclusions and observations reached through the articles seen in the previous chapters and to propose suggestions for future work, to improve the optimization developed.

Conclusions

Distillation columns are of great importance in the chemical industry, being the main purification and separation equipment. The cost of distillation columns is high, and it is important to try to reduce them. The literature presents optimization works that seek to minimize the costs of distillation columns, but these works do not always aim at the complete sizing of the tray.

Therefore, the present thesis proposes an optimal distillation column design able to size all the independent variables of the tray. This formulation is solved using two different optimization techniques, MINLP formulation and Set Trimming, and two alternative objective functions, minimization of column cost and mass. Both techniques used were better than the heuristic techniques, they present optimal results that one designer could hardly obtain.

Comparing the techniques, the Set Trimming procedure presents a better result than the MINLP formulation using global solvers. The results of the Set Trimming procedure always obtained the lowest column cost or mass, while the MINLP formulation obtained a local optimal or did not converge. The Set Trimming procedure shows 354 feasible solutions for the example with the same optimal cost, while the MINLP formulation shows only 3 of these solutions in three times as much time as the Set Trimming procedure. Then, the Set Trimming procedure is more robust than the MINLP formulation.

Seeking to increase formulation accuracy, the present thesis also proposes a readjustment of literature correlations of flooding and entrainment. Due to the significant error that the literature correlations show in certain regions of the graph. All the readjustments had a significant reduction in average error and maximum error, but the new parameters of flooding correlation of Kessler and Wankat (1987) and the entrainment correlation of Ogboja and Kuye (1990) present the best results. The comparison of the updated correlations with the correlations in the literature shows that the optimal tray found is an infeasible result for our readjustment (false positive) or results that should not be considered at the optimal tray (false negative).

From the results obtained in the thesis, it is concluded that the Set Trimming procedure is a good computational tool for the design of trays in distillation columns and that the new parameters of flooding and entrainment correlations can be used as a substitute for the original parameters of correlations.

Suggestions

To complement the optimal design of sieve trays in distillation columns, the following proposals are made as suggestions for future work:

- Update the formulation developed for other types of trays (bubble-cap and valved);
- Analyze the efficiency of the tray as an objective function and compare it with the column cost result;
- Include different flow rates in the formulation to obtain trays with greater flexibility;
- Apply the formulation developed for tray design in a distillation column where the number of the ideal tray and the flow rates are also variables. This formulation should have the equations of liquid vapor equilibrium, mass and energy balance.

REFERENCES

ABRAMS, D. S.; PRAUSNITZ, J. M. Statistical thermodynamics of liquid mixtures: a new expression for the excess Gibbs energy of partly or completely miscible systems. **AIChE Journal**, United States, v. 21, n. 1, p. 116–128, 1975.

AL-BAGHLI, N. A. *et al.* A rate-based model for the design of gas absorbers for the removal of CO_2 and H_2S using aqueous solutions of MEA and DEA. **Fluid Phase Equilibria**, Netherlands, v. 185, n. 1–2, p. 31–43, 2001.

AMACS PROCESS TOWER INTERNALS. **AMACS Fractionation Trays**. Houston: Amacs Process Tower Internals, 2012. Disponível em: https://amacs.com/wp-content/uploads/2012/09/AMACS-Tray-Brochure-web.pdf. Acesso em: 21 jun. 2020.

BANSAL, V. *et al.* The interactions of design and control: double-effect distillation. **Journal of Process Control**, United Kingdom, v. 10, n. 2–3, p. 219–227, 2000.

BANSAL, V.; PERKINS, J. D.; PISTIKOPOULOS, E. N. A case study in simultaneous design and control using rigorous, mixed-integer dynamic optimization models. **Industrial & Engineering Chemistry Research**, United States, v. 41, n. 4, p. 760–778, 2002.

BOUKOUVALAS, C.; MAGOULAS, K.; TASSIOS, D. Application of supercritical fluid extraction in industrial waste treatment: thermodynamic modeling and design. **Separation Science and Technology**, United States, v. 33, n. 3, p. 387–410, 1998.

BOX, M. J. A new method of constrained optimization and a comparison with other methods. **The Computer Journal**, United Kingdom, v. 8, n. 1, p. 42–52, 1965.

BUSSIECK, M. R.; MEERAUS, A. General algebraic modeling system (GAMS). *In*: KALLRATH, J. **Modeling languages in mathematical optimization**. New York: Springer, 2004. p. 137–157. Disponível em: https://doi.org/10.1007/978-1-4613-0215-5_8. Acesso em: 30 set. 2022.

CABALLERO, J. A. Logic hybrid simulation-optimization algorithm for distillation design. **Computers and Chemical Engineering**, United Kingdom, v. 72, p. 284–299, 2015.

CABALLERO, J. A.; MILÁN-YAÑEZ, D.; GROSSMANN, I. E. Rigorous design of distillation columns: integration of disjunctive programming and process simulators. **Industrial and Engineering Chemistry Research**, United States, v. 44, n. 17, p. 6760–6775, 2005.

CHÁVEZ-ISLAS, L. M.; HEARD, C. L. Design and analysis of an ammonia/water absorption refrigeration cycle by means of an equation-oriented method. **Industrial & Engineering Chemistry Research**, United States, v. 48, n. 4, p. 1944–1956, 2009.

CHEN, Y. *et al.* Integrated ionic liquid and process design involving azeotropic separation processes. **Chemical Engineering Science**, United Kingdom, v. 203, p. 402–414, 2019.

CHUANG, K. T.; NANDAKUMAR, K. DISTILLATION. Tray columns: design. *In*: WILSON, I. D. **Encyclopedia of separation science**. Cambridge: Academic Press, 2000. p. 1135–1140.

CICALESE, J. J. *et al.* Study of alkylation-plant isobutane tower performance. **Pet. Ref**, [*S. l.*], n. 26, p. 495, 1947.

COSTA, A. L. H.; BAGAJEWICZ, M. J. 110th Anniversary: on the departure from heuristics and simplified models toward globally optimal design of process equipment. **Industrial and Engineering Chemistry Research**, United States, v. 58, n. 40, p. 18684–18702, 2019.

COULSON, J. M.; RICHARDSON, J. F.; SINNOTT, R. K. **Chemical engineering design**. 4. ed. Oxford: Elsevier Butterworth-Heinemann, 2005.

COUPER, J. R. *et al.* Distillation and gas absorption. *In*: COUPER, J. R. *et al.* **Chemical process equipment**: selection and design. 3. ed. Boston: Butterworth-Heinemann, 2012. p. 399–486.

DOUGLAS, J. M. **Conceptual design of chemical processes**. New York: McGraw-Hill, 1988.

DOWLING, A. W.; BIEGLER, L. T. A framework for efficient large scale equation-oriented flowsheet optimization. **Computers & Chemical Engineering**, United Kingdom, v. 72, p. 3–20, 2015.

DRUD, A. CONOPT: a GRG code for large sparse dynamic nonlinear optimization problems. **Mathematical Programming**, Germany, v. 31, n. 2, p. 153–191, 1985.

DUTTA, B. K. **Principles of mass transfer and seperation processes**. New Delhi: PHI Learning Pvt. Ltd., 2007.

ECONOMOPOULOS, A. P. Computer design of sieve trays and tray columns. **Chemical Engineering**, New York, v. 85, n. 27, p. 109–120, 1978.

EDULJEE, H. E. Design of sieve-type distillation plates. **British Chemical Engineering**, United Kingdom, n. 54, p. 320, 1959.

ENGEL, V. **How to...Sieve Tray: How to design and optimize Sieve Trays.** [S. *l.*]: WelChem Process Technology, 2020. Disponível em: https://welchem.com/fileadmin/pub/WelChem_SieveTray_2020-1.pdf. Acesso em: 20 ago. 2021.

FAIR, J. R. How to predict sieve tray entrainment and flooding. **Petro/Chem Engineer**, United States, v. 33, n. 10, p. 45–52, 1961.

FAIR, J. R. Tray hydraulics: perfurated trays. *In*: SMITH, B. D. **Design of Equilibrium Stage Processes**. New York: McGraw-Hill, 1963. p. 539–569.

FLOUDAS, C. A. **Nonlinear and mixed-integer optimization**: fundamentals and applications. New York: Oxford University Press,USA, 1995.

GEORGIADIS, M. C. *et al.* The interactions of design control and operability in reactive distillation systems. **Computers & Chemical Engineering**, United Kingdom, v. 26, n. 4–5, p. 735–746, 2002.

GRADSHTEYN, I. S.; RYZHIK, I. M. **Table of integrals, series, and products**. 8. ed. London: Elsevier, 2015.

GUT, J. A. W.; PINTO, J. M. Optimal configuration design for plate heat exchangers. **International Journal of Heat and Mass Transfer**, United Kingdom, v. 47, n. 22, p. 4833–4848, 2004.

HUMPHREY, J. Separation processes: playing a critical role. **Chemical Engineering Progress**, United States, v. 91, n. 10, p. 43–54, 1995.

HUNT, C. D.; HANSON, D. N.; WILKE, C. R. Capacity factors in the performance of perforated-plate columns. **AIChE Journal**, United States, v. 1, n. 4, p. 441–451, 1955.

IBRAHIM, D.; JOBSON, M.; GUILLÉN-GOSÁLBEZ, G. Optimization-based design of crude oil distillation units using rigorous simulation models. **Industrial and Engineering Chemistry Research**, United States, v. 56, n. 23, p. 6728–6740, 2017.

JAĆIMOVIĆ, B. M. *et al.* Estimation of the number of trays for natural gas triethylene glycol dehydration column. **Chemical Engineering Research and Design**, United Kingdom, v. 89, n. 6, p. 561–572, 2011.

JAVALOYES-ANTÓN, J.; RUIZ-FEMENIA, R.; CABALLERO, J. A. Rigorous design of complex distillation columns using process simulators and the particle swarm optimization algorithm. **Industrial and Engineering Chemistry Research**, United States, v. 52, n. 44, p. 15621–15634, 2013.

KENNEDY, J.; EBERHART, R. Particle swarm optimization. *In*: ICNN'95 - INTERNATIONAL CONFERENCE ON NEURAL NETWORKS, 1995, Perth. **Proceedings [...]**. Perth: IEEE, 1995. p. 1942–1948.

KESSLER, D. P.; WANKAT, P. C. Correlations for column parameters. **Chemical Engineering**, New York, p. 72–74, 1988.

KISS, A. A.; IGNAT, R. M. Enhanced methanol recovery and glycerol separation in biodiesel production: DWC makes it happen. **Applied Energy**, United Kingdom, v. 99, p. 146–153, 2012.

KISTER, H. Z. **Distillation Design**. New York: McGraw-Hill, Inc, 1992.

KISTER, H. Z. **Distillation Operation**. New York: McGraw-Hill, Inc, 1990.

KISTER, H. Z. *et al.* Section 14 equipment for distillation, gas absorption, phase dispersion, and phase separation. *In*: GREEN, D. W.; PERRY, R. H. **Perry's chemical engineers' handbook**. 8. ed. New York: McGraw-Hill Education, 2008. p. 1–129.

KONG, L.; MARAVELIAS, C. T. From graphical to model-based distillation column design: a McCabe-Thiele-inspired mathematical programming approach. **AIChE Journal**, United States, v. 65, n. 11, p. 1–11, 2019.

KOOIJMAN, H. A.; TAYLOR, R. **The chemsep book**. 2. ed. [S. *l.*]: H.A. Kooijman and R. Taylor, 2006. Disponível em: http://www.chemsep.org/downloads/docs/book2.pdf. Acesso em: 21 mar. 2021.

LAHIRI, S. K. New design methodology. *In*: **Profit maximization techniques for operating chemical plants**. 5. ed. Hoboken: John Wiley & Sons, Ltd, 2020. p. 231–257.

LAHIRI, S. K. Particle swarm optimization technique for the optimal design of plate-type distillation column. *In*: VALADI, J.; SIARRY, P. **Applications of metaheuristics in process engineering**. New York: Springer, 2014. p. 153–182.

LEMOS, J. C.; COSTA, A. L. H.; BAGAJEWICZ, M. J. Set trimming procedure for the design optimization of shell and tube heat exchangers. **Industrial & Engineering Chemistry Research**, United States, v. 59, n. 31, p. 14048–14054, 2020.

LYGEROS, A. I.; MAGOULAS, K. G. Column flooding and entrainment. **Hydrocarbon Processing**, United States, v. 65, p. 43–44, 1986.

LYU, H. *et al.* Population-distributed stochastic optimization for distillation processes: implementation and distribution strategy. **Chemical Engineering Research and Design**, United Kingdom, v. 168, p. 357–368, 2021.

MCCABE, W. L.; SMITH, J. C.; HARRIOTT, P. **Unit Operations of Chemical Engineering**. 5. ed. New York: McGraw-Hill, 1993.

MIRANDA, M. *et al.* Integrating process design and control: an application of optimal control to chemical processes. **Chemical Engineering and Processing: process intensification**, Switzerland, v. 47, n. 11, p. 2004–2018, 2008.

MISENER, R.; FLOUDAS, C. A. ANTIGONE: algorithms for coNTinuous / integer global optimization of nonlinear equations. **Journal of Global Optimization**, Netherlands, v. 59, n. 2–3, p. 503–526, 2014.

MITCHELL, M. *et al.* **Engauge digitizer**: extracts data points from images of graphs. [S. *l.*], 2019. Disponível em: https://markummitchell.github.io/engauge-digitizer/. Acesso em: 12 out. 2019.

NAHES, A. L. M. *et al.* Computational study of the use of set trimming for the globally optimal design of gasketed-plate heat exchangers. **Industrial & Engineering Chemistry Research**, United States, v. 60, n. 4, p. 1746–1755, 2021.

NELDER, J. A.; MEAD, R. A simplex method for function minimization. **The Computer Journal**, United Kingdom, v. 7, n. 4, p. 308–313, 1965.

OBERG, E. *et al.* **Machinery's Handbook**. 27. ed. New York: Industrial Press Inc., 2004.

OGBOJA, O.; KUYE, A. A procedure for the design and optimization of sieve trays. **Chemical Engineering Research and Design**, United Kingdom, v. 68, n. 5, p. 445–452, 1990.

PEREIRA, F. E. *et al.* Integrated solvent and process design using a SAFT-VR thermodynamic description: high-pressure separation of carbon dioxide and methane. **Computers & Chemical Engineering**, United Kingdom, v. 35, n. 3, p. 474–491, 2011.

PLOUFFE, S. **The first 498 bernoulli numbers**. Champaign: Project Gutenberg, 2001. Disponível em: http://www.gutenberg.org/ebooks/2586. Acesso em: 13 set. 2020.

REDLICH, O.; KWONG, J. N. S. On the thermodynamics of solutions v. an equation-of-state. fugacities of gaseous solutions. **Chem. Rev.**, [*S. l.*], v. 44, p. 223–244, 1979.

SAHINIDIS, N. V. BARON: A general purpose global optimization software package. **Journal of Global Optimization**, Netherlands, v. 8, n. 2, p. 201–205, 1996.

SEADER, J.; HENLEY, E. J.; ROPER, D. K. **Separation process principles**. 3. ed. New York: John Wiley & Sons, Inc., 2011.

SOUZA, A. R. C.; BAGAJEWICZ, M. J.; COSTA, A. L. H. Globally optimal distillation tray design using a mathematical programming approach. **Chemical Engineering Research and Design**, United Kingdom, v. 180, p. 1–12, 2022.

SOUZA, A. R. C.; BAGAJEWICZ, M. J.; COSTA, A. L. H. Set Trimming approach for the globally optimal design of sieve trays in separation columns. **AIChE Journal**, United States, v. 69, n. 5, p. 1–14, 2023.

SPENDLEY, W.; HEXT, G. R.; HIMSWORTH, F. R. Sequential application of simplex designs in optimisation and evolutionary operation. **Technometrics**, United States, v. 4, n. 4, p. 441–461, 1962.

TAYLOR, R.; KOOIJMAN, H. A.; HUNG, J. S. A second generation nonequilibrium model for computer simulation of multicomponent separation processes. **Computers & Chemical Engineering**, United Kingdom, v. 18, n. 3, p. 205–217, 1994.

TOWLER, G.; SINNOTT, R. **Chemical engineering design principles:** practice and economics of plant and process design. 2. ed. Oxford: Elsevier, 2013.

VISWANATHAN, J.; GROSSMANN, I. E. An alternate MINLP model for finding the number of trays required for a specified separation objective. **Computers & Chemical Engineering**, United Kingdom, v. 17, n. 9, p. 949–955, 1993.

WANKAT, P. C. **Separations in chemical engineering**: equilibrium staged separations. New York: Elsevier, 1988.

YEOH, K. P.; HUI, C. W. Rigorous NLP distillation models for simultaneous optimization to reduce utility and capital costs. **Cleaner Engineering and Technology**, United Kingdom, v. 2, p. 100066, 2021.

YEOMANS, H.; GROSSMANN, I. E. Disjunctive programming models for the optimal design of distillation columns and separation sequences. **Industrial and Engineering Chemistry Research**, United States, v. 39, n. 6, p. 1637–1648, 2000.

APPENDIX A – Supplementary Material of Article 1

The heuristic design procedure presented in Section 1.6 of the paper was applied to the design example described in Section 1.7. This Supplementary Material describes the details of the search for a feasible solution using the heuristic design procedure. Five iterations needed to finish the procedure, which are presented below.

Iteration 1

The application of Steps 1, 2, and 3 yielded the results shown in Table 41. The column diameter is smaller than 0.60 m, therefore it was necessary to return to Step 2, reducing the tray spacing.

Table 41 – Results of Iteration 1

Variables	Valor
lt	0.6096 m
FAdc	12%
Dc	0.5696 m

Source: The author, 2022.

Iteration 2

The tray spacing was reduced to 0.4572 m in the return to Step 2. Then, the procedure went to Steps 3, where it was checked that the infeasibility of the column diameter was corrected. After Step 3, the procedure followed to Steps 4, 5, and 6. In Step 6, it stopped, because the constraint of the downcomer backup was infeasible. Table 42 presents the results of the second iteration.

Aiming at correcting the identified problem, the procedure returned to Step 4, increasing the percentage of the hole area to fix the identified problem.

Table 42 – Results of Iteration 2

Variables	Valor
lt	0.4572 m
FAdc	12%
Dc	0.7307 m
FAh	10%
tt	0.0034 m
dh	0.0048 m
hw	0.0508 m
hdwap	0.01 m
lay	triangular
lp	0.012 m
lw	0.5550
wus	0.0381 m

Source: The author, 2022.

Iteration 3

The percentage of the hole area was increased to 12% in the return to Step 4. Then, the procedure followed to Steps 5 and 6. In Step 6, it was verified that the problem of the violation of the downcomer backup constraint was solved. The subsequent steps were then checked: Steps 7, 8, 9 and 10. In Step 10, the procedure stopped because the flooding constraint was violated. Table 43 presents the results associated with the third iteration.

After the identification that the flooding constraint was violated, the procedure returned to Step 4, increasing the tray spacing to fix the problem.

Table 43 – Results of Iteration 3

Variables	Valor
lt	0.4572 m
FAdc	12%
Dc	0.7307 m
FAh	12%
tt	0.0034 m
dh	0.0048 m
hw	0.0508 m
hdwap	0.01 m
lay	triangular
lp	0.011 m
lw	0.5550
wus	0.0381 m

Source: The author, 2022.

Iteration 4

The spacing tray was increased to 0.6096 m in the return to Step 4. Then, the procedure followed to Steps 5, 6, 7, 8, 9, and 10. In Step 10, it was observed that the constraint of flooding was still not feasible. Table 44 presents the results associated with the fourth iteration.

After the identification that the flooding constraint was violated, the procedure returned to Step 4, increasing the tray spacing further to fix the constraint violation.

Table 44 – Results of Iteration 4

Variables	Valor
lt	0.6096 m
FAdc	12%
Dc	0.7307 m
FAh	12%
tt	0.0034 m
dh	0.0048 m
hw	0.0508 m
hdwap	0.01 m
lay	triangular
lp	0.011 m
lw	0.5550
wus	0.0381 m

Source: The author, 2022.

Iteration 5

The tray spacing was increased to 0.9144 m in the return to Step 4. Then, all the remaining steps yielded positive results, i.e. no constraints were violated. Therefore, the column design was finalized. Table 45 depicts the corresponding values of the variables.

Table 45 – Results of Iteration 5

Variables	Valor
lt	0.9144 m
FAdc	12%
Dc	0.7307 m
FAh	12%
tt	0.0034 m
dh	0.0048 m
hw	0.0508 m
hdwap	0.01 m
lay	triangular
lp	0.011 m
lw	0.5550
wus	0.0381 m

Source: The author, 2022.

APPENDIX B – Supplementary Material of Article 2

Table 46 – Comparison between Set Trimming and mathematical programming – objective function cost – mass flow rates (x1) original values

Examples	Total number of candidates	Set Trimming		ANTIGONE		BARON	
		Optimal solution ($)	Computational time (s)	Optimal solution ($)	Computational time (s)	Optimal solution ($)	Computational time (s)
1	7,931,520	28915.69	43.66	28915.69	72.70	32644,00	135.84
2	9,331,200	28915.69	52.46	29914.09	77.61	28915.69	56.72
3	10,730,880	28915.69	66.77	28915.69	51.80	28915.69	20.82
4	12,130,560	28915.69	82.75	28915.69	89.35	28915.69	69.07

Source: The author, 2022.

Table 47 – Comparison between Set Trimming and mathematical programming – objective function cost – mass flow rates (x0.5) original values

Examples	Total number of candidates	Set Trimming		ANTIGONE		BARON	
		Optimal solution ($)	Computational time (s)	Optimal solution ($)	Computational time (s)	Optimal solution ($)	Computational time (s)
1	7,931,520	25076.82	43.02	25076.82	10.31	25076.82	63.40
2	9,331,200	24767.20	50.73	25076.82	66.25	no converge	
3	10,730,880	24767.20	59.55	24767.20	62.77	no converge	
4	12,130,560	24767.20	72.98	25076.82	105.58	no converge	

Source: The author, 2022.

Table 48 – Comparison between Set Trimming and mathematical programming – objective function cost – mass flow rates (x2) original values

Examples	Total number of candidates	Set Trimming		ANTIGONE		BARON	
		Optimal solution ($)	Computational time (s)	Optimal solution ($)	Computational time (s)	Optimal solution ($)	Computational time (s)
1	7,931,520	45604.67	46.67	45604.67	51.26	no converge	
2	9,331,200	38845.80	53.53	45604.67	48.41	38845.80	48.79
3	10,730,880	38845.80	69.92	42691.48	52.51	38845.80	105.83
4	12,130,560	38845.80	88.35	38845.80	29.60	42691.48	53.49

Source: The author, 2022.

Table 49 – Comparison between Set Trimming and mathematical programming – objective function cost – mass flow rates (x3) original values

Examples	Total number of candidates	Set Trimming		ANTIGONE		BARON	
		Optimal solution ($)	Computational time (s)	Optimal solution ($)	Computational time (s)	Optimal solution ($)	Computational time (s)
1	7,931,520	51658.05	51.52	51658.05	37.34	no converge	
2	9,331,200	51658.05	58.35	51658.05	45.47	51658.05	67.85
3	10,730,880	48593.50	67.88	48593.50	65.60	49092.81	90.23
4	12,130,560	48593.50	94.35	48593.50	35.46	49092.81	30.46

Source: The author, 2022.

Table 50 – Comparison between Set Trimming and mathematical programming – objective function weight – mass flow rates (x1) original values

Examples	Total number of candidates	Set Trimming		ANTIGONE		BARON	
		Optimal solution (kg)	Computational time (s)	Optimal solution (kg)	Computational time (s)	Optimal solution (kg)	Computational time (s)
1	7,931,520	1335.52	43.99	1335.52	19.64	1335.52	36.26
2	9,331,200	1335.52	51.24	1335.52	41.60	1335.52	89.04
3	10,730,880	1335.52	65.09	1477.05	74.13	1335.52	98.76
4	12,130,560	1335.52	86.26	1853.85	49.28	1335.52	39.22

Source: The author, 2022.

Table 51 – Comparison between Set Trimming and mathematical programming – objective function weight – mass flow rates (x0.5) original values

Examples	Total number of candidates	Set Trimming		ANTIGONE		BARON	
		Optimal solution (kg)	Computational time (s)	Optimal solution (kg)	Computational time (s)	Optimal solution (kg)	Computational time (s)
1	7,931,520	1007	42.74	1501	34.04	1007	119.14
2	9,331,200	895	49.65	1045	42.49	895	140.05
3	10,730,880	895	52.78	1045	42.93	895	101.88
4	12,130,560	895	65.97	1078	68.69	895	63.83

Source: The author, 2022.

Table 52 – Comparison between Set Trimming and mathematical programming – objective function weight – mass flow rates (x2) original values

Examples	Total number of candidates	Set Trimming		ANTIGONE		BARON	
		Optimal solution (kg)	Computational time (s)	Optimal solution (kg)	Computational time (s)	Optimal solution (kg)	Computational time (s)
1	7,931,520	3146	45.00	3146	94.34	3146	45.49
2	9,331,200	2574	53.41	2574	92.99	3146	116.04
3	10,730,880	2574	65.32	2574	54.78	2574	69.77
4	12,130,560	2574	84.54	2854	97.60	2577	108.02

Source: The author, 2022.

Table 53 – Comparison between Set Trimming and mathematical programming – objective function weight – mass flow rates (x3) original values

Examples	Total number of candidates	Set Trimming		ANTIGONE		BARON	
		Optimal solution (kg)	Computational time (s)	Optimal solution (kg)	Computational time (s)	Optimal solution (kg)	Computational time (s)
1	7,931,520	3686	49.17	3686	69.12	3686	56.32
2	9,331,200	3686	57.62	3686	66.26	3686	43.78
3	10,730,880	3420	72.40	3420	63.47	3421	87.35
4	12,130,560	3420	96.64	4022	44.92	3421	106.44

Source: The author, 2022.

APPENDIX C – Supplementary Material of Article 3

Data Collection

Table 54 – Data collection to flooding correlation

Flv	6 in	9 in	12 in	18 in	24 in	36 in
0.0101859	0.1289470	0.1568780	0.2017750	0.2589700	0.3459780	-
0.0101971	0.1289470	0.1569060	0.2018000	0.2589700	0.3460170	-
0.0102755	0.1289470	0.1571080	0.2019800	0.2589700	0.3462840	-
0.0104160	0.1289470	0.1574670	0.2022990	0.2589700	0.3467580	-
0.0106396	0.1289470	0.1580300	0.2027990	0.2589700	0.3475010	-
0.0109474	0.1289470	0.1587880	0.2034720	0.2589700	0.3485000	-
0.0109594	0.1289700	0.1588170	0.2034980	0.2589700	0.3485390	-
0.0110438	0.1291370	0.1590220	0.2036800	0.2594410	0.3488080	-
0.0118694	0.1307090	0.1609580	0.2053940	0.2639120	0.3488080	-
0.0123889	0.1316520	0.1621200	0.2064190	0.2666050	0.3504850	-
0.0125638	0.1319630	0.1625020	0.2067560	0.2669810	0.3510350	-
0.0126500	0.1321140	0.1626880	0.2067560	0.2671650	0.3513040	-
0.0126652	0.1321410	0.1627060	0.2067560	0.2671980	0.3513510	-
0.0133152	0.1332560	0.1634540	0.2067560	0.2685480	0.3540870	-
0.0134061	0.1334080	0.1635560	0.2067560	0.2685480	0.3544600	-
0.0136942	0.1338850	0.1638740	0.2072480	0.2685480	0.3556300	-
0.0139100	0.1342370	0.1642720	0.2076110	0.2685480	0.3564930	-
0.0142078	0.1347150	0.1648120	0.2081040	0.2685480	0.3571270	-
0.0143049	0.1348690	0.1649860	0.2082630	0.2685480	0.3573310	-
0.0150401	0.1360090	0.1662720	0.2082630	0.2685480	0.3588380	-
0.0151672	0.1362010	0.1664490	0.2082630	0.2685480	0.3590910	-
0.0159332	0.1373320	0.1674850	0.2082630	0.2685480	0.3590910	-
0.0163010	0.1378590	0.1674850	0.2082630	0.2685480	0.3590910	-
0.0164050	0.1380070	0.1674850	0.2082630	0.2685480	0.3590910	-
0.0164115	0.1380160	0.1674850	0.2082710	0.2685480	0.3590910	-
0.0168742	0.1386610	0.1674850	0.2088550	0.2695870	0.3590910	-
0.0171244	0.1386610	0.1674850	0.2091650	0.2701390	0.3590910	-
0.0173938	0.1386610	0.1681440	0.2094940	0.2707260	0.3590910	-
0.0176256	0.1386610	0.1687060	0.2097740	0.2712240	0.3602900	-
0.0176316	0.1386610	0.1687060	0.2097810	0.2712370	0.3603210	-
0.0181357	0.1386610	0.1687060	0.2097810	0.2723010	0.3628880	-
0.0184269	0.1386610	0.1687060	0.2097810	0.2729050	0.3643460	-
0.0188136	0.1386610	0.1687060	0.2097810	0.2736930	0.3643460	-
0.0189432	0.1386610	0.1687060	0.2102170	0.2739550	0.3643460	-
0.0198045	0.1386610	0.1692880	0.2130600	0.2756520	0.3643460	-
0.0202069	0.1386610	0.1695520	0.2143590	0.2764240	0.3668150	-

Flv	6 in	9 in	12 in	18 in	24 in	36 in
0.0202207	0.1386610	0.1695610	0.2144030	0.2764500	0.3668990	-
0.0202288	0.1386610	0.1695660	0.2144030	0.2764650	0.3669480	-
0.0202377	0.1386610	0.1695720	0.2144030	0.2764650	0.3670020	-
0.0208048	0.1386610	0.1699350	0.2144030	0.2764650	0.3670020	-
0.0215763	0.1386610	0.1706290	0.2144030	0.2764650	0.3670020	-
0.0217175	0.1386610	0.1707540	0.2145590	0.2764650	0.3670020	-
0.0217410	0.1386610	0.1707750	0.2145850	0.2764650	0.3670020	-
0.0217507	0.1386610	0.1707830	0.2145960	0.2764650	0.3670020	-
0.0221997	0.1386610	0.1711740	0.2150870	0.2764650	0.3678430	-
0.0226776	0.1386610	0.1715830	0.2156010	0.2764650	0.3687210	-
0.0230229	0.1386610	0.1718730	0.2159660	0.2764650	0.3693450	-
0.0231985	0.1386610	0.1720190	0.2157820	0.2764650	0.3696590	-
0.0232090	0.1386610	0.1720280	0.2157710	0.2764650	0.3696780	-
0.0236882	0.1386610	0.1724220	0.2152780	0.2764650	0.3696780	-
0.0245660	0.1386610	0.1724220	0.2144030	0.2764650	0.3696780	-
0.0249058	0.1386610	0.1724220	0.2144030	0.2764650	0.3696780	-
0.0249327	0.1386920	0.1724220	0.2144030	0.2764650	0.3696780	-
0.0249441	0.1387040	0.1724220	0.2144030	0.2764810	0.3696780	-
0.0252762	0.1390740	0.1724220	0.2144030	0.2769420	0.3696780	-
0.0262129	0.1400980	0.1724220	0.2144030	0.2782140	0.3696780	-
0.0264133	0.1403130	0.1724220	0.2144030	0.2784810	0.3696780	-
0.0267683	0.1406910	0.1724220	0.2144030	0.2780650	0.3696780	-
0.0268088	0.1406910	0.1724220	0.2144030	0.2780180	0.3696780	-
0.0269706	0.1406910	0.1724220	0.2144030	0.2778300	0.3696780	-
0.0281837	0.1406910	0.1731880	0.2144030	0.2764650	0.3696780	-
0.0288130	0.1406910	0.1735740	0.2144030	0.2764650	0.3696780	-
0.0289872	0.1406910	0.1736790	0.2144030	0.2764650	0.3696780	-
0.0302686	0.1406910	0.1736790	0.2144030	0.2764650	0.3696780	-
0.0302786	0.1406910	0.1736790	0.2144030	0.2764650	0.3696780	-
0.0302906	0.1406910	0.1736790	0.2144030	0.2764650	0.3696780	-
0.0303044	0.1406910	0.1736790	0.2144030	0.2764650	0.3696780	-
0.0323084	0.1406910	0.1736790	0.2144030	0.2764650	0.3696780	-
0.0323359	0.1406910	0.1736790	0.2143870	0.2764650	0.3696780	-
0.0325314	0.1406910	0.1736790	0.2142790	0.2764650	0.3694280	-
0.0325551	0.1406910	0.1736790	0.2142660	0.2764650	0.3693980	-
0.0345033	0.1406910	0.1736790	0.2132230	0.2764650	0.3670020	-
0.0349634	0.1406910	0.1736790	0.2129860	0.2764650	0.3670020	-
0.0349888	0.1406910	0.1736650	0.2129730	0.2764650	0.3670020	-
0.0352276	0.1406910	0.1735330	0.2128510	0.2764650	0.3670020	-
0.0370826	0.1406910	0.1725390	0.2128510	0.2764650	0.3670020	-
0.0373068	0.1406910	0.1724220	0.2128510	0.2764650	0.3667550	-
0.0373344	0.1406910	0.1724220	0.2128510	0.2764650	0.3667240	-
0.0378611	0.1406910	0.1724220	0.2128510	0.2760320	0.3661500	-

Flv	6 in	9 in	12 in	18 in	24 in	36 in
0.0395681	0.1406910	0.1724220	0.2122610	0.2746720	0.3643460	-
0.0403859	0.1406910	0.1724220	0.2119870	0.2740440	0.3643460	-
0.0404332	0.1406910	0.1724220	0.2119720	0.2740080	0.3643460	-
0.0421578	0.1406910	0.1724220	0.2114150	0.2727300	0.3628160	-
0.0424899	0.1405670	0.1724220	0.2113110	0.2724900	0.3625290	-
0.0434050	0.1402320	0.1724220	0.2113110	0.2718410	0.3617520	-
0.0434554	0.1402140	0.1724020	0.2113110	0.2718050	0.3617090	-
0.0449834	0.1396720	0.1718030	0.2113110	0.2707560	0.3617090	-
0.0453383	0.1397370	0.1716670	0.2113110	0.2705180	0.3617090	-
0.0453558	0.1397410	0.1716600	0.2112920	0.2705060	0.3617090	-
0.0453764	0.1397440	0.1716520	0.2112710	0.2704930	0.3617090	-
0.0466494	0.1399740	0.1711740	0.2099660	0.2697400	0.3594750	-
0.0483765	0.1402760	0.1711740	0.2082630	0.2687540	0.3565600	-
0.0484172	0.1402830	0.1711740	0.2082630	0.2687310	0.3564930	-
0.0487459	0.1403390	0.1711740	0.2082630	0.2685480	0.3562500	-
0.0504995	0.1406330	0.1711740	0.2082630	0.2685480	0.3549830	0.4337980
0.0505151	0.1406360	0.1711630	0.2082630	0.2685480	0.3549720	0.4337850
0.0505352	0.1406390	0.1711470	0.2082550	0.2685480	0.3549580	0.4337670
0.0505731	0.1406450	0.1711180	0.2082390	0.2685480	0.3549310	0.4337350
0.0508493	0.1406910	0.1709100	0.2081250	0.2685480	0.3547360	0.4334970
0.0538837	0.1388760	0.1687060	0.2069130	0.2685480	0.3526700	0.4309720
0.0542569	0.1386610	0.1687060	0.2067690	0.2685480	0.3524250	0.4306720
0.0542908	0.1386610	0.1687060	0.2067560	0.2685480	0.3524030	0.4306450
0.0543131	0.1386610	0.1687060	0.2067560	0.2685480	0.3523890	0.4306270
0.0543532	0.1386610	0.1687060	0.2067560	0.2685280	0.3523620	0.4305950
0.0559257	0.1386610	0.1687060	0.2067560	0.2677570	0.3513510	0.4289840
0.0574959	0.1386610	0.1687060	0.2067560	0.2670110	0.3504610	0.4274260
0.0583495	0.1386610	0.1687060	0.2067560	0.2666150	0.3499880	0.4265990
0.0583727	0.1386610	0.1687060	0.2067390	0.2666050	0.3499750	0.4265760
0.0604719	0.1386610	0.1687060	0.2052720	0.2645030	0.3488450	0.4246000
0.0604905	0.1386610	0.1687000	0.2052590	0.2644850	0.3488350	0.4245830
0.0605408	0.1386610	0.1686860	0.2052420	0.2644360	0.3488080	0.4245360
0.0622844	0.1386610	0.1682040	0.2046560	0.2627590	0.3478120	0.4229550
0.0641541	0.1386610	0.1677040	0.2040470	0.2618910	0.3467770	0.4213140
0.0649920	0.1386610	0.1674850	0.2037800	0.2615110	0.3463230	0.4211240
0.0650119	0.1386610	0.1674790	0.2037740	0.2615020	0.3463130	0.4211190
0.0650659	0.1386610	0.1674630	0.2037270	0.2614770	0.3462840	0.4211070
0.0664590	0.1386610	0.1670660	0.2025440	0.2608580	0.3452290	0.4207970
0.0684331	0.1386610	0.1665200	0.2009210	0.2598980	0.3437780	0.4203700
0.0693480	0.1386610	0.1662720	0.2001890	0.2594630	0.3426290	0.4201760
0.0703352	0.1386610	0.1662720	0.1994130	0.2590020	0.3414110	0.4199690
0.0703552	0.1386610	0.1662720	0.1993970	0.2589920	0.3413860	0.4199650
0.0703752	0.1386610	0.1662670	0.1993810	0.2589830	0.3413620	0.4199610

Flv	6 in	9 in	12 in	18 in	24 in	36 in
0.0704040	0.1386610	0.1662590	0.1993810	0.2589700	0.3413270	0.4199550
0.0724944	0.1386610	0.1657160	0.1993810	0.2582070	0.3388200	0.4195290
0.0750708	0.1386610	0.1650690	0.1993810	0.2573000	0.3376290	0.4190200
0.0755933	0.1386610	0.1649540	0.1993810	0.2571210	0.3373930	0.4189190
0.0756363	0.1386550	0.1649440	0.1993810	0.2571060	0.3373740	0.4189110
0.0756664	0.1386500	0.1649380	0.1993720	0.2570960	0.3373610	0.4189050
0.0779130	0.1383040	0.1644520	0.1987200	0.2558860	0.3363670	0.4184790
0.0790716	0.1381300	0.1642080	0.1983920	0.2552770	0.3363670	0.4182650
0.0806820	0.1378920	0.1638740	0.1979450	0.2544490	0.3363670	0.4150890
0.0807058	0.1378890	0.1638690	0.1979380	0.2544370	0.3363670	0.4150420
0.0807728	0.1378790	0.1638560	0.1979200	0.2544030	0.3363670	0.4149120
0.0837633	0.1374520	0.1632570	0.1971160	0.2529160	0.3333000	0.4092490
0.0855665	0.1372020	0.1629070	0.1966460	0.2520490	0.3315160	0.4083250
0.0861151	0.1371270	0.1628020	0.1965060	0.2517890	0.3312490	0.4080490
0.0867126	0.1370460	0.1626880	0.1961150	0.2515080	0.3309610	0.4077490
0.0905448	0.1365410	0.1615110	0.1936880	0.2497610	0.3291630	0.4058830
0.0905705	0.1365380	0.1615010	0.1936720	0.2497490	0.3291510	0.4058710
0.0906066	0.1365330	0.1614860	0.1936640	0.2497330	0.3291350	0.4058540
0.0906457	0.1365280	0.1614710	0.1936560	0.2497220	0.3291170	0.4058350
0.0960581	0.1358530	0.1593870	0.1925270	0.2482670	0.3248700	0.4033460
0.0966124	0.1357870	0.1591820	0.1924160	0.2481230	0.3244510	0.4026790
0.0967202	0.1357740	0.1591820	0.1923940	0.2480950	0.3243700	0.4025490
0.0973403	0.1357000	0.1591820	0.1922700	0.2479360	0.3240220	0.4018090
0.0973790	0.1356950	0.1591820	0.1922550	0.2479260	0.3240010	0.4017630
0.1008830	0.1352860	0.1591820	0.1908890	0.2464580	0.3220820	0.3976930
0.1009120	0.1352830	0.1591770	0.1908790	0.2464460	0.3220670	0.3976610
0.1009950	0.1352730	0.1591640	0.1908470	0.2464120	0.3220230	0.3975670
0.1010280	0.1352690	0.1591590	0.1908340	0.2463990	0.3220010	0.3975290
0.1084240	0.1344560	0.1580300	0.1881360	0.2434920	0.3174480	0.3928400
0.1084530	0.1344530	0.1580250	0.1881260	0.2434810	0.3174310	0.3928220
0.1085420	0.1344430	0.1580120	0.1881080	0.2434470	0.3173780	0.3927680
0.1108690	0.1342000	0.1576750	0.1876620	0.2425820	0.3166260	0.3913710
0.1150230	0.1337790	0.1570910	0.1868910	0.2407900	0.3153240	0.3889600
0.1156620	0.1337160	0.1570040	0.1867750	0.2405210	0.3151290	0.3882930
0.1157230	0.1337090	0.1569950	0.1867640	0.2404960	0.3151100	0.3882300
0.1158170	0.1336980	0.1569830	0.1867280	0.2404560	0.3150810	0.3881310
0.1165280	0.1336150	0.1568860	0.1864570	0.2401600	0.3144340	0.3873960
0.1191540	0.1333160	0.1561050	0.1854740	0.2390830	0.3120880	0.3847270
0.1235770	0.1328270	0.1548360	0.1838780	0.2379880	0.3082900	0.3804020
0.1243070	0.1327480	0.1546310	0.1836210	0.2378120	0.3081070	0.3797080
0.1243370	0.1327380	0.1546230	0.1836110	0.2378040	0.3080990	0.3796800
0.1262270	0.1321090	0.1543880	0.1829550	0.2373530	0.3076310	0.3779070
0.1263190	0.1320780	0.1543770	0.1829230	0.2373180	0.3076090	0.3778220

Flv	6 in	9 in	12 in	18 in	24 in	36 in
0.1308060	0.1306340	0.1538350	0.1814160	0.2356540	0.3065290	0.3763480
0.1328140	0.1300090	0.1535990	0.1808590	0.2349320	0.3060580	0.3757070
0.1336310	0.1297580	0.1535040	0.1806360	0.2346420	0.3049260	0.3754490
0.1347860	0.1294070	0.1531910	0.1803230	0.2342350	0.3033410	0.3750870
0.1356610	0.1291430	0.1529560	0.1800880	0.2339300	0.3021560	0.3744950
0.1376840	0.1285420	0.1524200	0.1795510	0.2327690	0.2994610	0.3731430
0.1394980	0.1280130	0.1519480	0.1790780	0.2317470	0.2990670	0.3719510
0.1405810	0.1280760	0.1516690	0.1787990	0.2311460	0.2988340	0.3712490
0.1447500	0.1283120	0.1506220	0.1776330	0.2288870	0.2979550	0.3686080
0.1479760	0.1284900	0.1498370	0.1767580	0.2280410	0.2972940	0.3666280
0.1510480	0.1286560	0.1491080	0.1759470	0.2272560	0.2957590	0.3647920
0.1511470	0.1286620	0.1490980	0.1759210	0.2272310	0.2957100	0.3647330
0.1565560	0.1289470	0.1485710	0.1745410	0.2264270	0.2931010	0.3616130
0.1613420	0.1281660	0.1481210	0.1733680	0.2257410	0.2908860	0.3589620
0.1623380	0.1280080	0.1480290	0.1731290	0.2256010	0.2902850	0.3584230
0.1624450	0.1279910	0.1480070	0.1731030	0.2255860	0.2902210	0.3583650
0.1682560	0.1270870	0.1468470	0.1717460	0.2224110	0.2868130	0.3553010
0.1707800	0.1267700	0.1463580	0.1711740	0.2210800	0.2853820	0.3540110
0.1709740	0.1267450	0.1463210	0.1711350	0.2209790	0.2852730	0.3539120
0.1721520	0.1265990	0.1460960	0.1708980	0.2203680	0.2846160	0.3529950
0.1732170	0.1264680	0.1458940	0.1706860	0.2198200	0.2841740	0.3521730
0.1745810	0.1263020	0.1456640	0.1704160	0.2191260	0.2836130	0.3511300
0.1756920	0.1261670	0.1454770	0.1701990	0.2188460	0.2831600	0.3502890
0.1823690	0.1250650	0.1443880	0.1689240	0.2172070	0.2805110	0.3453840
0.1835420	0.1248770	0.1442010	0.1687060	0.2169260	0.2801480	0.3445480
0.1861620	0.1244610	0.1437900	0.1681710	0.2163080	0.2793490	0.3427070
0.1876280	0.1242320	0.1434850	0.1678760	0.2159660	0.2789080	0.3416920
0.1918660	0.1235810	0.1426210	0.1670380	0.2149960	0.2776550	0.3388200
0.1945130	0.1231840	0.1420940	0.1665260	0.2144030	0.2768890	0.3373980
0.1958420	0.1229860	0.1418320	0.1662720	0.2139130	0.2765100	0.3366940
0.1959980	0.1229630	0.1418020	0.1662300	0.2138550	0.2764650	0.3366120
0.2501550	0.1161070	0.1327480	0.1538660	0.1970230	0.2529700	0.3123370
0.2520220	0.1159040	0.1325490	0.1535040	0.1965310	0.2522860	0.3116250
0.2540420	0.1156870	0.1323360	0.1532300	0.1960050	0.2515540	0.3108630
0.2632590	0.1147210	0.1313890	0.1520120	0.1936720	0.2485590	0.3074830
0.2672740	0.1143130	0.1309890	0.1514970	0.1926890	0.2472990	0.3060580
0.2688500	0.1141550	0.1308340	0.1512980	0.1923090	0.2468110	0.3053340
0.2689110	0.1141490	0.1308220	0.1512900	0.1922940	0.2467920	0.3053060
0.2707370	0.1139680	0.1304880	0.1509870	0.1918580	0.2462310	0.3044740
0.2710630	0.1139400	0.1304290	0.1509330	0.1917800	0.2461310	0.3043260
0.2808970	0.1131250	0.1286830	0.1493470	0.1894970	0.2426200	0.2999840
0.2848020	0.1128100	0.1280130	0.1487370	0.1887080	0.2412730	0.2983180
0.2909700	0.1123240	0.1276680	0.1477950	0.1874890	0.2391970	0.2957520

Flv	6 in	9 in	12 in	18 in	24 in	36 in
0.3017080	0.1113030	0.1270870	0.1462160	0.1854460	0.2357270	0.2914610
0.3018860	0.1112870	0.1270490	0.1461900	0.1854120	0.2356710	0.2913920
0.3020000	0.1112760	0.1270250	0.1461740	0.1853810	0.2356350	0.2913480
0.3039570	0.1110950	0.1266120	0.1458940	0.1848450	0.2349540	0.2905900
0.3087010	0.1106620	0.1256270	0.1451370	0.1835670	0.2333290	0.2887800
0.3196060	0.1096980	0.1234480	0.1434540	0.1807330	0.2297270	0.2843230
0.3221090	0.1094830	0.1230170	0.1430780	0.1801030	0.2289260	0.2833310
0.3222300	0.1094730	0.1229960	0.1430600	0.1800800	0.2288870	0.2832830
0.3243220	0.1092940	0.1226400	0.1427490	0.1796890	0.2282250	0.2824630
0.3293800	0.1088690	0.1217920	0.1418610	0.1787570	0.2266470	0.2805110
0.3360810	0.1083180	0.1206980	0.1407140	0.1775510	0.2246110	0.2779060
0.3410160	0.1076130	0.1199120	0.1398890	0.1766840	0.2231490	0.2760360
0.3436910	0.1072370	0.1197030	0.1394490	0.1762210	0.2223690	0.2750380
0.3438160	0.1072190	0.1196930	0.1394290	0.1761780	0.2223330	0.2749920
0.3485520	0.1065640	0.1193270	0.1386610	0.1745640	0.2208050	0.2732550
0.3511970	0.1062030	0.1191250	0.1381920	0.1736790	0.2199640	0.2722990
0.3538670	0.1058440	0.1189230	0.1377240	0.1730910	0.2191260	0.2713460
0.3585950	0.1052160	0.1185700	0.1369080	0.1720650	0.2178270	0.2696830
0.3638690	0.1043480	0.1181830	0.1360150	0.1709420	0.2164060	0.2678650
0.3719010	0.1030640	0.1170730	0.1346910	0.1692780	0.2143000	0.2651690
0.3747240	0.1026230	0.1166910	0.1342250	0.1687060	0.2135750	0.2642420
0.3775720	0.1021830	0.1163100	0.1337600	0.1680630	0.2128510	0.2633160
0.3826900	0.1014050	0.1156360	0.1329370	0.1669260	0.2114110	0.2616790
0.4023980	0.0985578	0.1131540	0.1299120	0.1627530	0.2061260	0.2556620
0.4024850	0.0985578	0.1131430	0.1299000	0.1627350	0.2061040	0.2556370
0.4025720	0.0985578	0.1131320	0.1298870	0.1627170	0.2060810	0.2556110
0.4027140	0.0985578	0.1131140	0.1298710	0.1626880	0.2060450	0.2555690
0.4294470	0.0985578	0.1099030	0.1270970	0.1580700	0.1994750	0.2480720
0.4295450	0.0985578	0.1098950	0.1270870	0.1580540	0.1994520	0.2480460
0.4296910	0.0985578	0.1098820	0.1270710	0.1580300	0.1994180	0.2480070
0.4299940	0.0985578	0.1098560	0.1270370	0.1579730	0.1993470	0.2479260
0.4324810	0.0985578	0.1096430	0.1267600	0.1575150	0.1987680	0.2471770
0.4515890	0.0971363	0.1080620	0.1247050	0.1541190	0.1944830	0.2416370
0.4550320	0.0966415	0.1077870	0.1243480	0.1535300	0.1937390	0.2406770
0.4551820	0.0966200	0.1077750	0.1243260	0.1535040	0.1937070	0.2406350
0.4582200	0.0961888	0.1075340	0.1238880	0.1530200	0.1930590	0.2397970
0.4614520	0.0957354	0.1071830	0.1234260	0.1525110	0.1923760	0.2389150
0.4619560	0.0956959	0.1071280	0.1233550	0.1524320	0.1922700	0.2387780
0.4888330	0.0936718	0.1043460	0.1197080	0.1483960	0.1886510	0.2318020
0.4929070	0.0933398	0.1039440	0.1191820	0.1478130	0.1881260	0.2307960
0.5144860	0.0916448	0.1018920	0.1165020	0.1448380	0.1827830	0.2256680
0.5148430	0.0916176	0.1018590	0.1164590	0.1447880	0.1826980	0.2255860
0.5217740	0.0910950	0.1012270	0.1156360	0.1438150	0.1810620	0.2239020

Flv	6 in	9 in	12 in	18 in	24 in	36 in
0.5259140	0.0907876	0.1008550	0.1151250	0.1432430	0.1801030	0.2229130
0.5450080	0.0894134	0.0991956	0.1128480	0.1406910	0.1761000	0.2185040
0.5493260	0.0891121	0.0988320	0.1123500	0.1401940	0.1752260	0.2175400
0.5567210	0.0886038	0.0982188	0.1115110	0.1393560	0.1737550	0.2158700
0.5571070	0.0885776	0.0981871	0.1114770	0.1393130	0.1736790	0.2157840
0.5815170	0.0869677	0.0962472	0.1093550	0.1366620	0.1694400	0.2105170
0.5859180	0.0866877	0.0959102	0.1089860	0.1358330	0.1687060	0.2096050
0.5940150	0.0861803	0.0952995	0.1083180	0.1343360	0.1673760	0.2079530
0.6028340	0.0856388	0.0946482	0.1075160	0.1327480	0.1659610	0.2061950
0.6068710	0.0853947	0.0943547	0.1071550	0.1321910	0.1653240	0.2054030
0.6162180	0.0848383	0.0935503	0.1063320	0.1309230	0.1638740	0.2036020
0.6200340	0.0846145	0.0932272	0.1060020	0.1304150	0.1631950	0.2028790
0.6202530	0.0846045	0.0932088	0.1059830	0.1303860	0.1631570	0.2028380
0.6385890	0.0837803	0.0916999	0.1040550	0.1280130	0.1599920	0.1994610
0.6390320	0.0837608	0.0916642	0.1040090	0.1279570	0.1599170	0.1993810
0.6434290	0.0835680	0.0913128	0.1035610	0.1274060	0.1591820	0.1984480
0.6475180	0.0833903	0.0909893	0.1031480	0.1268980	0.1584210	0.1975890
0.6570410	0.0829822	0.0902708	0.1022030	0.1257350	0.1566800	0.1956250
0.6615770	0.0827906	0.0899343	0.1017990	0.1251910	0.1558670	0.1947060
0.6764650	0.0817649	0.0888541	0.1005020	0.1234480	0.1532650	0.1917630
0.6815840	0.0814202	0.0884911	0.1000660	0.1229790	0.1523930	0.1907760
0.7058870	0.0798377	0.0868237	0.0980659	0.1208260	0.1488450	0.1862560
0.7063450	0.0798079	0.0867931	0.0980293	0.1207870	0.1487800	0.1861730
0.7110840	0.0795010	0.0864786	0.0976523	0.1202790	0.1481130	0.1853230
0.7267550	0.0785086	0.0856380	0.0964333	0.1186370	0.1459580	0.1825790
0.7431090	0.0775083	0.0847882	0.0950901	0.1169850	0.1437900	0.1798190
0.7482390	0.0772016	0.0845272	0.0946786	0.1164790	0.1430440	0.1789740
0.7587180	0.0765854	0.0840021	0.0938523	0.1152590	0.1415460	0.1772790
0.7698600	0.0759447	0.0832644	0.0929939	0.1139950	0.1399940	0.1755190
0.7807830	0.0753306	0.0825576	0.0920698	0.1127870	0.1385100	0.1738350
0.7818050	0.0752765	0.0824923	0.0919845	0.1126750	0.1383730	0.1736790
0.7871750	0.0749936	0.0821513	0.0915393	0.1120930	0.1376580	0.1727010
0.7926100	0.0747103	0.0818100	0.0910940	0.1115110	0.1370230	0.1717230
0.8041030	0.0741211	0.0811005	0.0901693	0.1099030	0.1357030	0.1696940
0.8043680	0.0741076	0.0810843	0.0901482	0.1098870	0.1356730	0.1696480
0.8451670	0.0721181	0.0786928	0.0870417	0.1074770	0.1315070	0.1628590
0.8462440	0.0720563	0.0786322	0.0869632	0.1074160	0.1314010	0.1626880
0.8520760	0.0717243	0.0783061	0.0865408	0.1070860	0.1308340	0.1618140
0.8579680	0.0713928	0.0779802	0.0861192	0.1067560	0.1300660	0.1609420
0.9029020	0.0689840	0.0756084	0.0830591	0.1025230	0.1245200	0.1546230
0.9084120	0.0687024	0.0753306	0.0827017	0.1020290	0.1238750	0.1537710
0.9214580	0.0680468	0.0745223	0.0818701	0.1008830	0.1223760	0.1517930
0.9356810	0.0674190	0.0736638	0.0809860	0.0996654	0.1207870	0.1496960

Flv	6 in	9 in	12 in	18 in	24 in	36 in
0.9489680	0.0668462	0.0728821	0.0801807	0.0985578	0.1193890	0.1477920
0.9622800	0.0662852	0.0721181	0.0793930	0.0974103	0.1180240	0.1459340
0.9703010	0.0659531	0.0716499	0.0789272	0.0967329	0.1172180	0.1448380
0.9902770	0.0651449	0.0705135	0.0777955	0.0950898	0.1152630	0.1421830
1.0049200	0.0645687	0.0697060	0.0769902	0.0939234	0.1138750	0.1403000
1.0128000	-	0.0692800	0.0767211	0.0933086	0.1131430	-
1.0346100	-	0.0681319	0.0759924	0.0916527	0.1113350	-
1.0722400	-	0.0662485	0.0747854	0.0889406	0.1083650	-
1.0728600	-	0.0662184	0.0747467	0.0888972	0.1083180	-
1.0954500	-	0.0651449	0.0733698	0.0873539	0.1063130	-
1.1279700	-	0.0641910	0.0714786	0.0852314	0.1035600	-
1.1604300	-	0.0632793	0.0696914	0.0834529	0.1009580	-
1.2213000	-	0.0608785	0.0665828	0.0803412	0.0964333	-
1.2929600	-	0.0583084	0.0632793	0.0770078	0.0910416	-
1.2933600	-	0.0582948	0.0632659	0.0769902	0.0910134	-
1.3030400	-	0.0579668	0.0629394	0.0764128	0.0903308	-
1.3401900	-	0.0567470	0.0617245	0.0742757	0.0880543	-
1.3602000	-	0.0560954	0.0610936	0.0731734	0.0868775	-
1.4003100	-	0.0548388	0.0598746	0.0713436	0.0846145	-
1.4508700	-	0.0533435	0.0584200	0.0691725	0.0823743	-
1.4833500	-	0.0524308	0.0573121	0.0678509	0.0810060	-
1.5258700	-	0.0512885	0.0559286	0.0662007	0.0787287	-
1.5702400	-	0.0501551	0.0542129	0.0645676	0.0764839	-
1.5936400	-	0.0494119	0.0533482	0.0637406	0.0753505	-
1.6755200	-	0.0469758	0.0505208	0.0613698	0.0716356	-
1.6874400	-	0.0466412	0.0502957	0.0610418	0.0711253	-
1.6885500	-	0.0466171	0.0502748	0.0610113	0.0710780	-
1.7374800	-	0.0455839	0.0493777	0.0597070	0.0692398	-
1.7749000	-	0.0448281	0.0487189	0.0580781	0.0678996	-
1.8272300	-	0.0438178	0.0476597	0.0559286	0.0661140	-
1.8277100	-	0.0438088	0.0476503	0.0559096	0.0660981	-
1.8801500	-	0.0428471	0.0466412	0.0538937	0.0640339	-
1.9209600	-	0.0421314	0.0458898	0.0524125	0.0625106	-
1.9500100	-	0.0416381	0.0453716	0.0514012	0.0614672	-

Source: The author, 2022.

Table 55 – Data collection to entrainment correlation

Flv	90%	80%	70%	60%	50%	45%	40%	35%	30%
0.00504	0.43167	0.29191	0.19396	0.12534	0.07524	0.04387	0.02190	0.01046	0.00427
0.00507	0.43041	0.29106	0.19340	0.12474	0.07486	0.04368	0.02182	0.01043	0.00426
0.00514	0.42790	0.28936	0.19227	0.12356	0.07412	0.04331	0.02167	0.01038	0.00425
0.00533	0.42170	0.28516	0.18948	0.12065	0.07228	0.04239	0.02130	0.01026	0.00422
0.00544	0.41802	0.28267	0.18783	0.11893	0.07121	0.04185	0.02108	0.01018	0.00421
0.00556	0.41437	0.28020	0.18619	0.11724	0.07014	0.04131	0.02087	0.01011	0.00419
0.00568	0.41075	0.27776	0.18456	0.11558	0.06910	0.04072	0.02065	0.01003	0.00418
0.00572	0.40955	0.27695	0.18402	0.11500	0.06875	0.04053	0.02058	0.01001	0.00418
0.00597	0.40243	0.27213	0.18082	0.11159	0.06672	0.03938	0.02016	0.00987	0.00414
0.00601	0.40126	0.27134	0.18022	0.11103	0.06638	0.03920	0.02009	0.00984	0.00414
0.00614	0.39775	0.26897	0.17842	0.10920	0.06528	0.03864	0.01988	0.00977	0.00412
0.00619	0.39659	0.26818	0.17783	0.10859	0.06492	0.03848	0.01982	0.00975	0.00411
0.00627	0.39428	0.26662	0.17664	0.10739	0.06420	0.03816	0.01968	0.00970	0.00410
0.00641	0.39084	0.26429	0.17488	0.10605	0.06340	0.03768	0.01948	0.00963	0.00408
0.00650	0.38856	0.26275	0.17372	0.10517	0.06287	0.03737	0.01934	0.00959	0.00407
0.00664	0.38517	0.26046	0.17199	0.10386	0.06209	0.03691	0.01914	0.00953	0.00406
0.00669	0.38404	0.25970	0.17141	0.10327	0.06177	0.03675	0.01908	0.00951	0.00406
0.00688	0.37958	0.25668	0.16914	0.10093	0.06050	0.03614	0.01882	0.00944	0.00405
0.00693	0.37847	0.25593	0.16857	0.10035	0.06018	0.03598	0.01875	0.00941	0.00404
0.00698	0.37737	0.25517	0.16801	0.09978	0.05987	0.03581	0.01869	0.00938	0.00404
0.00708	0.37517	0.25366	0.16689	0.09883	0.05925	0.03548	0.01856	0.00933	0.00403
0.00723	0.37189	0.25141	0.16452	0.09743	0.05833	0.03500	0.01837	0.00925	0.00400
0.00733	0.36973	0.24992	0.16296	0.09650	0.05772	0.03468	0.01824	0.00921	0.00399
0.00739	0.36865	0.24918	0.16218	0.09601	0.05742	0.03452	0.01818	0.00918	0.00398
0.00744	0.36757	0.24823	0.16141	0.09552	0.05713	0.03436	0.01812	0.00916	0.00398
0.00771	0.36224	0.24354	0.15844	0.09312	0.05566	0.03357	0.01781	0.00906	0.00394
0.00776	0.36116	0.24261	0.15786	0.09265	0.05537	0.03342	0.01775	0.00903	0.00394
0.00782	0.36009	0.24180	0.15727	0.09218	0.05508	0.03327	0.01768	0.00901	0.00393
0.00793	0.35796	0.24019	0.15611	0.09125	0.05451	0.03296	0.01755	0.00897	0.00392
0.00816	0.35374	0.23701	0.15301	0.08941	0.05338	0.03236	0.01729	0.00889	0.00389
0.00821	0.35269	0.23622	0.15225	0.08895	0.05311	0.03221	0.01723	0.00886	0.00388
0.00833	0.35008	0.23464	0.15073	0.08805	0.05256	0.03192	0.01710	0.00882	0.00388
0.00845	0.34749	0.23308	0.14922	0.08716	0.05201	0.03162	0.01697	0.00877	0.00387
0.00851	0.34620	0.23230	0.14848	0.08672	0.05174	0.03151	0.01690	0.00875	0.00387
0.00869	0.34237	0.22999	0.14626	0.08542	0.05094	0.03116	0.01670	0.00868	0.00386
0.00876	0.34110	0.22913	0.14553	0.08500	0.05067	0.03104	0.01664	0.00866	0.00386
0.00882	0.33996	0.22829	0.14481	0.08457	0.05041	0.03093	0.01657	0.00863	0.00386
0.00901	0.33657	0.22576	0.14265	0.08331	0.04963	0.03058	0.01638	0.00857	0.00384
0.00914	0.33433	0.22409	0.14122	0.08220	0.04911	0.03026	0.01625	0.00852	0.00383
0.00927	0.33211	0.22243	0.14005	0.08111	0.04860	0.02995	0.01612	0.00848	0.00382
0.00933	0.33088	0.22144	0.13946	0.08057	0.04835	0.02979	0.01606	0.00845	0.00381
0.00940	0.32965	0.22046	0.13888	0.08024	0.04810	0.02963	0.01599	0.00843	0.00380
0.00947	0.32843	0.21948	0.13831	0.07990	0.04785	0.02948	0.01593	0.00841	0.00380
0.00967	0.32479	0.21657	0.13658	0.07891	0.04714	0.02901	0.01574	0.00834	0.00378
0.00974	0.32359	0.21548	0.13590	0.07858	0.04690	0.02886	0.01568	0.00832	0.00378
0.00988	0.32120	0.21334	0.13455	0.07793	0.04643	0.02856	0.01559	0.00828	0.00377

Flv	90%	80%	70%	60%	50%	45%	40%	35%	30%
0.00995	0.32001	0.21227	0.13387	0.07754	0.04620	0.02841	0.01554	0.00826	0.00376
0.01002	0.31882	0.21121	0.13320	0.07715	0.04597	0.02826	0.01550	0.00823	0.00376
0.01009	0.31764	0.21015	0.13254	0.07676	0.04574	0.02811	0.01545	0.00821	0.00375
0.01024	0.31529	0.20806	0.13122	0.07600	0.04528	0.02781	0.01536	0.00816	0.00374
0.01031	0.31412	0.20722	0.13056	0.07562	0.04506	0.02767	0.01531	0.00814	0.00374
0.01038	0.31296	0.20640	0.12991	0.07524	0.04483	0.02753	0.01527	0.00811	0.00373
0.01046	0.31180	0.20557	0.12926	0.07486	0.04461	0.02739	0.01520	0.00809	0.00373
0.01053	0.31064	0.20475	0.12861	0.07449	0.04439	0.02725	0.01514	0.00806	0.00372
0.01060	0.30926	0.20393	0.12797	0.07412	0.04416	0.02712	0.01507	0.00804	0.00371
0.01076	0.30652	0.20230	0.12669	0.07338	0.04358	0.02685	0.01494	0.00799	0.00370
0.01091	0.30380	0.20069	0.12543	0.07265	0.04300	0.02658	0.01481	0.00794	0.00369
0.01099	0.30245	0.19988	0.12480	0.07228	0.04271	0.02647	0.01475	0.00792	0.00368
0.01114	0.29977	0.19822	0.12356	0.07156	0.04215	0.02625	0.01463	0.00787	0.00367
0.01130	0.29711	0.19657	0.12215	0.07085	0.04173	0.02603	0.01450	0.00783	0.00365
0.01138	0.29579	0.19575	0.12146	0.07050	0.04152	0.02592	0.01444	0.00781	0.00365
0.01147	0.29448	0.19494	0.12076	0.07009	0.04131	0.02582	0.01438	0.00780	0.00364
0.01155	0.29317	0.19412	0.12007	0.06969	0.04110	0.02571	0.01432	0.00778	0.00363
0.01163	0.29187	0.19332	0.11939	0.06930	0.04090	0.02558	0.01427	0.00776	0.00363
0.01171	0.29057	0.19235	0.11871	0.06890	0.04069	0.02545	0.01422	0.00775	0.00362
0.01179	0.28936	0.19139	0.11811	0.06851	0.04049	0.02532	0.01416	0.00773	0.00361
0.01196	0.28695	0.18948	0.11693	0.06773	0.04007	0.02507	0.01406	0.00770	0.00360
0.01213	0.28457	0.18759	0.11577	0.06694	0.03966	0.02482	0.01396	0.00767	0.00359
0.01222	0.28338	0.18665	0.11519	0.06655	0.03945	0.02470	0.01390	0.00765	0.00359
0.01231	0.28220	0.18572	0.11461	0.06616	0.03925	0.02457	0.01385	0.00763	0.00358
0.01240	0.28102	0.18479	0.11404	0.06578	0.03904	0.02445	0.01379	0.00760	0.00358
0.01248	0.27978	0.18387	0.11338	0.06539	0.03884	0.02433	0.01373	0.00758	0.00357
0.01257	0.27853	0.18295	0.11272	0.06501	0.03864	0.02421	0.01367	0.00756	0.00357
0.01266	0.27729	0.18204	0.11206	0.06463	0.03842	0.02409	0.01362	0.00754	0.00356
0.01293	0.27361	0.17932	0.11011	0.06383	0.03777	0.02373	0.01345	0.00747	0.00355
0.01303	0.27240	0.17842	0.10947	0.06356	0.03755	0.02361	0.01340	0.00745	0.00354
0.01312	0.27119	0.17753	0.10883	0.06330	0.03734	0.02349	0.01335	0.00743	0.00354
0.01321	0.26998	0.17664	0.10821	0.06303	0.03712	0.02337	0.01330	0.00740	0.00353
0.01331	0.26863	0.17576	0.10759	0.06277	0.03694	0.02326	0.01325	0.00738	0.00353
0.01340	0.26729	0.17488	0.10698	0.06251	0.03675	0.02314	0.01320	0.00736	0.00352
0.01369	0.26330	0.17227	0.10516	0.06127	0.03620	0.02279	0.01305	0.00729	0.00351
0.01379	0.26199	0.17141	0.10455	0.06086	0.03602	0.02268	0.01301	0.00727	0.00350
0.01388	0.26068	0.17052	0.10403	0.06045	0.03584	0.02257	0.01297	0.00725	0.00350
0.01398	0.25937	0.16964	0.10351	0.06015	0.03566	0.02245	0.01293	0.00723	0.00349
0.01408	0.25829	0.16876	0.10300	0.05985	0.03546	0.02234	0.01289	0.00721	0.00349
0.01428	0.25615	0.16702	0.10197	0.05926	0.03504	0.02212	0.01281	0.00717	0.00347
0.01449	0.25402	0.16529	0.10095	0.05866	0.03464	0.02190	0.01274	0.00712	0.00346
0.01459	0.25296	0.16443	0.10045	0.05837	0.03443	0.02179	0.01270	0.00710	0.00345
0.01470	0.25190	0.16358	0.09978	0.05808	0.03423	0.02168	0.01266	0.00708	0.00344
0.01480	0.25085	0.16280	0.09911	0.05775	0.03403	0.02157	0.01260	0.00706	0.00343
0.01501	0.24835	0.16126	0.09780	0.05709	0.03365	0.02136	0.01247	0.00702	0.00342
0.01512	0.24711	0.16049	0.09715	0.05676	0.03345	0.02125	0.01241	0.00700	0.00341
0.01533	0.24465	0.15896	0.09586	0.05612	0.03307	0.02104	0.01229	0.00696	0.00340

Flv	90%	80%	70%	60%	50%	45%	40%	35%	30%
0.01544	0.24342	0.15821	0.09522	0.05580	0.03288	0.02095	0.01223	0.00694	0.00340
0.01555	0.24221	0.15730	0.09459	0.05547	0.03270	0.02086	0.01216	0.00691	0.00340
0.01566	0.24100	0.15641	0.09396	0.05515	0.03253	0.02078	0.01211	0.00689	0.00339
0.01589	0.23859	0.15463	0.09271	0.05451	0.03221	0.02060	0.01201	0.00685	0.00338
0.01612	0.23622	0.15286	0.09148	0.05387	0.03189	0.02043	0.01191	0.00681	0.00337
0.01623	0.23503	0.15199	0.09096	0.05356	0.03173	0.02035	0.01186	0.00679	0.00337
0.01635	0.23386	0.15098	0.09044	0.05325	0.03157	0.02025	0.01181	0.00677	0.00336
0.01646	0.23269	0.14997	0.08992	0.05294	0.03141	0.02015	0.01177	0.00675	0.00335
0.01658	0.23153	0.14898	0.08941	0.05264	0.03129	0.02006	0.01172	0.00673	0.00334
0.01670	0.23037	0.14823	0.08890	0.05234	0.03116	0.01996	0.01168	0.00671	0.00334
0.01694	0.22807	0.14675	0.08788	0.05175	0.03091	0.01977	0.01159	0.00668	0.00332
0.01706	0.22693	0.14602	0.08730	0.05145	0.03079	0.01968	0.01155	0.00666	0.00331
0.01718	0.22580	0.14529	0.08672	0.05116	0.03058	0.01958	0.01151	0.00664	0.00331
0.01755	0.22243	0.14312	0.08500	0.05034	0.02998	0.01929	0.01138	0.00659	0.00329
0.01767	0.22116	0.14231	0.08443	0.05007	0.02978	0.01919	0.01133	0.00657	0.00329
0.01792	0.21864	0.14068	0.08331	0.04954	0.02938	0.01900	0.01124	0.00654	0.00328
0.01805	0.21739	0.13988	0.08276	0.04928	0.02919	0.01891	0.01119	0.00652	0.00328
0.01818	0.21615	0.13908	0.08220	0.04902	0.02899	0.01880	0.01114	0.00650	0.00327
0.01844	0.21369	0.13750	0.08111	0.04849	0.02866	0.01858	0.01105	0.00646	0.00326
0.01857	0.21262	0.13670	0.08057	0.04822	0.02850	0.01848	0.01100	0.00644	0.00326
0.01870	0.21156	0.13590	0.08011	0.04794	0.02834	0.01837	0.01096	0.00642	0.00325
0.01897	0.20945	0.13432	0.07920	0.04740	0.02801	0.01816	0.01088	0.00638	0.00323
0.01911	0.20841	0.13354	0.07875	0.04713	0.02785	0.01807	0.01084	0.00636	0.00323
0.01938	0.20633	0.13199	0.07785	0.04659	0.02753	0.01789	0.01076	0.00633	0.00321
0.01952	0.20530	0.13122	0.07741	0.04632	0.02737	0.01780	0.01072	0.00631	0.00320
0.01966	0.20420	0.13034	0.07696	0.04605	0.02721	0.01771	0.01068	0.00629	0.00320
0.01980	0.20311	0.12948	0.07651	0.04578	0.02705	0.01763	0.01064	0.00627	0.00319
0.02008	0.20095	0.12776	0.07562	0.04525	0.02674	0.01745	0.01056	0.00623	0.00318
0.02022	0.19988	0.12691	0.07518	0.04498	0.02658	0.01736	0.01053	0.00621	0.00317
0.02036	0.19874	0.12606	0.07474	0.04472	0.02645	0.01728	0.01049	0.00620	0.00317
0.02051	0.19761	0.12522	0.07430	0.04446	0.02632	0.01719	0.01045	0.00618	0.00316
0.02066	0.19648	0.12451	0.07387	0.04420	0.02618	0.01710	0.01041	0.00616	0.00315
0.02110	0.19313	0.12239	0.07240	0.04343	0.02579	0.01685	0.01029	0.00611	0.00313
0.02125	0.19203	0.12169	0.07192	0.04318	0.02566	0.01676	0.01025	0.00609	0.00313
0.02140	0.19091	0.12099	0.07144	0.04293	0.02554	0.01668	0.01021	0.00607	0.00312
0.02155	0.18980	0.12030	0.07097	0.04268	0.02539	0.01660	0.01017	0.00605	0.00312
0.02171	0.18869	0.11950	0.07050	0.04243	0.02525	0.01651	0.01012	0.00604	0.00312
0.02233	0.18433	0.11635	0.06864	0.04147	0.02467	0.01619	0.00996	0.00597	0.00310
0.02249	0.18326	0.11558	0.06818	0.04123	0.02453	0.01611	0.00991	0.00595	0.00309
0.02265	0.18221	0.11481	0.06773	0.04100	0.02439	0.01602	0.00986	0.00593	0.00309
0.02281	0.18117	0.11414	0.06727	0.04076	0.02425	0.01594	0.00981	0.00591	0.00308
0.02364	0.17606	0.11085	0.06506	0.03975	0.02355	0.01555	0.00956	0.00580	0.00305
0.02380	0.17503	0.11020	0.06463	0.03955	0.02341	0.01547	0.00954	0.00578	0.00304
0.02397	0.17401	0.10956	0.06420	0.03936	0.02328	0.01538	0.00951	0.00576	0.00304
0.02414	0.17299	0.10883	0.06377	0.03916	0.02315	0.01530	0.00948	0.00574	0.00303
0.02432	0.17199	0.10811	0.06335	0.03890	0.02301	0.01521	0.00945	0.00572	0.00302
0.02502	0.16801	0.10526	0.06168	0.03787	0.02249	0.01486	0.00934	0.00565	0.00299

Flv	90%	80%	70%	60%	50%	45%	40%	35%	30%
0.02519	0.16705	0.10455	0.06127	0.03762	0.02236	0.01479	0.00931	0.00563	0.00298
0.02537	0.16610	0.10386	0.06086	0.03737	0.02223	0.01472	0.00925	0.00562	0.00297
0.02555	0.16515	0.10317	0.06045	0.03716	0.02210	0.01464	0.00919	0.00560	0.00296
0.02574	0.16421	0.10248	0.06005	0.03695	0.02197	0.01457	0.00913	0.00558	0.00295
0.02592	0.16327	0.10180	0.05965	0.03673	0.02184	0.01450	0.00909	0.00557	0.00295
0.02629	0.16141	0.10045	0.05886	0.03632	0.02159	0.01435	0.00901	0.00553	0.00294
0.02648	0.16034	0.09978	0.05847	0.03611	0.02146	0.01428	0.00898	0.00552	0.00293
0.02666	0.15927	0.09911	0.05808	0.03590	0.02134	0.01421	0.00894	0.00550	0.00293
0.02685	0.15821	0.09845	0.05769	0.03569	0.02122	0.01414	0.00890	0.00549	0.00293
0.02724	0.15611	0.09715	0.05693	0.03528	0.02098	0.01400	0.00883	0.00545	0.00292
0.02743	0.15507	0.09650	0.05655	0.03507	0.02086	0.01393	0.00879	0.00544	0.00291
0.02763	0.15404	0.09586	0.05617	0.03487	0.02074	0.01386	0.00876	0.00542	0.00291
0.02782	0.15327	0.09522	0.05580	0.03467	0.02062	0.01379	0.00873	0.00540	0.00290
0.02802	0.15250	0.09459	0.05543	0.03446	0.02048	0.01372	0.00870	0.00538	0.00289
0.02822	0.15174	0.09396	0.05506	0.03426	0.02035	0.01364	0.00867	0.00536	0.00289
0.02903	0.14873	0.09148	0.05361	0.03321	0.01981	0.01333	0.00854	0.00528	0.00287
0.02924	0.14798	0.09087	0.05325	0.03295	0.01968	0.01326	0.00850	0.00526	0.00286
0.02945	0.14683	0.09026	0.05289	0.03270	0.01958	0.01318	0.00846	0.00524	0.00285
0.02966	0.14569	0.08966	0.05254	0.03254	0.01948	0.01311	0.00842	0.00523	0.00285
0.03051	0.14122	0.08730	0.05096	0.03193	0.01910	0.01285	0.00826	0.00517	0.00282
0.03095	0.13958	0.08614	0.05019	0.03162	0.01891	0.01273	0.00819	0.00513	0.00281
0.03117	0.13877	0.08557	0.04981	0.03144	0.01878	0.01266	0.00815	0.00512	0.00280
0.03139	0.13796	0.08494	0.04948	0.03126	0.01865	0.01260	0.00812	0.00510	0.00280
0.03206	0.13556	0.08311	0.04849	0.03071	0.01828	0.01241	0.00802	0.00505	0.00278
0.03229	0.13477	0.08250	0.04817	0.03053	0.01816	0.01235	0.00799	0.00503	0.00278
0.03252	0.13387	0.08191	0.04785	0.03035	0.01804	0.01229	0.00796	0.00501	0.00277
0.03275	0.13298	0.08131	0.04753	0.03018	0.01795	0.01223	0.00793	0.00499	0.00276
0.03299	0.13210	0.08072	0.04722	0.02998	0.01786	0.01216	0.00790	0.00497	0.00276
0.03346	0.13034	0.07955	0.04659	0.02958	0.01768	0.01203	0.00784	0.00494	0.00275
0.03370	0.12948	0.07897	0.04628	0.02938	0.01760	0.01196	0.00781	0.00492	0.00274
0.03418	0.12776	0.07793	0.04566	0.02899	0.01742	0.01182	0.00775	0.00490	0.00273
0.03442	0.12691	0.07741	0.04536	0.02880	0.01733	0.01175	0.00772	0.00489	0.00272
0.03467	0.12606	0.07689	0.04506	0.02863	0.01722	0.01169	0.00768	0.00488	0.00272
0.03491	0.12522	0.07638	0.04476	0.02847	0.01710	0.01162	0.00765	0.00486	0.00271
0.03541	0.12356	0.07537	0.04416	0.02815	0.01688	0.01148	0.00757	0.00484	0.00270
0.03592	0.12192	0.07420	0.04358	0.02783	0.01665	0.01135	0.00749	0.00480	0.00269
0.03617	0.12111	0.07362	0.04329	0.02767	0.01654	0.01128	0.00746	0.00479	0.00268
0.03643	0.12030	0.07305	0.04300	0.02748	0.01645	0.01122	0.00742	0.00477	0.00268
0.03669	0.11950	0.07249	0.04271	0.02730	0.01635	0.01115	0.00739	0.00475	0.00267
0.03695	0.11871	0.07192	0.04243	0.02712	0.01626	0.01110	0.00735	0.00473	0.00267
0.03721	0.11791	0.07138	0.04215	0.02694	0.01617	0.01104	0.00732	0.00471	0.00266
0.03775	0.11635	0.07029	0.04159	0.02658	0.01598	0.01093	0.00726	0.00468	0.00265
0.03801	0.11570	0.06976	0.04131	0.02640	0.01589	0.01088	0.00723	0.00466	0.00265
0.03829	0.11506	0.06923	0.04103	0.02623	0.01580	0.01082	0.00719	0.00465	0.00264
0.03856	0.11442	0.06870	0.04076	0.02605	0.01570	0.01077	0.00716	0.00463	0.00263
0.03883	0.11379	0.06818	0.04049	0.02588	0.01560	0.01071	0.00713	0.00462	0.00263
0.03911	0.11316	0.06765	0.04022	0.02571	0.01551	0.01066	0.00710	0.00460	0.00262

Flv	90%	80%	70%	60%	50%	45%	40%	35%	30%
0.03939	0.11253	0.06713	0.03999	0.02556	0.01542	0.01061	0.00707	0.00459	0.00262
0.04023	0.10969	0.06557	0.03931	0.02513	0.01514	0.01045	0.00697	0.00455	0.00260
0.04052	0.10876	0.06506	0.03909	0.02498	0.01505	0.01040	0.00694	0.00454	0.00259
0.04110	0.10693	0.06420	0.03864	0.02470	0.01486	0.01029	0.00688	0.00451	0.00258
0.04139	0.10603	0.06377	0.03838	0.02454	0.01477	0.01024	0.00685	0.00450	0.00258
0.04198	0.10424	0.06293	0.03787	0.02422	0.01459	0.01012	0.00679	0.00446	0.00256
0.04258	0.10248	0.06209	0.03744	0.02390	0.01442	0.01001	0.00673	0.00443	0.00255
0.04319	0.10075	0.06045	0.03702	0.02359	0.01424	0.00990	0.00667	0.00440	0.00254
0.04412	0.09821	0.05926	0.03639	0.02313	0.01399	0.00974	0.00658	0.00435	0.00252
0.04539	0.09493	0.05769	0.03544	0.02253	0.01365	0.00952	0.00647	0.00428	0.00249
0.06290	0.06420	0.04106	0.02622	0.01665	0.01032	0.00737	0.00528	0.00361	0.00221
0.06335	0.06377	0.04076	0.02605	0.01654	0.01026	0.00733	0.00525	0.00359	0.00221
0.06380	0.06335	0.04053	0.02588	0.01643	0.01019	0.00729	0.00522	0.00358	0.00220
0.06564	0.06168	0.03961	0.02520	0.01600	0.00995	0.00713	0.00512	0.00353	0.00218
0.06610	0.06127	0.03938	0.02503	0.01589	0.00989	0.00709	0.00510	0.00351	0.00217
0.06657	0.06086	0.03916	0.02486	0.01579	0.00982	0.00705	0.00507	0.00350	0.00216
0.06705	0.06045	0.03890	0.02470	0.01568	0.00976	0.00701	0.00504	0.00349	0.00216
0.06849	0.05926	0.03813	0.02428	0.01537	0.00956	0.00689	0.00496	0.00344	0.00214
0.06898	0.05886	0.03787	0.02414	0.01527	0.00950	0.00685	0.00494	0.00343	0.00213
0.06947	0.05847	0.03762	0.02400	0.01517	0.00944	0.00681	0.00492	0.00342	0.00213
0.07046	0.05769	0.03712	0.02373	0.01496	0.00931	0.00673	0.00488	0.00339	0.00211
0.07096	0.05731	0.03687	0.02357	0.01486	0.00925	0.00670	0.00485	0.00337	0.00211
0.07147	0.05693	0.03663	0.02341	0.01477	0.00919	0.00666	0.00483	0.00336	0.00210
0.07249	0.05617	0.03614	0.02310	0.01457	0.00908	0.00658	0.00479	0.00334	0.00209
0.07300	0.05580	0.03590	0.02295	0.01447	0.00903	0.00654	0.00477	0.00333	0.00209
0.07405	0.05481	0.03543	0.02264	0.01428	0.00893	0.00647	0.00473	0.00331	0.00208
0.07457	0.05433	0.03519	0.02249	0.01419	0.00888	0.00643	0.00470	0.00330	0.00208
0.07510	0.05384	0.03496	0.02234	0.01409	0.00883	0.00639	0.00468	0.00329	0.00207
0.07564	0.05337	0.03472	0.02219	0.01400	0.00877	0.00636	0.00466	0.00328	0.00207
0.07618	0.05289	0.03449	0.02205	0.01390	0.00871	0.00632	0.00463	0.00327	0.00206
0.07727	0.05219	0.03397	0.02175	0.01372	0.00859	0.00625	0.00459	0.00324	0.00205
0.07837	0.05150	0.03345	0.02146	0.01354	0.00848	0.00617	0.00455	0.00322	0.00203
0.07893	0.05116	0.03320	0.02132	0.01343	0.00842	0.00614	0.00453	0.00320	0.00203
0.07949	0.05082	0.03295	0.02118	0.01333	0.00837	0.00610	0.00451	0.00319	0.00202
0.08006	0.05048	0.03270	0.02104	0.01323	0.00832	0.00606	0.00449	0.00318	0.00202
0.08120	0.04948	0.03219	0.02076	0.01303	0.00821	0.00599	0.00445	0.00315	0.00200
0.08236	0.04849	0.03169	0.02048	0.01283	0.00811	0.00592	0.00441	0.00312	0.00199
0.08295	0.04817	0.03145	0.02035	0.01273	0.00806	0.00589	0.00438	0.00311	0.00199
0.08354	0.04785	0.03120	0.02021	0.01263	0.00801	0.00586	0.00436	0.00309	0.00198
0.08473	0.04722	0.03079	0.01994	0.01244	0.00791	0.00579	0.00432	0.00307	0.00197
0.08533	0.04690	0.03058	0.01981	0.01234	0.00786	0.00576	0.00430	0.00305	0.00196
0.08594	0.04659	0.03038	0.01968	0.01225	0.00781	0.00573	0.00428	0.00304	0.00196
0.08655	0.04628	0.03018	0.01955	0.01216	0.00776	0.00570	0.00425	0.00303	0.00195
0.08717	0.04587	0.02998	0.01942	0.01208	0.00771	0.00567	0.00423	0.00302	0.00195
0.08779	0.04546	0.02978	0.01929	0.01200	0.00766	0.00564	0.00422	0.00300	0.00194
0.08904	0.04466	0.02925	0.01903	0.01184	0.00757	0.00559	0.00418	0.00298	0.00193
0.08968	0.04426	0.02899	0.01889	0.01177	0.00752	0.00556	0.00416	0.00297	0.00193

Flv	90%	80%	70%	60%	50%	45%	40%	35%	30%
0.09031	0.04387	0.02880	0.01874	0.01169	0.00747	0.00553	0.00415	0.00296	0.00192
0.09160	0.04310	0.02842	0.01846	0.01153	0.00737	0.00546	0.00411	0.00293	0.00191
0.09226	0.04271	0.02823	0.01832	0.01146	0.00732	0.00542	0.00409	0.00292	0.00190
0.09357	0.04196	0.02785	0.01804	0.01130	0.00722	0.00535	0.00405	0.00290	0.00189
0.09424	0.04159	0.02767	0.01790	0.01123	0.00718	0.00531	0.00403	0.00289	0.00188
0.09491	0.04122	0.02742	0.01776	0.01115	0.00714	0.00528	0.00401	0.00288	0.00187
0.09764	0.03978	0.02646	0.01722	0.01076	0.00697	0.00515	0.00393	0.00283	0.00186
0.09834	0.03942	0.02623	0.01709	0.01067	0.00693	0.00512	0.00391	0.00282	0.00185
0.09904	0.03916	0.02600	0.01696	0.01057	0.00689	0.00508	0.00389	0.00281	0.00185
0.09974	0.03890	0.02576	0.01683	0.01050	0.00685	0.00505	0.00387	0.00280	0.00184
0.10045	0.03864	0.02554	0.01670	0.01043	0.00680	0.00502	0.00386	0.00279	0.00184
0.10261	0.03762	0.02486	0.01632	0.01023	0.00667	0.00493	0.00380	0.00275	0.00182
0.10334	0.03729	0.02467	0.01620	0.01016	0.00662	0.00490	0.00378	0.00274	0.00181
0.10408	0.03696	0.02448	0.01607	0.01009	0.00658	0.00487	0.00376	0.00273	0.00180
0.10482	0.03663	0.02429	0.01594	0.01001	0.00654	0.00484	0.00374	0.00272	0.00180
0.10557	0.03630	0.02410	0.01582	0.00993	0.00649	0.00481	0.00371	0.00271	0.00179
0.10708	0.03566	0.02373	0.01558	0.00978	0.00641	0.00475	0.00367	0.00268	0.00178
0.10860	0.03503	0.02337	0.01534	0.00963	0.00632	0.00470	0.00363	0.00266	0.00177
0.10938	0.03472	0.02319	0.01522	0.00956	0.00628	0.00467	0.00361	0.00265	0.00176
0.11094	0.03411	0.02284	0.01498	0.00944	0.00620	0.00462	0.00358	0.00262	0.00175
0.11173	0.03381	0.02266	0.01486	0.00937	0.00615	0.00459	0.00357	0.00261	0.00174
0.11253	0.03351	0.02249	0.01473	0.00931	0.00611	0.00456	0.00355	0.00260	0.00174
0.11413	0.03292	0.02210	0.01447	0.00919	0.00603	0.00451	0.00352	0.00258	0.00173
0.11495	0.03262	0.02190	0.01434	0.00907	0.00599	0.00449	0.00350	0.00257	0.00172
0.11576	0.03233	0.02170	0.01422	0.00901	0.00595	0.00446	0.00349	0.00256	0.00172
0.11659	0.03205	0.02151	0.01409	0.00895	0.00591	0.00444	0.00347	0.00255	0.00171
0.11742	0.03176	0.02132	0.01400	0.00889	0.00587	0.00441	0.00345	0.00254	0.00171
0.11909	0.03120	0.02095	0.01381	0.00877	0.00580	0.00435	0.00342	0.00251	0.00170
0.11994	0.03089	0.02076	0.01372	0.00871	0.00576	0.00432	0.00341	0.00250	0.00169
0.12080	0.03058	0.02058	0.01363	0.00865	0.00572	0.00429	0.00339	0.00249	0.00169
0.12166	0.03028	0.02039	0.01354	0.00858	0.00568	0.00426	0.00337	0.00248	0.00168
0.12252	0.02998	0.02021	0.01345	0.00850	0.00564	0.00423	0.00335	0.00247	0.00168
0.12427	0.02938	0.01986	0.01321	0.00835	0.00557	0.00418	0.00331	0.00245	0.00167
0.12605	0.02886	0.01950	0.01298	0.00820	0.00549	0.00414	0.00328	0.00243	0.00165
0.12695	0.02861	0.01933	0.01286	0.00815	0.00546	0.00411	0.00326	0.00242	0.00165
0.12785	0.02835	0.01916	0.01275	0.00809	0.00542	0.00409	0.00324	0.00241	0.00164
0.12876	0.02810	0.01899	0.01265	0.00804	0.00538	0.00406	0.00322	0.00240	0.00163
0.12968	0.02785	0.01882	0.01255	0.00799	0.00535	0.00404	0.00320	0.00239	0.00163
0.13246	0.02697	0.01833	0.01227	0.00783	0.00524	0.00397	0.00316	0.00236	0.00161
0.13341	0.02669	0.01816	0.01218	0.00776	0.00521	0.00395	0.00314	0.00235	0.00161
0.13436	0.02640	0.01800	0.01208	0.00769	0.00517	0.00393	0.00312	0.00234	0.00160
0.13531	0.02617	0.01784	0.01198	0.00762	0.00514	0.00391	0.00311	0.00232	0.00160
0.13628	0.02594	0.01768	0.01187	0.00755	0.00510	0.00388	0.00309	0.00231	0.00160
0.13822	0.02548	0.01737	0.01166	0.00742	0.00504	0.00383	0.00306	0.00229	0.00159
0.13921	0.02525	0.01722	0.01156	0.00736	0.00500	0.00380	0.00305	0.00228	0.00158
0.14020	0.02503	0.01707	0.01146	0.00731	0.00497	0.00378	0.00303	0.00227	0.00157
0.14220	0.02450	0.01676	0.01128	0.00720	0.00490	0.00373	0.00300	0.00224	0.00156

Flv	90%	80%	70%	60%	50%	45%	40%	35%	30%
0.14423	0.02398	0.01647	0.01110	0.00709	0.00484	0.00368	0.00297	0.00223	0.00155
0.14526	0.02373	0.01632	0.01102	0.00704	0.00481	0.00365	0.00296	0.00222	0.00154
0.14629	0.02352	0.01618	0.01093	0.00699	0.00477	0.00363	0.00294	0.00221	0.00154
0.14733	0.02331	0.01603	0.01083	0.00693	0.00474	0.00361	0.00293	0.00220	0.00153
0.14944	0.02290	0.01575	0.01064	0.00680	0.00468	0.00356	0.00290	0.00218	0.00152
0.15050	0.02269	0.01561	0.01055	0.00674	0.00465	0.00354	0.00288	0.00217	0.00152
0.15157	0.02249	0.01547	0.01046	0.00668	0.00462	0.00352	0.00287	0.00216	0.00151
0.15265	0.02229	0.01534	0.01036	0.00662	0.00459	0.00350	0.00285	0.00215	0.00151
0.15374	0.02210	0.01520	0.01025	0.00658	0.00456	0.00348	0.00284	0.00214	0.00150
0.15594	0.02170	0.01493	0.01002	0.00649	0.00450	0.00344	0.00281	0.00212	0.00149
0.15816	0.02132	0.01467	0.00985	0.00641	0.00444	0.00340	0.00278	0.00210	0.00148
0.15929	0.02109	0.01449	0.00976	0.00636	0.00441	0.00337	0.00277	0.00209	0.00148
0.16042	0.02085	0.01432	0.00967	0.00632	0.00438	0.00335	0.00276	0.00208	0.00148
0.16157	0.02062	0.01415	0.00959	0.00626	0.00435	0.00333	0.00274	0.00207	0.00147
0.16272	0.02040	0.01398	0.00950	0.00621	0.00432	0.00331	0.00273	0.00206	0.00147
0.16387	0.02019	0.01381	0.00941	0.00615	0.00428	0.00328	0.00271	0.00205	0.00146
0.16621	0.01976	0.01357	0.00924	0.00605	0.00422	0.00324	0.00268	0.00203	0.00145
0.16740	0.01955	0.01345	0.00915	0.00599	0.00419	0.00322	0.00266	0.00202	0.00145
0.16859	0.01935	0.01333	0.00907	0.00594	0.00415	0.00320	0.00265	0.00201	0.00144
0.16979	0.01916	0.01321	0.00899	0.00589	0.00412	0.00319	0.00263	0.00200	0.00144
0.17100	0.01897	0.01309	0.00891	0.00583	0.00409	0.00317	0.00262	0.00199	0.00143
0.17468	0.01841	0.01268	0.00867	0.00568	0.00401	0.00311	0.00258	0.00197	0.00142
0.17592	0.01821	0.01254	0.00859	0.00564	0.00399	0.00309	0.00257	0.00196	0.00141
0.17717	0.01802	0.01241	0.00852	0.00559	0.00396	0.00307	0.00256	0.00195	0.00141
0.17843	0.01783	0.01229	0.00844	0.00555	0.00393	0.00305	0.00254	0.00195	0.00140
0.17970	0.01764	0.01216	0.00837	0.00551	0.00390	0.00303	0.00253	0.00194	0.00140
0.18098	0.01745	0.01204	0.00829	0.00547	0.00387	0.00301	0.00252	0.00193	0.00139
0.18357	0.01703	0.01180	0.00815	0.00538	0.00381	0.00297	0.00249	0.00191	0.00138
0.18487	0.01683	0.01169	0.00807	0.00534	0.00378	0.00295	0.00247	0.00190	0.00137
0.18751	0.01643	0.01148	0.00792	0.00526	0.00373	0.00291	0.00244	0.00188	0.00136
0.18885	0.01629	0.01138	0.00784	0.00522	0.00370	0.00289	0.00243	0.00187	0.00136
0.19019	0.01614	0.01128	0.00777	0.00518	0.00368	0.00287	0.00242	0.00186	0.00135
0.19155	0.01600	0.01118	0.00769	0.00514	0.00365	0.00285	0.00240	0.00185	0.00135
0.19291	0.01586	0.01108	0.00762	0.00509	0.00363	0.00284	0.00239	0.00184	0.00134
0.19428	0.01572	0.01096	0.00755	0.00504	0.00361	0.00282	0.00237	0.00183	0.00134
0.19567	0.01558	0.01084	0.00748	0.00499	0.00358	0.00280	0.00236	0.00182	0.00133
0.19706	0.01538	0.01073	0.00741	0.00494	0.00356	0.00278	0.00235	0.00182	0.00133
0.19988	0.01500	0.01050	0.00727	0.00485	0.00351	0.00274	0.00232	0.00180	0.00132
0.20130	0.01481	0.01040	0.00720	0.00481	0.00349	0.00272	0.00231	0.00179	0.00131
0.20273	0.01462	0.01029	0.00713	0.00476	0.00346	0.00271	0.00230	0.00178	0.00131
0.20417	0.01444	0.01019	0.00707	0.00472	0.00344	0.00269	0.00229	0.00177	0.00130
0.20563	0.01426	0.01009	0.00700	0.00468	0.00341	0.00267	0.00227	0.00176	0.00130
0.20856	0.01390	0.00989	0.00688	0.00460	0.00336	0.00263	0.00225	0.00174	0.00129
0.21154	0.01366	0.00965	0.00676	0.00452	0.00331	0.00260	0.00223	0.00173	0.00128
0.21305	0.01354	0.00954	0.00669	0.00448	0.00328	0.00258	0.00222	0.00172	0.00127
0.21457	0.01342	0.00942	0.00661	0.00444	0.00326	0.00257	0.00220	0.00171	0.00127
0.21609	0.01330	0.00931	0.00654	0.00440	0.00323	0.00255	0.00219	0.00170	0.00126

Flv	90%	80%	70%	60%	50%	45%	40%	35%	30%
0.21763	0.01318	0.00923	0.00647	0.00436	0.00321	0.00253	0.00218	0.00169	0.00126
0.21918	0.01304	0.00915	0.00641	0.00432	0.00319	0.00251	0.00217	0.00168	0.00125
0.22074	0.01290	0.00907	0.00634	0.00428	0.00316	0.00250	0.00215	0.00168	0.00125
0.22231	0.01276	0.00896	0.00628	0.00424	0.00314	0.00248	0.00214	0.00167	0.00124
0.22390	0.01263	0.00885	0.00622	0.00421	0.00311	0.00246	0.00213	0.00166	0.00124
0.22549	0.01249	0.00875	0.00615	0.00417	0.00309	0.00245	0.00212	0.00165	0.00123
0.22871	0.01220	0.00854	0.00603	0.00411	0.00305	0.00242	0.00209	0.00163	0.00122
0.23363	0.01177	0.00827	0.00587	0.00402	0.00299	0.00237	0.00206	0.00160	0.00121
0.23529	0.01162	0.00818	0.00582	0.00399	0.00297	0.00235	0.00204	0.00159	0.00120
0.23697	0.01149	0.00809	0.00577	0.00395	0.00295	0.00234	0.00203	0.00159	0.00120
0.23865	0.01135	0.00801	0.00572	0.00392	0.00293	0.00232	0.00202	0.00158	0.00119
0.24035	0.01121	0.00793	0.00566	0.00388	0.00290	0.00230	0.00201	0.00157	0.00119
0.24206	0.01108	0.00785	0.00560	0.00385	0.00288	0.00229	0.00200	0.00156	0.00119
0.24552	0.01084	0.00770	0.00548	0.00378	0.00284	0.00226	0.00197	0.00155	0.00118
0.24727	0.01073	0.00762	0.00542	0.00374	0.00281	0.00224	0.00196	0.00154	0.00117
0.24903	0.01062	0.00755	0.00537	0.00370	0.00279	0.00223	0.00195	0.00153	0.00117
0.25080	0.01050	0.00747	0.00531	0.00366	0.00277	0.00221	0.00194	0.00152	0.00116
0.25438	0.01022	0.00732	0.00521	0.00358	0.00273	0.00219	0.00192	0.00151	0.00115
0.25620	0.01008	0.00723	0.00516	0.00355	0.00271	0.00217	0.00191	0.00150	0.00115
0.25802	0.00994	0.00715	0.00510	0.00352	0.00269	0.00216	0.00190	0.00149	0.00115
0.26171	0.00967	0.00698	0.00500	0.00346	0.00265	0.00213	0.00187	0.00148	0.00114
0.26357	0.00954	0.00689	0.00494	0.00343	0.00263	0.00211	0.00186	0.00147	0.00113
0.26544	0.00941	0.00682	0.00489	0.00340	0.00261	0.00210	0.00185	0.00146	0.00113
0.26733	0.00928	0.00675	0.00484	0.00337	0.00259	0.00209	0.00184	0.00145	0.00113
0.26924	0.00916	0.00668	0.00479	0.00334	0.00257	0.00207	0.00182	0.00144	0.00112
0.27308	0.00891	0.00654	0.00469	0.00328	0.00253	0.00204	0.00180	0.00143	0.00111
0.27503	0.00879	0.00645	0.00464	0.00325	0.00251	0.00203	0.00179	0.00142	0.00111
0.27698	0.00867	0.00636	0.00459	0.00322	0.00249	0.00201	0.00178	0.00141	0.00110
0.28294	0.00832	0.00611	0.00445	0.00313	0.00243	0.00197	0.00175	0.00139	0.00109
0.28496	0.00821	0.00604	0.00441	0.00311	0.00241	0.00195	0.00174	0.00138	0.00109
0.28698	0.00809	0.00597	0.00436	0.00308	0.00239	0.00194	0.00173	0.00137	0.00108
0.28903	0.00802	0.00590	0.00432	0.00305	0.00237	0.00192	0.00172	0.00136	0.00108
0.29316	0.00788	0.00576	0.00423	0.00299	0.00233	0.00190	0.00170	0.00135	0.00107
0.29524	0.00781	0.00569	0.00419	0.00296	0.00230	0.00189	0.00168	0.00134	0.00107
0.29946	0.00767	0.00555	0.00411	0.00290	0.00227	0.00186	0.00166	0.00132	0.00106
0.30374	0.00747	0.00542	0.00403	0.00284	0.00224	0.00184	0.00164	0.00131	0.00105
0.30590	0.00737	0.00536	0.00399	0.00282	0.00223	0.00182	0.00163	0.00130	0.00105
0.30808	0.00727	0.00529	0.00395	0.00279	0.00221	0.00181	0.00162	0.00129	0.00104
0.31027	0.00718	0.00523	0.00391	0.00277	0.00220	0.00180	0.00161	0.00129	0.00104
0.31920	0.00680	0.00498	0.00375	0.00267	0.00212	0.00175	0.00156	0.00126	0.00103
0.32376	0.00662	0.00486	0.00368	0.00261	0.00209	0.00173	0.00154	0.00124	0.00102
0.33072	0.00636	0.00469	0.00357	0.00251	0.00203	0.00170	0.00151	0.00122	0.00101
0.33784	0.00611	0.00453	0.00346	0.00244	0.00198	0.00166	0.00148	0.00120	0.00100
0.34024	0.00603	0.00447	0.00343	0.00242	0.00196	0.00165	0.00147	0.00119	0.00099
0.34266	0.00595	0.00442	0.00340	0.00239	0.00195	0.00164	0.00146	0.00119	0.00099
0.34510	0.00587	0.00437	0.00336	0.00237	0.00193	0.00163	0.00145	0.00118	0.00098
0.35503	0.00560	0.00416	0.00323	0.00229	0.00187	0.00159	0.00142	0.00115	0.00097

Flv	90%	80%	70%	60%	50%	45%	40%	35%	30%
0.36010	0.00544	0.00406	0.00317	0.00225	0.00184	0.00156	0.00140	0.00114	0.00096
0.37047	0.00512	0.00387	0.00304	0.00217	0.00178	0.00152	0.00136	0.00111	0.00095
0.38384	0.00474	0.00365	0.00289	0.00208	0.00170	0.00147	0.00132	0.00108	0.00093
0.39770	0.00447	0.00343	0.00275	0.00199	0.00162	0.00142	0.00127	0.00105	0.00091

Source: The author, 2022.

Parameter estimation for flooding correlation without split of the domain

The new parameters for flooding correlation without split the *Flv* domain were determined. The results for each model were shown in Tables 56, 57 and Figure 30 (Lygeros; Magoulas, 1986); Tables 58, 59 and Figure 31 (Kessler; Wankat, 1988); Tables 60, 61 and Figure 32 (Ogboja; Kuye, 1990); Tables 62, 63 and Figure 33 (Economopoulos, 1978).

Table 56 – New parameters for the correlation of Lygeros and Magoulas (1986)

Tray spacing (m)	$\theta_{Csb,1}$	$\theta_{Csb,2}$	$\theta_{Csb,3}$	$\theta_{Csb,4}$	$\theta_{Csb,5}$
0.1524	0.01915556	0.10122625	0.77982775	2.77286068	1.54949375
0.2286	0.01157324	0.12704042	0.75974423	1.49836952	1.08102670
0.3048	0.06460206	$-8.17281 \cdot 10^{-8}$	-11.6583	0.73138154	-0.55954042
0.4572	0.08323371	$-1.049484 \cdot 10^{-7}$	-17.6475	0.65513710	-0.60413469
0.6096	0.01608333	0.14477439	0.75252671	1.71753015	0.93773419
0.9144	0.01763829	0.14388256	0.75412396	1.64074437	0.79462743

Source: The author, 2022.

Table 57 – Errors of the flooding correlation by Lygeros and Magoulas (1986) with new parameters

Tray spacing (m)	Average error (%)	Maximum error (%)
0.1524	1.54	8.00
0.2286	1.97	9.88
0.3048	1.06	5.03
0.4572	0.89	5.44
0.6096	1.85	7.67
0.9144	0.47	1.82

Source: The author, 2022.

Figure 30 – Comparison of Fair’s data from Souders-Brown constant with the correlation proposed by Lygeros and Magoulas (1986) with new parameters

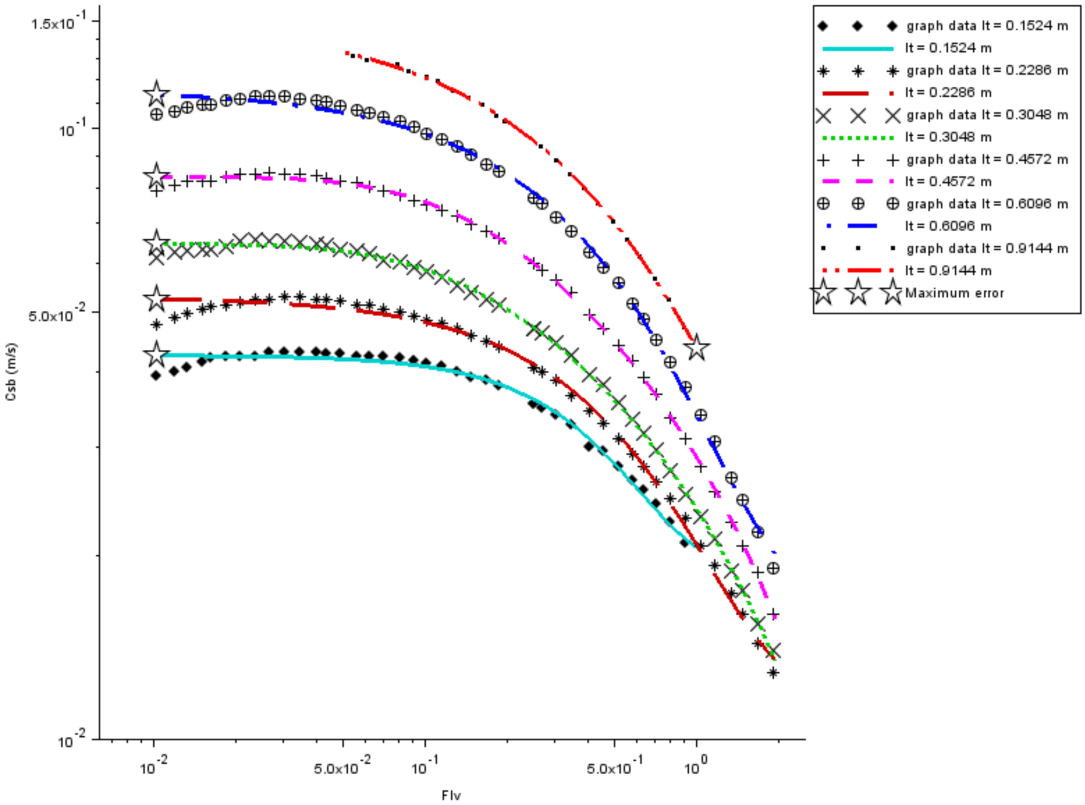

Source: The author, 2022.

Table 58 – New parameters of the quadratic correlation of Kessler and Wankat (1988)

Tray spacing (in)	$\theta_{Csb,1}$	$\theta_{Csb,2}$	$\theta_{Csb,3}$
6	1.1578	0.4515	0.1624
9	1.1483	0.5513	0.1938
12	1.1021	0.5841	0.1951
18	1.0165	0.6232	0.2094
24	0.9309	0.6666	0.2214
36	0.8305	0.6973	0.2633

Source: The author, 2022.

Table 59 – Error of flooding correlation by Kessler and Wankat (1988) with new parameters

Tray Spacing (in)	Average error (%)	Maximum error (%)
6	1.64	7.45
9	2.30	13.76
12	2.42	13.58
18	2.53	18.62
24	2. 60	17.08
36	0.82	4.94

Source: The author, 2022.

Figure 31 – Comparison of Fair's data from Souders-Brown constant with the quadratic correlation proposed by Kessler and Wankat (1988) with the new parameters

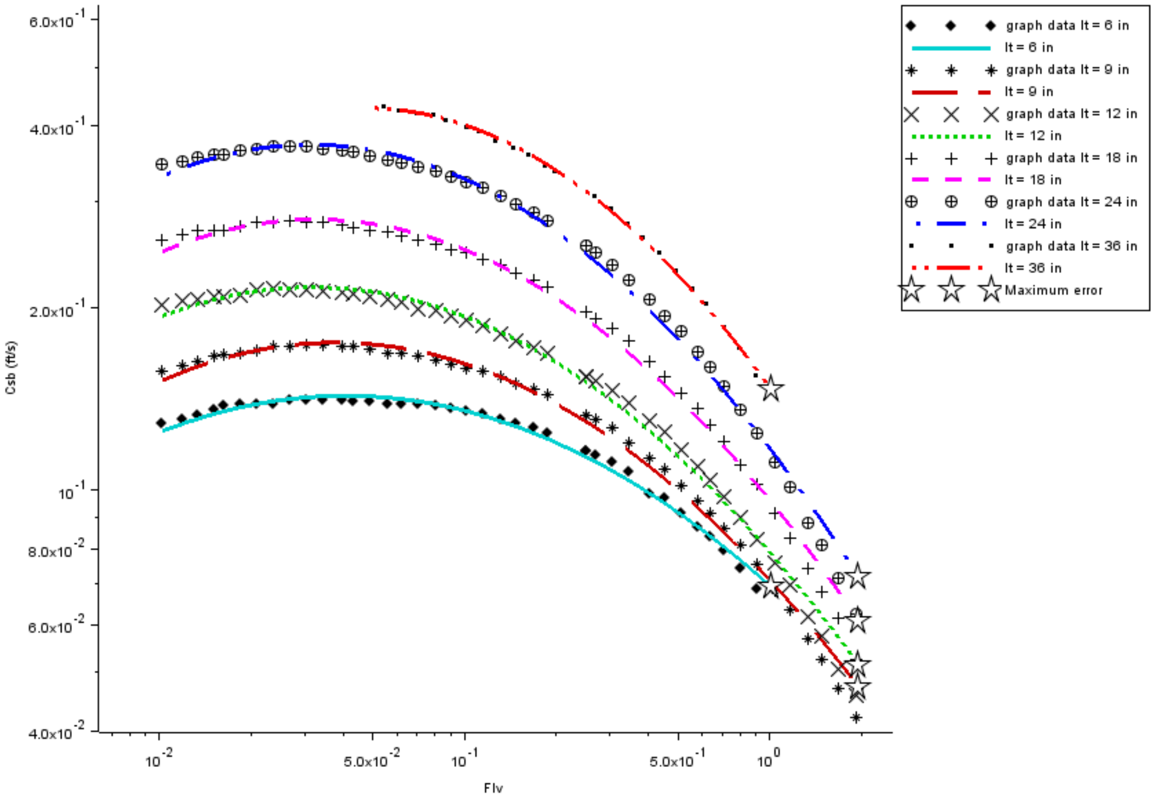

Source: The author, 2022.

Table 60 – New parameters for the correlation of Ogboja and Kuye (1990)

Tray spacing (m)	$\theta_{Csb,1}$	$\theta_{Csb,2}$	$\theta_{Csb,3}$	$\theta_{Csb,4}$	$\theta_{Csb,5}$	$\theta_{Csb,6}$
0.1524	0.0129	0.2011	0.0061	-0.2686	-0.008	0.1229
0.2286	0.0129	0.1731	0.0153	-0.2686	-0.008	0.0954
0.3048	0.0129	0.1688	0.0193	-0.2686	-0.008	0.0914
0.4572	0.0129	0.1535	0.0388	-0.2686	-0.008	0.0763
0.6096	0.0129	0.1589	0.0464	-0.2686	-0.008	0.0761
0.9144	0.0129	0.1373	0.0603	-0.2686	-0.008	0.1116

Source: The author, 2022.

Table 61 – Error the flooding correlation by Ogboja and Kuye (1990) with new parameters

Tray spacing (m)	Average error (%)	Maximum error (%)
0.1524	1.94	9.90
0.2286	3.21	18.81
0.3048	4.13	29.10
0.4572	4.56	37.23
0.6096	5.47	43.77
0.9144	2.01	10.38

Source: The author, 2022.

Figure 32 – Comparison of Fair's data from Souders-Brown constant with the correlation proposed by Ogboja and Kuye (1990) with new parameters

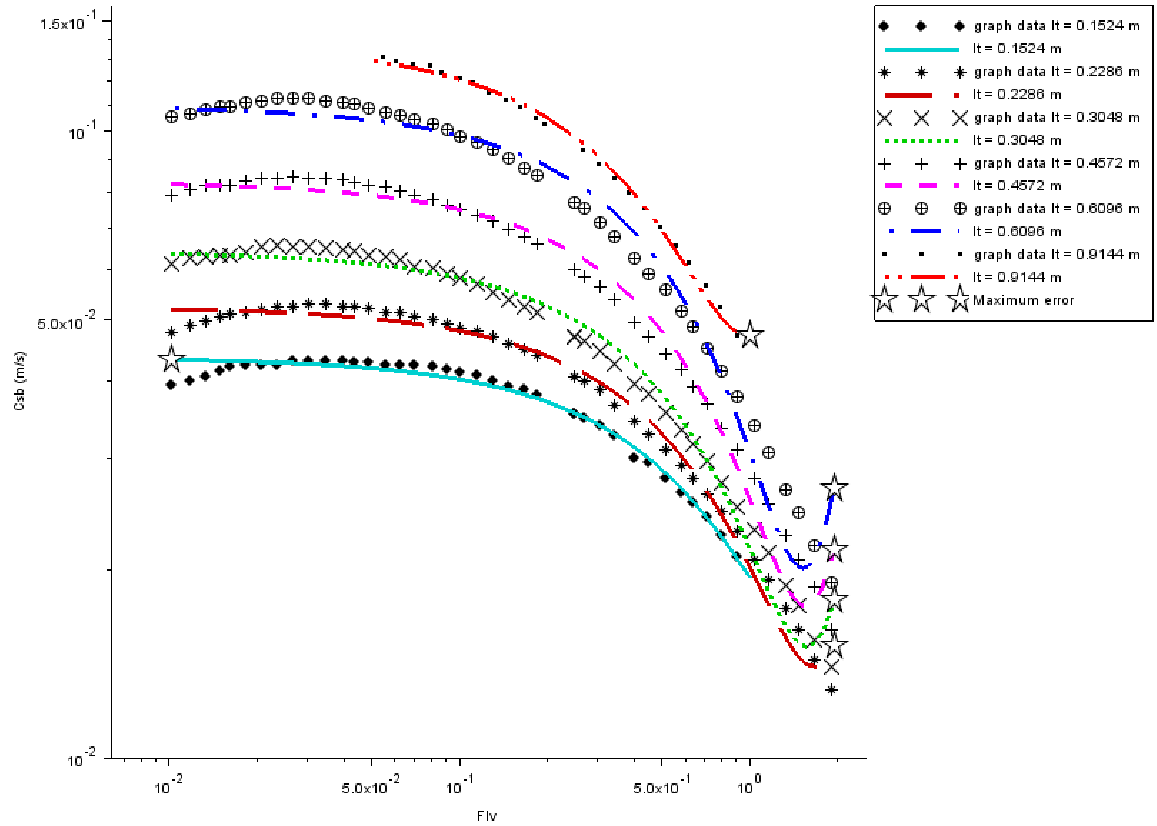

Source: The author, 2022.

Table 62 – New parameters for the correlation of Economopoulos (1978)

Tray spacing (in)	$\theta_{Csb,1}$	$\theta_{Csb,2}$	$\theta_{Csb,3}$	$\theta_{Csb,4}$	$\theta_{Csb,5}$	$\theta_{Csb,6}$
6	4.6144707	-0.5853533	4.9526855	-0.9774971	4.9179433	- 2.3130686
9	2.3786258	-0.2944786	-4.962861	-0.6446075	- 4.8080764	2.7702027
12	3.0359264	- 0.2228002	- 4.9247237	- 0.4620664	- 4.2113957	2.5712821
18	4.9446145	- 0.1615520	- 4.8172325	- 0.3025193	- 4.7330993	3.2151896
24	4.5304367	- 0.1055046	4.785858	- 0.2199283	4.9397237	- 3.6547326
36	3.6044579	4.359803	4.1460763	- 0.1339737	4.7870535	- 3.0333122

Source: The author, 2022.

Table 63 – Errors of the flooding correlation by Economopoulos (1978) with new parameters

Tray spacing (in)	Average error (%)	Maximum error (%)
6	1.85	6.77
9	2.49	8.04
12	2.57	9.87
18	2.36	6.39
24	2.42	7.36
36	3.44	13.41

Source: The author, 2022.

Figure 33 – Comparison of Fair's data from Souders-Brown constant with the correlation proposed by Economopoulos (1978)with new parameters

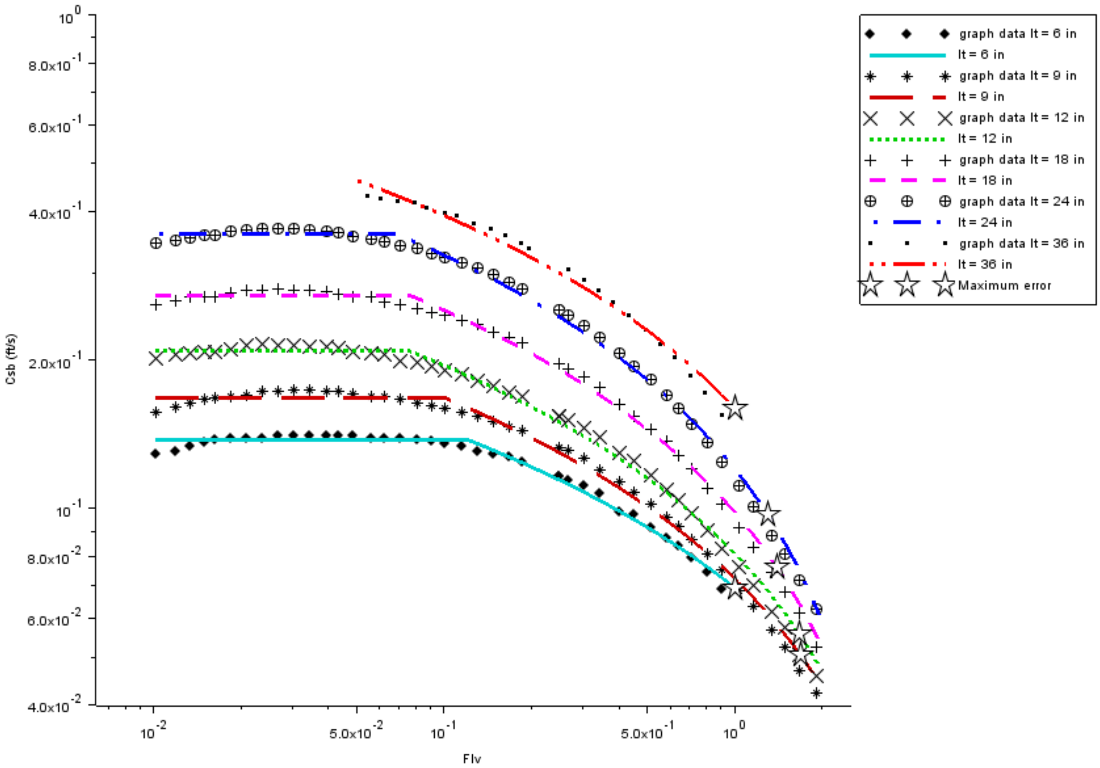

Source: The author, 2022.

Parameter estimation for entrainment correlation without split of the domain

The new parameters for entrainment correlation without split in regions were determined. The results for each model were shown in Tables 64, 65 and Figure 34 (Economopoulos, 1978); Tables 66, 67 and Figure 35 (Ogboja; Kuye, 1990).

Table 64 – New parameters of the correlation of Economopoulos (1978) for evaluation of the fractional entrainment

	$\theta_{\psi,1}$	$\theta_{\psi,2}$	$\theta_{\psi,3}$	$\theta_{\psi,4}$
Parameters	6.5975	2.4158	-0.1115	0.6019

Source: The author, 2022.

Table 65 – Errors of entrainment correlations by Economopoulos (1978) with new parameters

Fflood (%)	Average error (%)	Maximum error (%)
90	8.10	38.62
80	7.83	32.28
70	9.38	28.34
60	5.03	15.68
50	10.34	24.23
45	6.67	16.51
40	3.71	7.85
35	4.38	16.90
30	15.33	45.65

Source: The author, 2022.

Figure 34 – Comparison of Fair's data from entrainment fraction with the correlation proposed by Economopoulos (1978) with new parameters

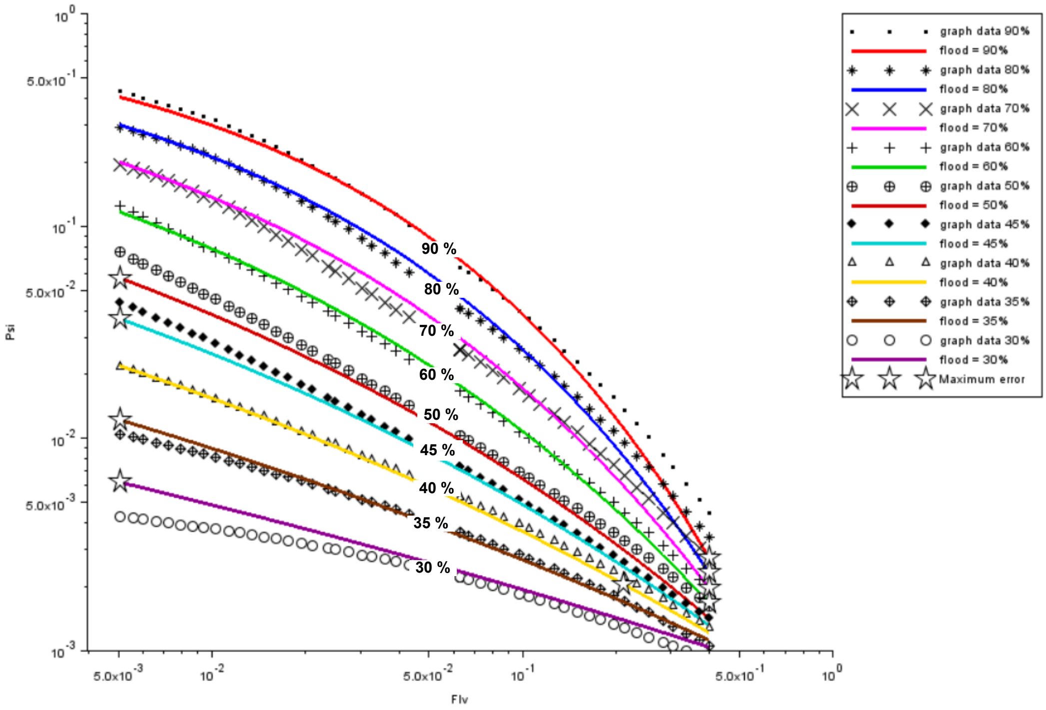

Source: The author, 2022.

Table 66 – New parameters of the correlation of Ogboja and Kuye (1990) for evaluation of the fractional entrainment

Parameters	$\theta_{\psi,1}$	$\theta_{\psi,2}$	$\theta_{\psi,3}$	$\theta_{\psi,4}$	$\theta_{\psi,5}$	$\theta_{\psi,6}$	$\theta_{\psi,7}$	$\theta_{\psi,8}$
	-7.7036	0.7153	-0.0499	2.2989	-0.2424	1.1750	-1.9799	0.8633

Source: The author, 2022.

Table 67 – Errors of the entrainment correlations of Ogboja and Kuye (1990) with new parameters

Fflood (%)	Average error (%)	Maximum error (%)
90	1.22	8.18
80	2.68	8.82
70	2.88	8.12
60	3.77	12.65
50	5.63	10.93
45	2.76	5.24
40	2.80	5.69
35	2.57	7.66
30	7.11	10.75

Source: The author, 2022.

Figure 35 – Comparison of the original data from entrainment fraction with the correlation proposed by Ogboja and Kuye (1990) with new parameters

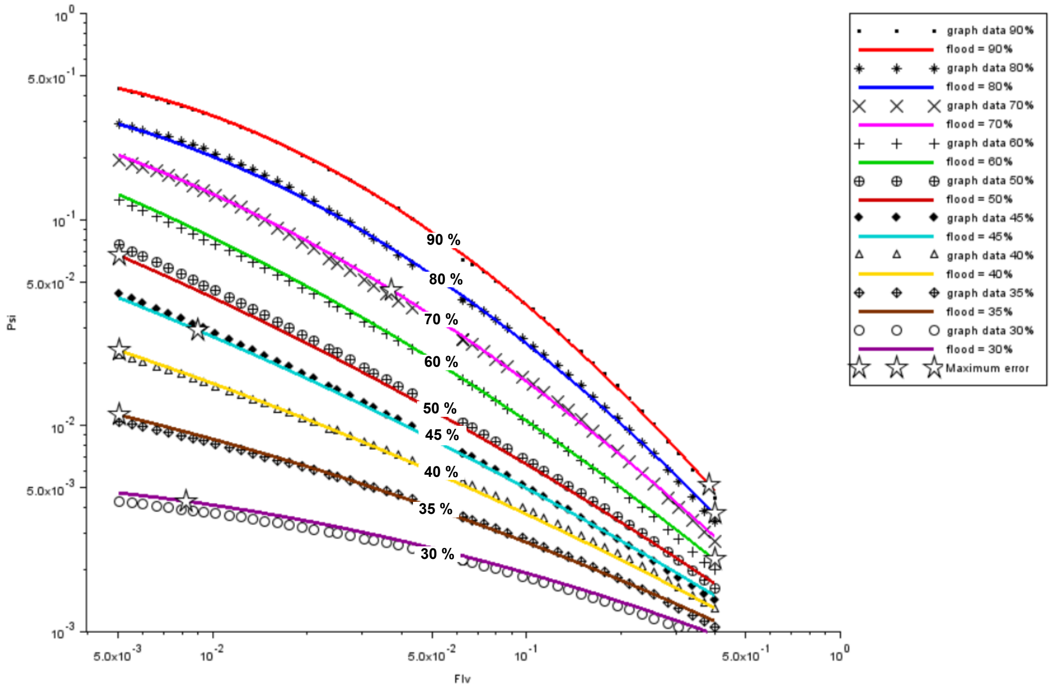

Source: The author, 2022.

Distillation design examples

Tray design variables

Tray design variables is composed by column diameter (*Dc*), hole diameter (*dh*), tray spacing (*lt*), the weir height (*hw*), the difference between weir and clearance height under the downcomer (*hdwap*), the weir lengh (*lw*), hole pitch (*lp*), tray thickness (*tt*), and hole layout (*lay*). Table 2 show discrete values adopted for this variables.

Table 2 –Discrete values of the design variables

Variables	Discrete values																
Dc (m)	0.61	0.76	0.91	1.07	1.27	1.47	1.68	1.93	2.18	2.44	2.74	3.05	3.35	3.71	4.06	4.42	4.83
dh (mm)	3.60	4.00	4.40	4.80	5.20	5.60	6.00	6.40									
hdwap (mm)	5.00	6.00	7.00	8.00	9.00	10.0											
hw (cm)	3.81	4.44	5.08	5.71	6.35	6.98	7.62	8.25	8.89								
lt (m)	0.15	0.23	0.31	0.47	0.62	0.91											
lw (m)	0.41	0.66	0.91	1.17	1.42	1.68	1.93	2.18	2.44	2.69	2.95	3.20	3.45	3.71	3.96		
lp (mm)	9.00	12.0	15.0	18.0	21.0	24.0											
tt (mm)	3.40																
lay	square		triangular														

Source: The author, 2022.

Example 1

Example 1 consists of a depropanizer column and was taken from Kister (1992), with changes in flow rates (multiplied by 2.0). The feed of the distillation column is crude oil, the top stream contains 99.5% mol of methane, ethane, and propane, and the bottom stream contains 1% mol of propane. The operational parameters of the nineteen ideal stages are shown in Table 68, where the feed tray is tray 9 and the reflux ratio is 1.5.

Table 68 – Operational parameters of Example 1

Stage	Vapor mass flow rate (kg/s)	Density of vapor (kg/m³)	Liquid mass flow rate (kg/s)	Density of liquid (kg/m³)	Sufarce tension (N/m)×10^3
1	27.61	38.43	18.60	477.66	5.31
2	30.40	39.64	21.38	448.17	3.37
3	30.49	39.69	21.48	447.61	3.30
4	30.04	39.50	21.03	451.50	3.35
5	29.74	39.31	20.72	456.48	3.44
6	29.47	39.07	20.45	461.57	3.53
7	28.87	38.54	19.86	467.85	3.66
8	27.50	37.24	18.49	482.49	4.44
9	20.85	48.33	35.02	464.99	3.40
10	23.55	49.90	37.72	455.82	3.60
11	25.26	51.05	39.43	451.05	3.41
12	26.65	52.07	40.82	447.45	3.28
13	27.98	53.02	42.15	444.26	3.16
14	29.14	53.90	43.31	441.68	3.07
15	29.98	54.62	44.15	439.76	3.00
16	30.81	55.25	44.98	438.00	2.94
17	31.44	55.85	45.61	436.78	2.90
18	31.88	56.59	46.05	436.09	2.87
19	32.48	57.89	46.66	435.55	2.84

Source: KISTER, 1992.

The result of the Set Trimming procedure for correlations of Economopoulos (1978), Ogboja and Kuye (1990) and our readjusted is shown in Table 69.

Table 69 – Results of Example 1

	Economopoulos (1978)	Ogboja and Kuye (1990)	Our readjusted correlations
Cost total ($)	316361.07	352484.38	441644.54
Dc (m)	3.0480	3.3528	4.064
dh (m)	0.0036	0.0036	0.0036
hdwap (m)	0.005	0.005	0.005
hw (m)	0.0508	0.0445	0.0381
lt (m)	0.9144	0.9144	0.9144
lw (m)	2.9464	3.2004	3.9624
lp (m)	0.009	0.012	0.012
lay	square	triangular	square

Source: The author, 2022.

Example 2

Example 2 was taken from Towler and Sinnott (2013), with changes in flow rates (multiplied by 2.0), where acetone is recovered from a 10% mol of acetone aqueous waste. The top stream of the distillation column must contain 95% mol of acetone and the bottom stream must not contain more than 1 mol of acetone.

The operational parameters of the nine ideal stages are shown in Table 70, the Stage 8 is the feed tray and the reflux ratio is 1.24. These were obtained by a simulation in the Aspen software using the property method UNIQ-RK, which employs the Redlich-Kwong equation of state and the UNIQUAC activity coefficient model.

Table 70 – Operational parameters of Example 2

Stage	Vapor mass flow rate (kg/s)	Density of vapor (kg/m³)	Liquid mass flow rate (kg/s)	Density of liquid (kg/m³)	Sufarce tension (N/m)×10^3
1	2.99	2.10	1.64	753.76	22.28
2	2.96	2.09	1.60	754.64	23.20
3	2.92	2.07	1.56	755.64	24.21
4	2.87	2.04	1.51	756.92	25.45
5	2.80	2.01	1.44	758.84	27.21
6	2.68	1.95	1.32	762.57	30.28
7	2.37	1.78	1.01	776.27	38.60
8	2.04	1.61	6.24	873.01	59.14
9	1.36	1.02	5.57	900.73	60.79

Source: TOWLER; SINNOTT, 2013.

Table 71 shows the result of the Set Trimming procedure for correlations of Economopoulos (1978), Ogboja and Kuye (1990) and our readjusted.

Table 71 – Results of Example 2

	Economopoulos (1978)	Ogboja and Kuye (1990)	Our readjusted correlations
Cost total ($)	36738.14	45604.67	40852.56
Dc (m)	0.9144	1.2700	1.2700
dh (m)	0.0036	0.0036	0.0036
hdwap (m)	0.005	0.005	0.005
hw (m)	0.0699	0.0381	0.0381
lt (m)	0.9144	0.6096	0.4572
lw (m)	0.6604	0.9144	0.9144
lp (m)	0.009	0.009	0.009
lay	square	square	square

Source: The author, 2022.

The comparison of the correlations of Economopoulos (1978) with our predictions is shown in Figure 36. It is possible to observe a small fraction of false positive and false negative candidates in both constraints. Despite the small number of false positive candidates, one of them is the solution of the optimization problem when the Economopoulos (1978) correlation is employed, associated with a cost of $36,738.14. The solution with our predictions in the model has a higher cost, \$40,852.57, i.e. the solution using the correlation of Economopoulos (1978) was another false positive.

Figure 36 – Example 2: Comparison between correlations of the Economopoulos (1978) and our readjusted correlations

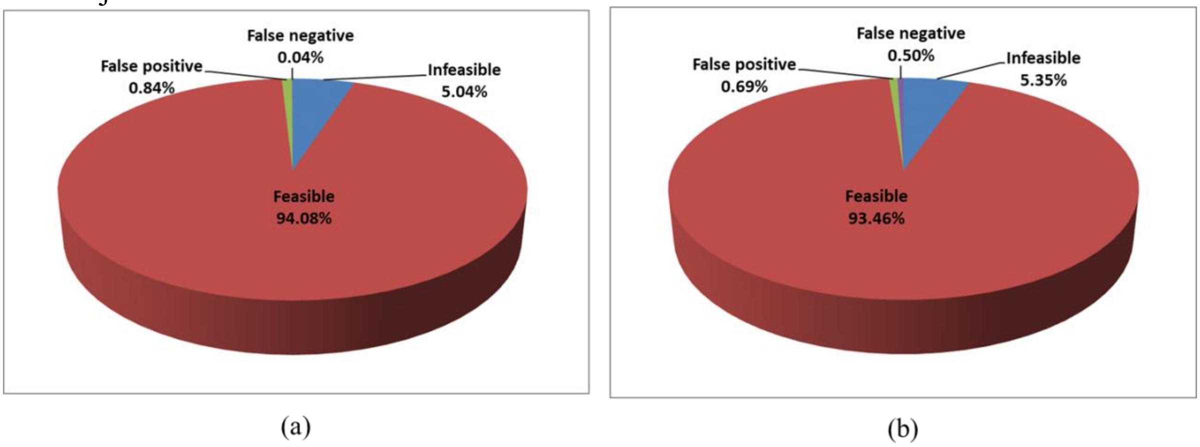

Subtitle: (a) Flooding, (b) Entrainment

Source: The author, 2022.

Figure 37 shows the results related to the correlations of Ogboja and Kuye (1990), where there is a small amount of false positive and false negative candidates. Here, the solution is also affected, but in an opposite way, the optimal solution has a cost of \$45,604.67, but there is another alternative, which is feasible according to the predictions of this paper, with a smaller cost, \$40,852.57, i.e. it is a false negative.

Figure 37 – Example 2: Comparison between correlations of the Ogboja and Kuye (1990) and our readjusted correlations

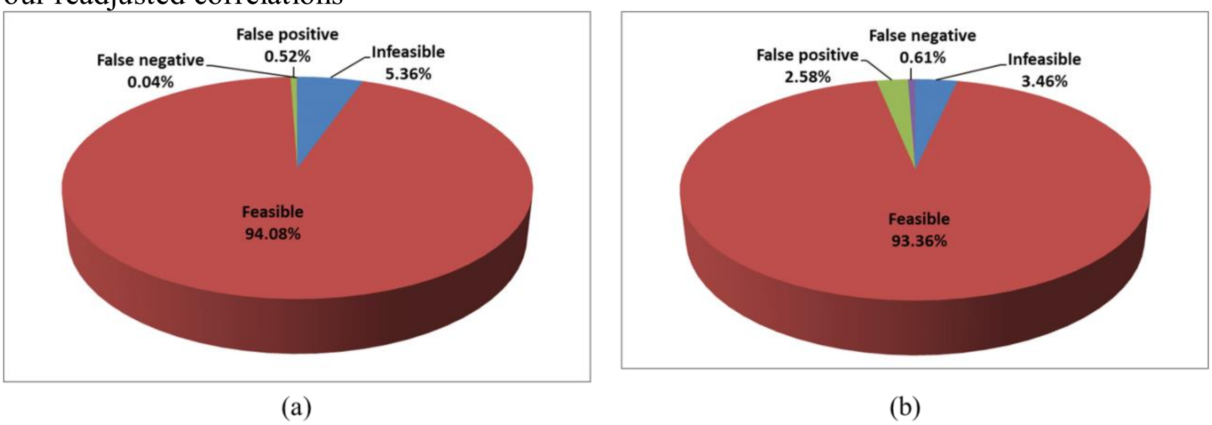

Subtitle: (a) Flooding, (b) Entrainment

Source: The author, 2022.

Example 3

Example 3 consists of a methanol purification column and was taken from Kiss and Ignat (2012), with changes in flow rates (multiplied by 0.5). The feed of the distillation column is a ternary mixture of methanol-water-glycerol (0.473–0.054–0.473 % mass). The top stream of the distillation column must contain 99.9% mass of methanol and the bottom stream must contain 90% mass of glycerol. To prevent the degradation of glycerol, the operating pressure is 0.5 bar.

The operational parameters of the fourteen ideal stages are shown in Table 72, Stage 9 is the feed tray and the reflux ratio is 1.4. These were obtained by a simulation in the Aspen software using the property method UNIQUAC activity coefficient model.

Table 72 – Operational parameters of Example 3

Stage	Vapor mass flow rate (kg/s)	Densityof vapor (kg/m^3)	Liquid mass flow rate (kg/s)	Density of liquid (kg/m^3)	Sufarce tension $(N/m)\times10^3$
1	0.456	0.600	0.266	765.503	20.411
2	0.456	0.600	0.266	765.566	20.464
3	0.455	0.600	0.265	765.671	20.551
4	0.455	0.599	0.265	765.844	20.694
5	0.454	0.598	0.264	766.130	20.928
6	0.452	0.597	0.262	766.604	21.311
7	0.450	0.594	0.260	767.395	21.934
8	0.445	0.585	0.255	768.729	22.943
9	0.441	0.581	0.647	898.886	30.101
10	0.421	0.564	0.633	904.710	32.018
11	0.376	0.508	0.588	926.350	38.349
12	0.292	0.399	0.505	984.956	51.279
13	0.236	0.297	0.449	1043.560	59.270

Source: Kiss; Ignat, 2012.

The result of the Set Trimming procedure is shown in Table 73 for correlations of Economopoulos (1978), Ogboja and Kuye (1990) and our readjusted.

Table 73 – Results of Example 3

	Economopoulos (1978)	Ogboja and Kuye (1990)	Our readjusted correlations
Cost total ($)	31955.10	31955.10	30643.87
Dc (m)	0.7620	0.7620	0.6096
dh (m)	0.0036	0.0036	0.0036
hdwap (m)	0.005	0.005	0.005
hw (m)	0.0381	0.0381	0.0381
lt (m)	0.4572	0.4572	0.6096
lw (m)	0.4064	0.4064	0.4064
lp (m)	0.009	0.009	0.009
lay	square	square	square

Source: The author, 2022.

Figures 38 and 39 show the comparison of the performance of the correlations of Economopoulos (1978) and Ogboja and Kuye (1990), respectively. These figures indicate a small percentage of false positive and negative candidates.

Figure 38 – Example 3: Comparison between correlations of the Economopoulos (1978) and our readjusted correlations

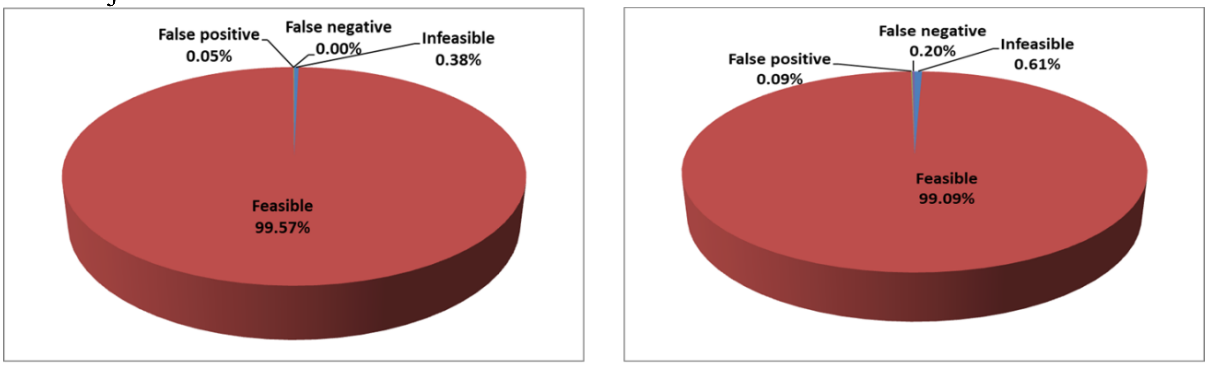

(a) (b)

Subtitle: (a) Flooding, (b) Entrainment

Source: The author, 2022.

Figure 39 – Example 3: Comparison between correlations of the Ogboja and Kuye (1990) and our readjusted correlations

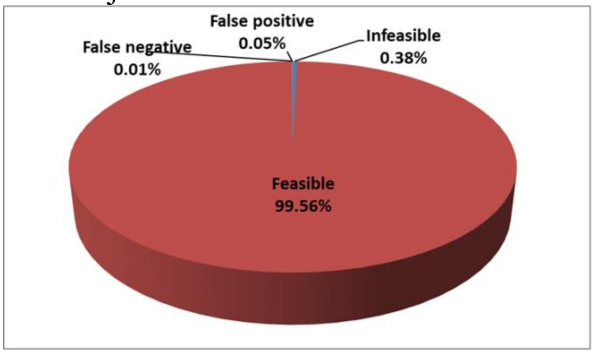

(a)

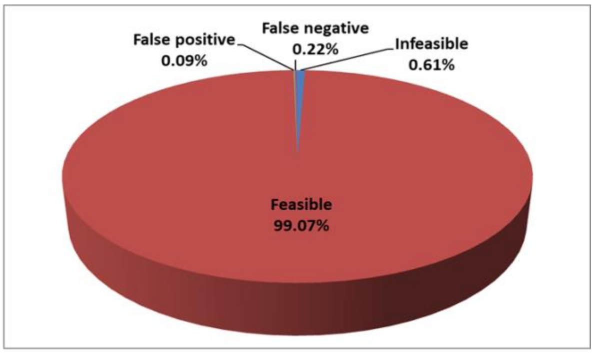

(b)

Subtitle: (a) Flooding, (b) Entrainment

Source: The author, 2022.

The results of Set Trimming optimization to minimize cost using the correlations of Economopoulos (1978) or Ogboja and Kuye (1990) have a cost of $31,955.10, while the result with our predictions is $ 30,643.874, i.e. another example of a false negative candidate.

APPENDIX D – Scientific Production

In this appendix the scientific production developed during the thesis period is presented. Only the first page of the complete paper is shown.

Journal: Chemical Engineering Research and Design, 2022.

- Title: Globally optimal distillation tray design using a mathematical programming approach. Authors: Aline R.C. Souza, Miguel J. Bagajewicz, André L.H. Costa.

Journal: AIChE Journal, 2023.

- Title: Set Trimming approach for the globally optimal design of sieve trays in separation columns. Authors: Aline R. da Cruz Souza, Miguel J. Bagajewicz, André Luiz Hemerly Costa.

Journal: Chemical Engineering Research and Design, 2024. (Received for publication).

- Title: Improved correlations for threshold flooding and entrainment in sieve trays in distillation/absorption columns. Authors: Aline R. C. Souza, Miguel J. Bagajewicz, André L. H. Costa.

Chemical Engineering Research and Design 180 (2022) 1–12

Contents lists available at ScienceDirect

Chemical Engineering Research and Design

journal homepage: www.elsevier.com/locate/cherd

Globally optimal distillation tray design using a mathematical programming approach

Aline R.C. Souza [a], *Miguel J. Bagajewicz* [a,b,c], *André L.H. Costa* [a,*]

[a] *Rio de Janeiro State University (UERJ), Rua São Francisco Xavier, 524, Maracanã, CEP 20550-900, Rio de Janeiro, RJ, Brazil*
[b] *School of Chemical, Biological and Materials Engineering, University of Oklahoma, Norman, Oklahoma, 73019, USA*
[c] *Federal University of Rio de Janeiro (UFRJ), Escola de Química, CT, Bloco E, Ilha do Fundão, CEP 21949-900, Rio de Janeiro, RJ, Brazil*

A R T I C L E I N F O

Article history:
Received 26 September 2021
Received in revised form 24 January 2022
Accepted 25 January 2022
Available online 29 January 2022

Keywords:
Distillation
Optimization
Design

A B S T R A C T

This article presents the optimization of the design of distillation column trays. We develop a mixed-integer nonlinear optimization model, which we solve using mathematical programming. The objective of this formulation is to size all geometric variables of the tray. Two possible alternative objective functions are tested: column cost and column mass. The utilization of the proposed approach is illustrated through a design example from the literature. In this example, the optimal result obtained through the proposed approach is compared with the one obtained following the spirit of a traditional heuristic design procedure employed in process equipment design textbooks. The comparison indicates a reduction of both objective functions tested as compared to the result of the heuristic procedure.

1. Introduction

In the United States, it is estimated that there are more than 40,000 distillation columns in operation, accounting for 90 % of the separation and purification processes. It is estimated that the capital invested in these systems is around US$ 8 billion (Humphrey, 1995). Because the costs associated with this equipment are high, a considerable number of papers have addressed the optimal design of distillation columns. The main focus of these procedures is to optimize the column diameter, the number of trays, and the reflux ratio to minimize the total annualized cost.

Several different mathematical programming approaches were used to address this design problem: nonlinear programming (NLP) (Dowling and Biegler, 2015; Yeoh and Hui, 2021), mixed-integer nonlinear programming (MINLP) (Viswanathan and Grossmann, 1993; Kong and Maravelias, 2019), and generalized disjunctive programming (GDP) (Yeomans and Grossmann, 2000). Additionally, a combination of mathematical programming and commercial simulators was proposed by Caballero et al. (2005) and Caballero (2015).

Aiming at avoiding convergence drawbacks and local optimality problems associated with mathematical programming, some authors proposed the utilization of stochastic optimization methods for the solution of the aforementioned optimal design problem. Different techniques were tested, such as, particle swarm optimization (PSO) (Javaloyes-Antón et al., 2013), genetic algorithms (GA) (Ibrahim et al., 2017) and differential evolution (DE) associated with parallel computing (Lyu et al., 2021).

In all the aforementioned approaches, the dimensions of the column internals, namely, tray spacing, weir length, weir height, etc., have been not included. The traditional approach for the design of distillation column trays is based on trial and verification schemes, as depicted in several textbooks: Fair (1963), Wankat (1988), Kister (1992), Chuang and Nandakumar (2000), and Towler and Sinnott (2013). These schemes are considered reliable, but they depend on the designer's experience to attain a feasible choice of the tray geometric dimensions, with no guarantee that the solution found will feature the lowest cost. We know of only two works that employ optimization techniques for identifying the optimal set of tray dimensions: Ogboja and Kuye (1990) and Lahiri (2014, 2020). Ogboja and Kuye (1990) developed a sieve tray optimization

* *Corresponding author.*
E-mail address: andrehc@uerj.br (A.L.H. Costa).
https://doi.org/10.1016/j.cherd.2022.01.036
0263-8762/

Received: 26 July 2022 | Revised: 30 September 2022 | Accepted: 18 October 2022
DOI: 10.1002/aic.18003

AIChE JOURNAL

RESEARCH ARTICLE
Process Systems Engineering

Set Trimming approach for the globally optimal design of sieve trays in separation columns

Aline R. da Cruz Souza[1] | Miguel J. Bagajewicz[1,2,3] | André Luiz Hemerly Costa[1]

[1]Rio de Janeiro State University (UERJ), Rua São Francisco Xavier, 524, Rio de Janeiro, RJ, 20550-900, Brazil
[2]Escola de Química, CT, Bloco E, Federal University of Rio de Janeiro (UFRJ), Ilha do Fundão, Rio de Janeiro, RJ, 21949-900, Brazil
[3]School of Chemical, Biological and Materials Engineering, University of Oklahoma, Norman, Oklahoma, 73019, USA

Correspondence
André Luiz Hemerly Costa, Rio de Janeiro State University (UERJ), Rua São Francisco Xavier, 524, Maracanã, CEP 20550-900, Rio de Janeiro, RJ, Brazil.
Email: andrehc@uerj.br

Funding information
Conselho Nacional de Desenvolvimento Científico e Tecnológico, Grant/Award Number: 310390/2019-2; Coordenação de Aperfeiçoamento de Pessoal de Nível Superior; Universidade do Estado do Rio de Janeiro

Abstract

In this article, we use Set Trimming to obtain the globally optimal design of distillation column trays, that is, the column diameter and the geometrical design of the trays (weir, downcomer, etc.) that minimize mass or cost. We assume that the operating conditions (vapor and liquid flow rates, compositions, temperatures) are given. The design task is, to this day, presented in textbooks as a trial and verification procedure. We show that Set Trimming guarantees global optimality and is amenable to exploring alternative global optima. Compared with the employment of a mixed-integer nonlinear programming (MINLP) approach using commercial global optimizers, we show that Set Trimming is a more robust option with competitive computational times for individual design problems. It also exhibits a significant reduction in computational effort when alternative optimal solutions are sought.

KEYWORDS
design, distillation, optimization, Set Trimming, tray

1 | INTRODUCTION

The design of column trays in separation columns has been traditionally handled using trial-and-verification procedures through step-by-step procedures.[1–8] Some of these procedures are based on bold assumptions and heuristics that facilitate obtaining viable answers, with the intended effect of keep changing the trial geometries until one is viable. For example, the area of the downcomer is assumed to be 10% of the total area right after the diameter is selected based on a flooding velocity.[8]

The utilization of optimization techniques for the design of column trays was addressed by a few works. Ogboja and Kuye[9] used the Complex Method to solve a sieve tray optimization. They obtained the optimal tray design by maximizing tray efficiency according to geometrical and phenomenological constraints. The problem formulation was restricted to optimizing only one plate and not the total set of column trays. Lahiri[10,11] presented a method to obtain the optimal tray design based on the minimization of the total annualized cost, showing better results when compared with a commercial simulator. More recently, Souza et al.[12] presented a mixed-integer nonlinear mathematical model (MINLM) solved using a global optimizer for the design of column trays, based on the equations presented in Towler and Sinnot.[8]

As shown by Souza et al.,[12] the solution to the tray design-optimization problem using mathematical programming can attain better results than the traditional trial and verification approach. However, further numerical tests indicate that the global solution of the tray design problem using mathematical programming may be difficult sometimes. Aiming at providing a fast and reliable optimization tool for the solution of the optimal tray design problem, we present in this work the application of Set Trimming.[13] According to the results presented in this article, the proposed technique for solving the tray design problem is more robust than mathematical programming using global solvers, presenting competitive computational times.

Another important aspect of the proposed technique is the solution based on optimal sets, instead of optimal points. Conventional optimization techniques identify a single optimal solution. However, Set Trimming can identify all of the optimal solutions with the lowest value of the objective function (if there is more than one). Therefore, the user can choose one of these solutions considering other

Improved Correlations for Threshold Flooding and Entrainment in Sieve Trays in Distillation/Absorption Columns

Aline R. C. Souza[a], Miguel J. Bagajewicz[a,b,c], André L. H. Costa[a]*

[a] Rio de Janeiro State University (UERJ), Rua São Francisco Xavier, 524, Maracanã, CEP 20550-900, Rio de Janeiro, RJ, Brazil

[b] School of Chemical, Biological and Materials Engineering, University of Oklahoma, Norman, Oklahoma USA 73019

[c] Federal University of Rio de Janeiro (UFRJ), Escola de Química, CT, Bloco E, Ilha do Fundão, CEP 21949-900, Rio de Janeiro, RJ, Brazil

ABSTRACT

The data available in the literature about flooding and entrainment in distillation/absorption columns were originally reported in graphs. Aiming at the use of these data for computational applications, several algebraic correlations were proposed for evaluation of the Souders-Brown flooding constant (*Csb*) and the fractional entrainment (ψ). In this article, we revisit these correlations, using the graphs presented by Fair (1961) as a source of data and targets to match. We digitized these graphs to obtain a set of points for each reported curve. Comparing these data with the correlations predictions, we show that there are considerable deviations. Therefore, we use the collected dataset to re-estimate the parameters of several correlations, also exploring the scheme of splitting the domain of a correlation in multiple regions and estimate parameters for each region. We found that our results reduce the error of the original

* Corresponding author.
E-mail address: andrehc@uerj.br (A. L. H. Costa)